

**WILLIAM LEONARD EURY
APPALACHIAN COLLECTION
APPALACHIAN STATE UNIVERSITY
BOONE, NORTH CAROLINA 28608**

Archives
Closed
LD
175
A40K
Th
640

COMPARATIVE MICROSCOPIC ANATOMY AND TENSILE STRENGTH OF PLUMAGE
FROM VARIOUS COLOR PHASES IN THE EASTERN SCREECH OWL
(*MEGASCOPS ASIO*)

A Thesis
By
EVAN LACY PANNKUK

Submitted to the Graduate School
Appalachian State University
In partial fulfillment of the requirements for the degree of
MASTER OF SCIENCE

August 2008
Major Department: Biology

COMPARATIVE MICROSCOPIC ANATOMY AND TENSILE STRENGTH OF PLUMAGE
FROM VARIOUS COLOR PHASES IN THE EASTERN SCREECH OWL
(*MEGASCOPS ASIO*)

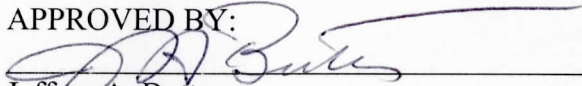
A Thesis

by

EVAN LACY PANNKUK

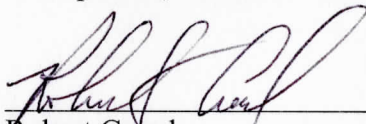
August 2008

APPROVED BY:



Jeffrey A. Butts

Chairperson, Thesis Committee



Robert Creed

Member, Thesis Committee



Robert Wayne Van Devender

Member, Thesis Committee



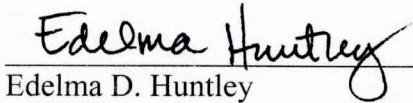
Lynn M. Siefferman

Member, Thesis Committee



Steven Seagle

Chairperson, Department of Biology



Edelma D. Huntley

Dean, Research and Graduate Studies

(COPYRIGHT PAGE)

Copyright by Evan Lacy Pannkuk 2008
All Rights Reserved

ABSTRACT

COMPARATIVE MICROSCOPIC ANATOMY AND TENSILE STRENGTH OF PLUMAGE FROM VARIOUS COLOR PHASES IN THE EASTERN SCREECH OWL

(*MEGASCOPS ASIO*). (August 2008)

Evan Lacy Pannkuk, B.S., Appalachian State University

M.S., Appalachian State University

Thesis Chairperson: Jeffrey A. Butts

The Eastern Screech Owl (*Megascops asio*) is a polymorphic species with rufous and gray tones that exhibits clinal variation. The rufous morph is virtually nonexistent in the northern and westernmost parts of its range. The rufous morph predominates in humid deciduous areas in the center of the eastern screech owl range. While color polymorphism is exhibited widely in birds there is no apparent explanation for the maintenance of clinal variation. Studies have noted differences in oxygen consumption across eastern screech owl color morphs. Differences in feather morphology could lead to difference in thermal insulation and physical resistance. To date there have been no studies investigating the plumage morphology of a color polymorphic bird. This study employed light, scanning, and transmission electron microscopy to investigate the microscopic anatomy of *M. asio* feathers. The tensile strength of contour feather barbs was also measured and the breakage point was imaged with scanning electron microscopy. Finally, Geographic Information Software (GIS) was used to determine habitat use associated with different color morphs. GIS land cover

analysis indicates that rufous morphs of the eastern screech owl are more closely associated with deciduous forests. Transmission microscopy indicates that the coloration of *M. asio* is caused by eumelanin (gray) and phaeomelanin (rufous) pigments deposited in the cortex wall of the feather barb. While the rufous morph exhibits lower ventral nodal pigmentation than the gray morph and a greater length between barbules, there does not appear to be a significant difference between gross morphological feather structures. Also, the two pigment variants do not differentially thicken the cortex wall or lead to a difference in tensile strength. The results of this study provide evidence that there may be a greater length between barbules in the rufous morphs that could lead to a lower thermal efficiency but there is no differences in strength that may impact differential eastern screech owl color variant range frequency.

ACKNOWLEDGEMENTS

I am happy to thank the individuals and organizations that supplied specimens of eastern screech owls: Nina Fishchesser of the Blue Ridge Raptor Rehabilitation Clinic; Dr. John Gerwin, Dr. Doug Pratt, and Becky Dejanarios of the North Carolina State Museum of Natural History; Christopher Hatton of the Avian and Exotic Animal Clinic of Indianapolis; Mathias Engelmann of Carolina Raptor Rehabilitation; Diana Flynn of the Florida Audubon Society; and the Ornithology Department at the American Museum of Natural History. I thank Dr. Phillip Russell, Dr. Michael Dexter, Dr. Peter Sttenheim, Dr. Fred Gehlbach, and Curtis Smalling of the North Carolina Audubon Society for responding to personal communications. Nolan Beasley entered light microscope measurements into a database, Dr. Guichuan Hou assisted with the electron microscopy, and Dr. Lou Germinario and Dr. Brad Snow of the Physical Chemistry Research Laboratory at Eastman Chemical Company assisted with the tensile strength test. Dr. Jill Thomas, Dr. Howard Nuefeld, and Dr. Robert Creed assisted with statistical analysis and design. I also thank my advisor, Dr. Jeffrey Butts, for his patience and advice. Dr. Wayne Van Devender, Dr. Robert Creed, and Dr. Lynn Sieffermann all served on my committee. The Graduate Student Association and the Office of Student Research at Appalachian State University provided funding.

TABLE OF CONTENTS

	<u>Page</u>
List of Tables	ix
List of Figures	xi
Chapter 1. Color Polymorphism and the Eastern Screech Owl	1
INTRODUCTION	1
Genetics.....	6
Physiology and Behavior	7
Environmental Conditions	8
Objectives	8
Chapter 2. GIS Analysis of Eastern Screech Owl Color Variant Clinal Variation.....	10
INTRODUCTION	10
MATERIALS AND METHODS.....	12
RESULTS	14
DISCUSSION	24
Chapter 3. Macro- and Microstructural Anatomy of Eastern Screech Owl Feathers	26
INTRODUCTION	26
MATERIALS AND METHODS.....	28
Owl Collection	28
Color Score	28
Light Microscopy and Macroscopic Measurements	29

Scanning Electron Microscopy	35
Transmission Electron Microscopy	35
RESULTS	37
Color Score	37
Light Microscopy and Macroscopic Measurements	37
Scanning Electron Microscopy	56
Transmission Electron Microscopy	62
DISCUSSION	65
Light Microscopy and Macroscopic Measurements	65
Scanning Electron Microscopy	67
Transmission Electron Microscopy	67
Chapter 4. Melanin Endocrinology, Biochemistry, and Biomechanics	69
INTRODUCTION	69
MATERIALS AND METHODS	75
RESULTS	77
DISCUSSION	80
Chapter 5. General Conclusions	82
References	85
Appendix A	97
Vita	101

LIST OF TABLES

	<u>Page</u>
Table 1. Majority zonal statistics of 200m United States Geological Survey (USGS) land cover data and rufous eastern screech owl density	15
Table 2. Levels of analysis of eastern screech owl feather morphological measurements.....	34
Table 3. Average color tristimulus scores on a number of pixels from the eastern screech owl dorsum	37
Table 4. Eigenvectors and percentage of variation for the first 3 principle components (PC) of morphological body measurements of eastern screech owl color variants.....	38
Table 5. <i>P</i> -values and <i>F</i> -values for a univariate one-way analysis of variance (ANOVA) and summary statistics for morphological measurements at the feather and barb level of eastern screech owl color variants	39
Table 6. <i>P</i> -values and <i>F</i> -values for a univariate one-way analysis of variance (ANOVA) and summary statistics for morphological measurements at the barbule level of eastern screech owl color variants	41-43
Table 7. <i>P</i> -values from subsequent univariate one-way analysis of variance (ANOVA) on the first 3 principle components (PC) for morphological measurements at the barbule segment level of eastern screech owl color variants	49-50
Table 8. Principle component loading factors for the first three principle components (PC) and <i>P</i> -values, percentage of variation, and <i>F</i> -values from subsequent analysis of variance (ANOVA) with significant <i>P</i> -values for morphological measurements at the barbule segment level of eastern screech owl color variants.....	50-56
Table 9. Summary statistics, <i>P</i> -value, and <i>T</i> -value from student's t-test of physical and chemical constituent percentages in eastern screech owl color variant feathers.....	64
Table 10. Terms and abbreviations for tensile strength tests of eastern screech owl dorsal feather barbs	77

Table 11. Pooled summary statistics of morphological measurements of the breakage point of eastern screech owl dorsal contour feathers.....78

Table 12. Summary statistics of morphological measurements and mechanical variables of the breakage point of eastern screech owl color variant dorsal feather barbs.....79

LIST OF FIGURES

	<u>Page</u>
Figure 1. Frequency of rufous eastern screech owls in North America.....	6
Figure 2. United State Geological Survey (USGS) 200m land cover (solid colors) and rufous screech owl density (outlined in color by county) for counties in North Carolina	16
Figure 3. United State Geological Survey (USGS) 200m land cover (solid colors) and rufous screech owl density (outlined in color by county) for counties in New Jersey.....	17
Figure 4. United State Geological Survey (USGS) 200m land cover (solid colors) and rufous screech owl density (outlined in color by county) for counties in South Carolina	18
Figure 5. United State Geological Survey (USGS) 200m land cover (solid colors) and rufous screech owl density (outlined in color by county) for counties in Tennessee.....	19
Figure 6. United State Geological Survey (USGS) 200m land cover (solid colors) and rufous screech owl density (outlined in color by county) for counties in Vermont	20
Figure 7. United State Geological Survey (USGS) 200m land cover (solid colors) and rufous screech owl density (outlined in color by county) for counties in Alabama.....	21
Figure 8. United State Geological Survey (USGS) 200m land cover (solid colors) and rufous screech owl density (outlined in color by county) for counties in Kansas.....	22
Figure 9. United State Geological Survey (USGS) 200m land cover (solid colors) and rufous screech owl density (outlined in color by county) for counties in Kentucky.....	23
Figure 10. Lateral pterylae of the great-horned owl (<i>Bubo virginianus</i>).....	30
Figure 11. Dorsal pterylae of the great-horned owl (<i>Bubo virginianus</i>).....	31

Figure 12. Topographic anatomy of an eastern screech owl dorsal contour feather32

Figure 13. Feather morphology at the barb, barbule, and barbule segment levels33

Figure 14. Scanning electron microscopy (SEM) micrographs of contour feathers from dorsal tract of the eastern screech owl59

Figure 15. Scanning electron microscopy (SEM) micrographs of contour feathers from femoral tract of the eastern screech owl.....60

Figure 16. Scanning electron microscopy (SEM) micrographs of contour feathers from humeral tract of the eastern screech owl61

Figure 17. Scanning electron microscopy (SEM) micrographs of contour feathers from medial pectoral tract of the eastern screech owl62

Figure 18. Transmission electron microscopy (TEM) micrograph (3000x) of the distal region of a rufous eastern screech owl dorsal feather barb and barbule63

Figure 19. Structure of eumelanin and pheomelanin71

Figure 20. The biochemical pathway for eumelanin and pheomelanin72

Figure 21. Rate reactions for beginning intermediates in pheomelanin and eumelanin production72

Figure 22. Average mean breaking force (N) and standard deviation for eastern screech owl dorsal barbs78

Figure 23. Average breaking stress (N mm⁻²) and standard deviation for eastern screech owl dorsal barbs78

Figure 24. Average cross-sectional area (mm²) and standard deviation for eastern screech owl dorsal barbs79

CHAPTER 1

COLOR POLYMORPHISM AND THE EASTERN SCREECH OWL

INTRODUCTION

Color polymorphism in birds is the existence of two or more distinct plumage colors in one species regardless of age, sex, or mass (Roulin 2004a). In Aves, color polymorphism is most common in Strigiformes (owls, 81%) and Caprimulgiformes (nightjars, 34%) but is also present in 61% of the other orders and 3.5% of all avian species (Fowlie and Kruger 2003; Galeotti et al. 2003). Since the early works of Huxley (1955) and Mayr (1963) researchers have attempted to demonstrate the maintenance of color polymorphism in nature (Van Valen 1965; Willson 1969; Soule and Stewart 1970; Johnson and Brush 1972; Paulson 1973; Baker 1974; Needham 1974; Endler 1978; Preston 1980; Wunderle 1981; Cooke et al. 1988; Bretagnolle 1993; Galeotti and Cesaris 1996; Hughes et al. 2001; Price and Bontrager 2001; Theron et al. 2001; Lank 2002; Fowlie and Kruger 2003; Galeottie et al. 2003; Mundy et al. 2003; Mundy and Kelly 2003; Niecke et al. 2003; Roulin et al. 2003; Roulin and Dijkstra 2003; Galeotti and Rubolini 2004; Roulin 2004a; Brommer et al. 2005; Brito 2005; Bond and Kamil 2006; Py et al. 2006; Roulin 2006). Despite this extensive literature, the maintenance of color polymorphism is still incompletely understood. Here I introduce evolutionary theories on color polymorphism, a review of color polymorphism in owls, and finally a broad review of research conducted on the maintenance of color polymorphism and clinal variation in eastern screech owls.

One hypothesis for the production and maintenance of a color polymorphism is apostatic selection or the avoidance-image hypothesis (Paulson 1973; Galeotti et al. 2003; Fowlie and Kruger 2003). Apostatic selection or avoidance-image hypothesis suggests that if a new and rare color morph emerges in a species, the morph will have an advantage in hunting and crypsis because prey and predators would have low visual recognition of the new morph (Paulson 1973). Because the rare morph has an advantage at capturing food, the morph should persist until equilibrium has been established. Paulson (1973) stated that a requirement of apostatic selection is high prey turnover. The prey may become accustomed to the new predator morph if the prey has a low turnover. The intelligence and visual acuity of prey species may be positively correlated with color polymorphism (Galeotti et al. 2003).

Fowlie and Kruger (2003) reviewed literature on birds of prey to determine if there is support for the predictions of apostatic selection. First, this hypothesis predicts an increase in color polymorphism in predators hunting birds and mammals because these two prey items are primarily vision oriented. Secondly, an increase in color polymorphism in migratory species may be observed since the predators would be taking advantage of different prey populations and no one single population would become used to a new color morph. The effects of population size and life history traits that correlate with color polymorphism in predatory birds were also reviewed. Fowlie and Kruger (2003) found no support for the apostatic selection hypothesis; color polymorphism did not correlate with any foraging variables. In a more recent review, Roulin and Wink (2004) found that color polymorphic raptors are more likely to prey on mammals compared to color monomorphic raptors. A large world population size seems to be the most important factor correlated with plumage polymorphism, probably because larger population sizes exhibit higher phenotypic variation

(Fowlie and Kruger 2003). Additional variables positively correlated with color polymorphism, including sexual plumage dimorphism, reproduction rate, migration pattern, niche breadth, and range size (Fowlie and Kruger 2003). Color polymorphism was negatively correlated with habitat productivity, and incubation-fledgling period.

Galeotti et al. (2003) reviewed the literature of all color polymorphic bird species and found no link between color polymorphism and apostatic selection. Color polymorphism is positively correlated with terrestrial species that occupy four or more habitats, nomadic species, and species with crepuscular habits (Galeotti et al. 2003). Vegetarian species of birds display higher frequencies of color polymorphism than predator species, which is in disagreement with apostatic selection (Galeotti et al. 2003). Birds with both nocturnal and diurnal habits displayed the highest color polymorphism suggesting that plumage dimorphism may be associated with light abundance (Galeotti et al. 2003).

Another hypothesis proposed to account for the persistence of color polymorphism in nature is the niche variation hypothesis (Van Valen 1965; Galeotti et al. 2003; Galeotti and Rubolini 2004). Niche variation is driven by disruptive selection (Schluter 2001). Disruptive selection occurs when an environmental pressure is placed on a unimodal color population leading to a bimodal distribution with each extreme color morphs being selected positively (Dale 2000; Galeotti and Rubolini 2004). A strong disruptive force lead may to higher levels of phenotypic variation (Schluter 2001). A prerequisite of disruptive selection is a large species pool or population size (Fowlie and Kruger 2003). Species with broad habitats would conceivably have an increased diversity of habitats to exploit. If a single species began utilizing different habitats and experienced separate ecological pressures then color polymorphism could be positively selected. Examples of ecological pressures include

competition leading to displacement (Grant and Grant 2003), environmental change (Avisé and Walker 1998; Brito 2005), or predation promoting crypsis (Huxley 1955; Bretagnolle 1993).

Niche variation was disputed by Willson (1969) and Soule and Stewart (1970). Willson (1969) could not find increased variation in morphological features in northern temperate and tropical lowland passerines. Soule and Stewart (1970) refuted niche variation on the basis that they could not find a difference in the variation of beak sizes of birds with broad diets vs. birds with narrow diets. However, Galeotti and Rubolini (2004) found species of greater polymorphism tended to inhabit wide niches. Furthermore, Galeotti and Rubolini (2004) argue that niche variation is a more parsimonious evolutionary explanation than apostatic selection because a bird can exploit a new habitat through genetic variation rather than being dependant on a predator or prey item being unable to recognize that new morph. Many individual color polymorphic species have also been studied.

In addition to the eastern screech owl, the barn owl (*Tyto alba*) and tawny owl (*Strix aluco*) serve as models for studying color polymorphism. Barn owl coloration can vary in melanin type, eumelanin or pheomelanin, and also amount of eumelanic spots (Roulin 2004a). There is evidence of barn owls exhibiting assortative mating based on coloration in Switzerland (Roulin 1999) but not in Hungarian races (Matics et al. 2002). Barn owls with higher degrees of eumelanic spots tend to have higher calcium levels (Roulin et al. 2006), do not preen as often (Roulin 2007), and females tend to breed earlier and have higher brood survival rates (Roulin and Altwegg 2007). Plumage coloration may also covary with diet in the barn owl (Roulin 2004b).

DNA evidence supports the hypothesis that color polymorphism arose in tawny owls in three allopatric groups during the Pleistocene glaciations (Brito 2005). It is thought that the allopatric groups of the tawny owl supposedly returned to a sympatric distribution and color polymorphism was maintained. While there is no evidence for environmental factors maintaining clinal variation in the tawny owl in Italy (Galeotti and Cesaris 1996), gray morphs tend to have higher survivorship than rufous morphs (Brommer et al. 2005), and have lower parasite loads (Galeotti and Sacchi 2003), yet rufous morphs have also produced higher quality chicks in experimentally reduced broods (Roulin et al. 2008).

The eastern screech owl, *Megascops asio* (Banks et al. 2003), displays color polymorphism (Hoffman 1931; Kelso 1938; Johnsgard 1988; Gehlbach 1994). Principle color morphs observed in the eastern screech owl are rufous and gray, and the two morphs exhibit clinal variation (Figure 1) (Gehlbach 1994; Dexter 1996). A low frequency of brown intermediates, which is a mix of gray and rufous pigments, also exists (Owen 1963a, 1963b). Persistence of color polymorphism in the eastern screech owl is related to several factors as illustrated below: 1) genetics (Hrubant 1955; Proudfoot et al. 2007), 2) physiology (Mosher and Henny 1976; Dexter 1996), 3) behavior (Dexter 1996), 4) environmental conditions (Gehlbach 1994), and 5) morphological variations (Gehlbach 2003).

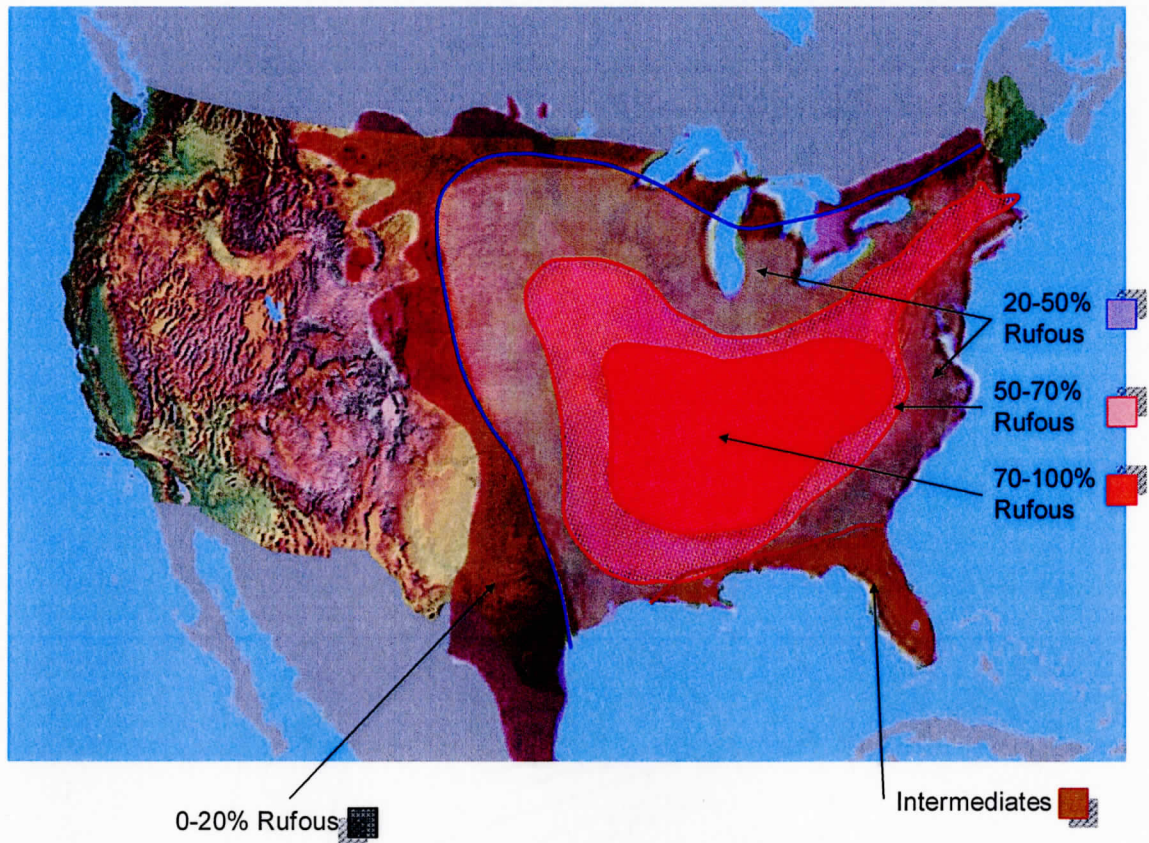


Figure 1. Frequency of rufous eastern screech owls in North America (adapted from Dexter 1996).

Genetics:

Phenotype is not inherited as a simple Mendelian trait in the eastern screech owl. Gray coloration is usually recessive to rufous in some areas and analysis of color in clutch suggests the presence of a multiple allelic system (Hrubant 1955). There are two main explanations for the morphs: 1) that one gene has two alleles, with brown under control of another gene, or 2) that one gene has three alleles accounting for all three morphs (Hrubant 1955).

Variation in the mitochondrial cytochrome b gene within the eastern screech owl is low (Proudfoot et al. 2007) and is not consistent with the current subspecies' standing (Gehlbach

2003). Four of five recognized subspecies share six out of seven haplotypes. The subspecies in Mexico (*M. a. mccallii*) differed by 4% from all others and was unique (Proudfoot et al. 2007).

Physiology and Behavior:

Climatic episodes could affect the distribution of alleles of the eastern screech owl if there is differential mortality rate of the color morphs under intense cold weather. Several physiological differences between color polymorphic birds have been reviewed by Roulin (2004a). Mosher and Henny (1976) found different oxygen consumption for morphs at different temperatures. The rufous owl had a higher metabolic rate at -5°C . At 30°C the rufous morph still had a higher O_2 consumption than the gray morph, but the difference was not as great (Mosher and Henny 1976; Daniels and Duke 1980; Lohrer 1985; Dexter 1996). Rufous morphs erect their feathers at a higher temperature than the gray morph (Dexter 1996). The gray morph reflects less light, and their body temperature increases much faster than the rufous morph (Cena and Monteith 1975a, 1975b; Dexter 1996). Gray eastern screech owls are more efficient than rufous morphs at basking due to lower radiant energy being reflected from their bodies (Dexter 1996). Rufous owls in northern Ohio had greater mortality rate in colder than normal winters than the gray morphs (VanCamp and Henny 1975). Higher winter mortality and a higher O_2 consumption have also been observed in rufous morphs of ruffed grouse (Gullion and Marshall 1968). The increased demand for nutrition required to sustain rufous owls in cold weather might account for a decreased rufous morph frequency in the northern part of the species range and could explain the higher rufous morph frequencies in areas of high *Peromyscus* density in Pennsylvania (Olson and Mooney 2001).

Other differences between the rufous and gray morph of the eastern screech owl have also been described. Screech owls have symmetrical ears (personal observation) and cannot

hear prey in thick grass or snow (Dexter 1996). Brittan-Powell et al. (2005) described variation in the hearing sensitivity of the color morphs. Rufous morphs have greater sensitivity and a lower threshold to auditory stimuli. The increased sensitivity in the rufous morph could enhance prey detection and allow them to outcompete the gray morphs for food resources in the center of the species range.

Environmental Conditions:

Gehlbach (1994) examined the effects of rainfall, temperature, humidity, and geographical location on the eastern screech owl in Texas. Gehlbach (1994) was interested in why the rufous morph persisted in nature as they were more brightly colored and should be more susceptible to predation. He concluded that rufous morphs are harder to see in rain or high humidity due to red wavelengths being more easily scattered by water (Cena and Monteith 1975c). Precipitation rates do increase from the northern range to the middle range, correlating to rufous morph density, although precipitation rates are the same from the middle of the owls' range into the southern range where the gray morph begins to predominate again. Rufous morphs persist in times of 'climatic minimums' or an absence of extreme cold (Gehlbach 1995). In the western range rufous morph concentration does not correlate with rainfall except in suburban areas, where humidity and warmth are thought to be greater and are associated with a higher density of rufous morphs. There is mixed support for the argument that clinal variation influences variation in color morphs of the eastern screech owl.

Objectives:

The purpose of this thesis was to investigate possible differences in feather morphology of eastern screech owl color morphs that may affect the thermal efficiency or

strength of plumage. Light and electron microscopy will be used to investigate the feathers of the gray and rufous morphs of the eastern screech owl in order to describe the macro- and microscopic characteristics of plumage. GIS techniques will be applied to existing eastern screech owl color morph data to elucidate land composition with color morph frequency. Effect of coloration on tensile strength of feathers across the color variant gradient will be examined to determine if melanin subtype contributes to differential strength.

CHAPTER 2
GIS ANALYSIS OF EASTERN SCREECH OWL COLOR VARIANT CLINAL
VARIATION

INTRODUCTION

There have been few attempts to create a distribution map of eastern screech owl color variants (Hasbrouck 1893a, 1893b; Owen 1963a, 1963b; Dexter 1996). Much of the available data on eastern screech owls ignores color phases. Hasbrouck (1893a, 1893b) conducted the first of such studies and found that gray morphs are more abundant in areas of high and low temperature extremes, gray morphs predominate in humid areas, and rufous morphs predominate in forests of deciduous trees while gray morphs predominate in forests of coniferous trees. However, as Hasbrouck's (1893a, 1893b) analysis was conducted over a century ago, changes in land use and morph frequency may have changed drastically. Owen (1963a, 1963b) revised the relationship between land use and morph frequency using 1,320 museum specimens of the eastern screech owl. His results supported Hasbrouck's (1893a, 1893b) analysis that gray morphs are more abundant in areas of temperature extremes; however, he found no evidence that gray morphs are more abundant in areas of higher humidity. Subsequent analyses demonstrate that the rufous morph predominates in areas of high humidity in Texas (Gehlbach 1994). Dexter (1996) provided the most recent investigation on eastern screech owl color variant distribution and his results were compatible with Owen's (1963a, 1963b). However, all the above analyses were performed using handwritten maps. The correlations made between eastern screech owl color morph

frequency and environmental and land cover variables could be more accurate by using GIS analysis.

The purpose of the present study is to use ArcGIS 9.2 software to compile maps of eastern screech owl color morph frequency overlaid with USGS 200m land cover data. Eastern screech owl data were compiled from Dexter (1996) and additional data was received from the Blue Ridge Raptor Rehabilitation Center (BRRC), Carolina Raptor Center (CRC), the Audubon Society of Florida, Olson and Mooney (2001), DeCandido (2005), and North Carolina Museum of Natural History (NCSM). States were chosen from the extreme parts of the eastern screech owl distribution.

By utilizing GIS data layers to compile eastern screech owl habitat maps, the results should theoretically be less prone to researcher bias. Previous maps were either handwritten or used overlays done by hand. The power of GIS is that standardized map layers can be downloaded and reproducibility of results greatly increases. A compilation of eastern screech owl color morph data and modern land cover data can offer new insight into correlations between land cover and color morph abundance.

MATERIALS AND METHODS

Analytical Geographical Information System (GIS) maps were compiled in ArcGIS 9.2 software for visual geospatial distribution models and descriptive summaries of landscape composition associated with *Megascops asio* color morph frequency (Environmental Systems Research Institutes [ESRI] 2005). Color morph data were collected from a number of published papers (Hasbrouck 1893a, 1893b; Schorger 1954; Hrubant 1955; Burleigh 1958; Owen 1963a, 1963b; Stupka 1963; Bull 1964; VanCamp and Henny 1975; Duley 1979; Fowler 1985; Gehlbach 1994, 1995, 2003; Pittaway 1995; Dexter 1996; Olson and Mooney 2001; DeCandido 2005; AMNH 2006; Audubon 2006; NCSM 2006), and also the Carolina Raptor Center (CRC), North Carolina Museum of Natural History (NCSM), the Audubon Society of Florida and North Carolina (Audubon), the American Museum of Natural History, and the Blue Ridge Raptor Rehabilitation Center (BRRC). A 200m land cover layer was obtained from the U.S. Geologic Survey (USGS) seamless data distribution (USGS 2007). A political county boundary data layer was obtained from the GIS data depot (GIS 2007).

State maps were compiled for Vermont (VT), North Carolina (NC), New Jersey (NJ), Kansas (KS), South Carolina (SC), Kentucky (KY), Tennessee (TN), and Alabama (AL). The above states were chosen based on the quality of available color morph data and to give a representation of the central and peripheral parts of the eastern screech owls range. The land cover layer from the USGS seamless data distribution are downloaded as a Raster tile, mosaiced as a new Raster, viewed and exported to visible extent of state political boundaries.

Because land cover data is downloaded as large squares, excess portions of the land cover layer is eliminated by viewing the land cover layer to the extent of state political boundaries. The political county boundary layer was downloaded as a polygon. Screech owl color morph data were compiled in an Excel spreadsheet and joined onto the shapefile of state counties.

Zonal statistics under the spatial analyst tab were performed in ArcGIS to determine the majority of land cover in counties with available color morph data. In the present study, the zone was defined as a group of counties with a similar rufous frequency (i.e. 70-100% rufous) and the value layer was the 200m land cover layer. For each defined zone (counties) the value layer (land cover) was used to give an output of majority of land cover squares contained within each county. The majority of land cover can offer insight into what types of habitats eastern screech owl color morphs tend to congregate.

RESULTS

The zonal majority statistics of the USGS 200m land cover data and eastern screech owl color morph density (Table 1) mirrored previously published data (Hasbrouck 1893a, 1893b; Owen 1963a, 1963b; VanCamp and Henny 1975; Gehlbach 1995; Dexter 1996). Areas that tended to have high rufous density were likely to consist mainly of deciduous forest while an increasing gray density coincided with increasing mixed and evergreen forest (Figure 2-9). In Kansas, the rufous density increased with the appearance of cultivated crops; however, total screech owl density was lower towards the Midwest grasslands (Sutton 1986; Fitton 1993).

Table 1. Majority zonal statistics of 200m United States Geological Survey (USGS) land cover data and rufous eastern screech owl density.

US Region	State	Rufous %	Majority
Northeast	VT	0-20	Deciduous Forest Some Mixed Forest
		20-50	Deciduous Forest
	NJ	20-50	Mixed Forest Some Developed Open Space
50-70		Deciduous Forest Developed Open Space	
Southeast	NC	20-50	Cultivated Crops Palustrine Forested Wetland
		50-70	Deciduous Forest Some Evergreen Forest
		70-100	Deciduous Forest
	SC	20-50	Evergreen Forest Cultivated Crops
		50-70	Evergreen Forest
		70-100	Deciduous Forest
	AL	50-70	Mixed Forest
		70-100	Deciduous Forest Some Mixed Forest
		Intermediate	Evergreen Forest Mixed Forest
	KY	70-100	Deciduous Forest Pasture/Hay Cultivated Crops
TN	70-100	Deciduous Forest Cultivated Crops	
Midwest	KS	0	Grassland
		0-20	Grassland
		20-50	Pasture/Grassland
		50-70	Pasture/Cultivated Crops

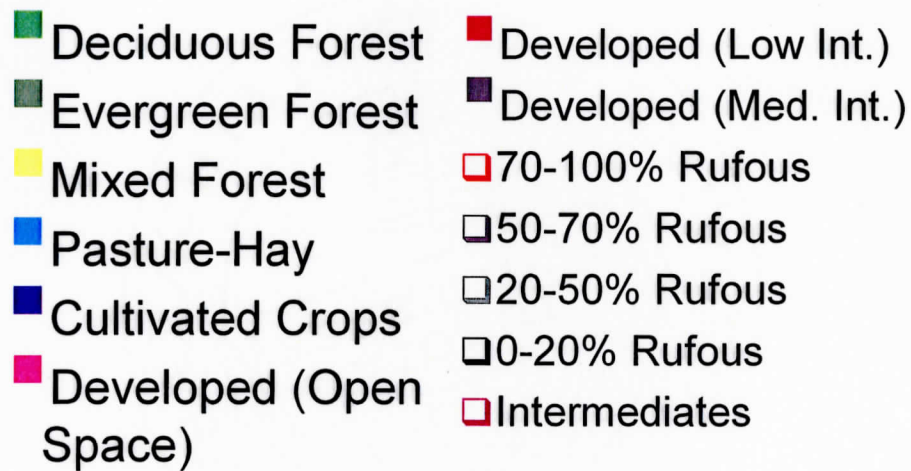
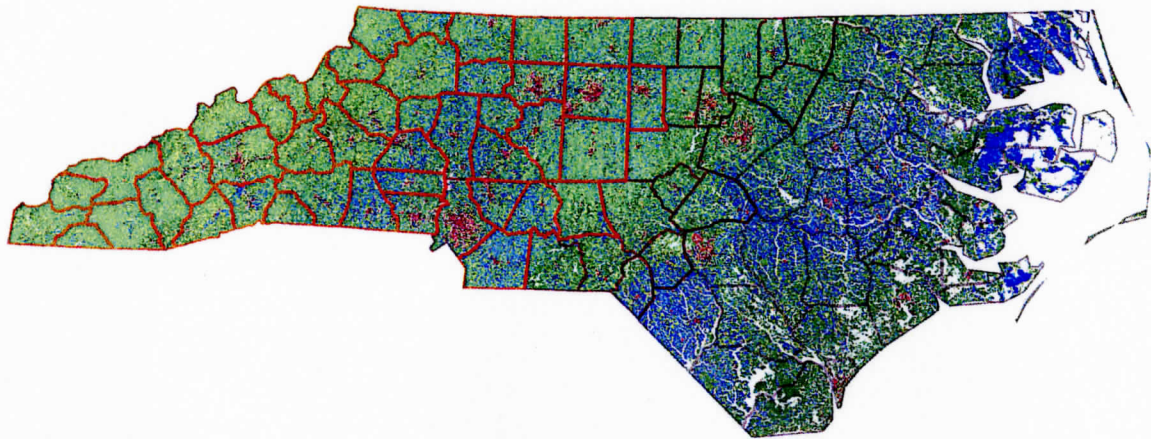


Figure 2. United State Geological Survey (USGS) 200m land cover (solid colors) and rufous screech owl density (outlined in color by county) for counties in North Carolina.

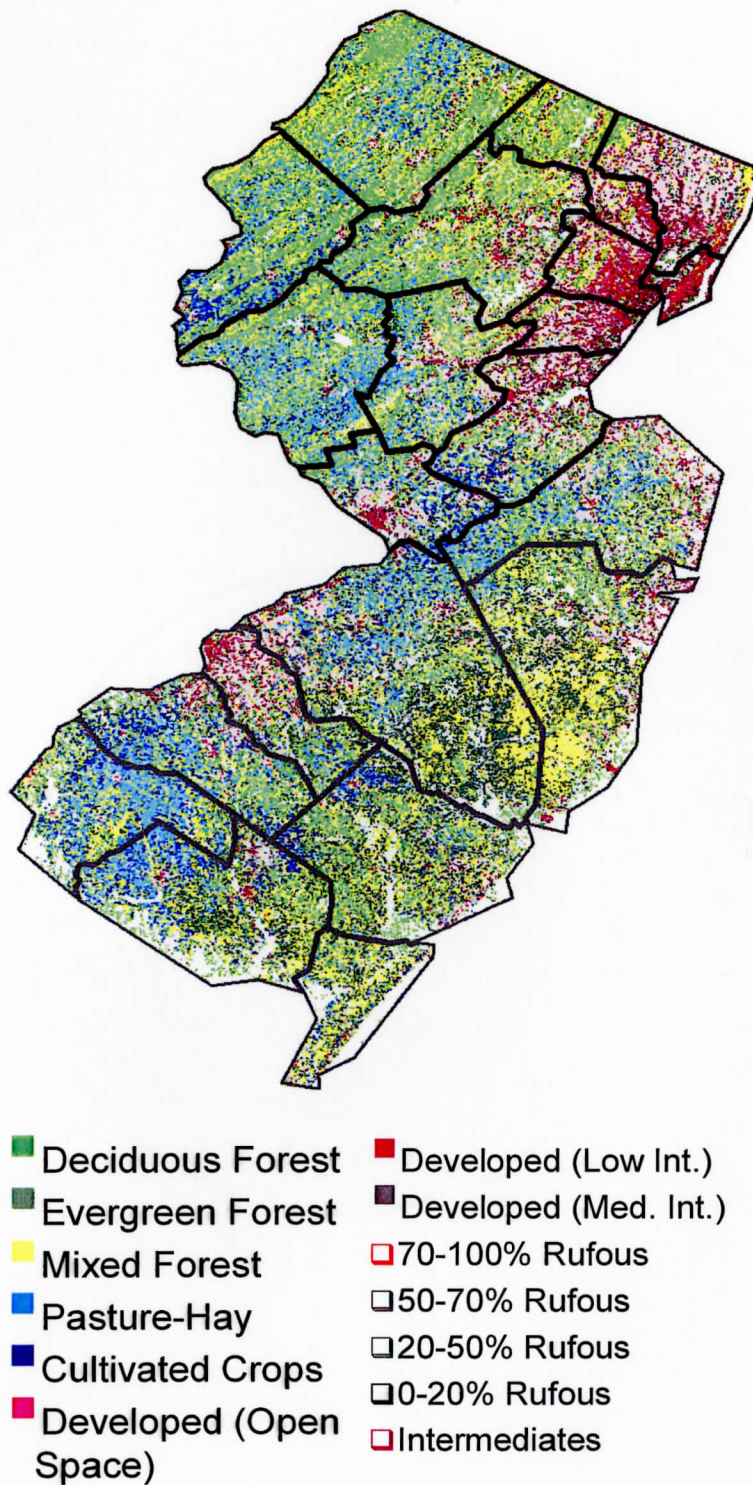


Figure 3. United State Geological Survey (USGS) 200m land cover (solid colors) and rufous screech owl density (outlined in color by county) for counties in New Jersey.

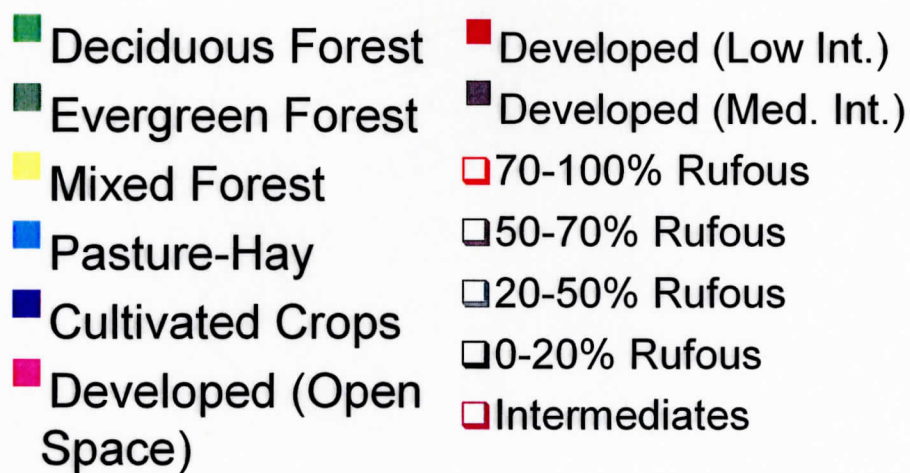
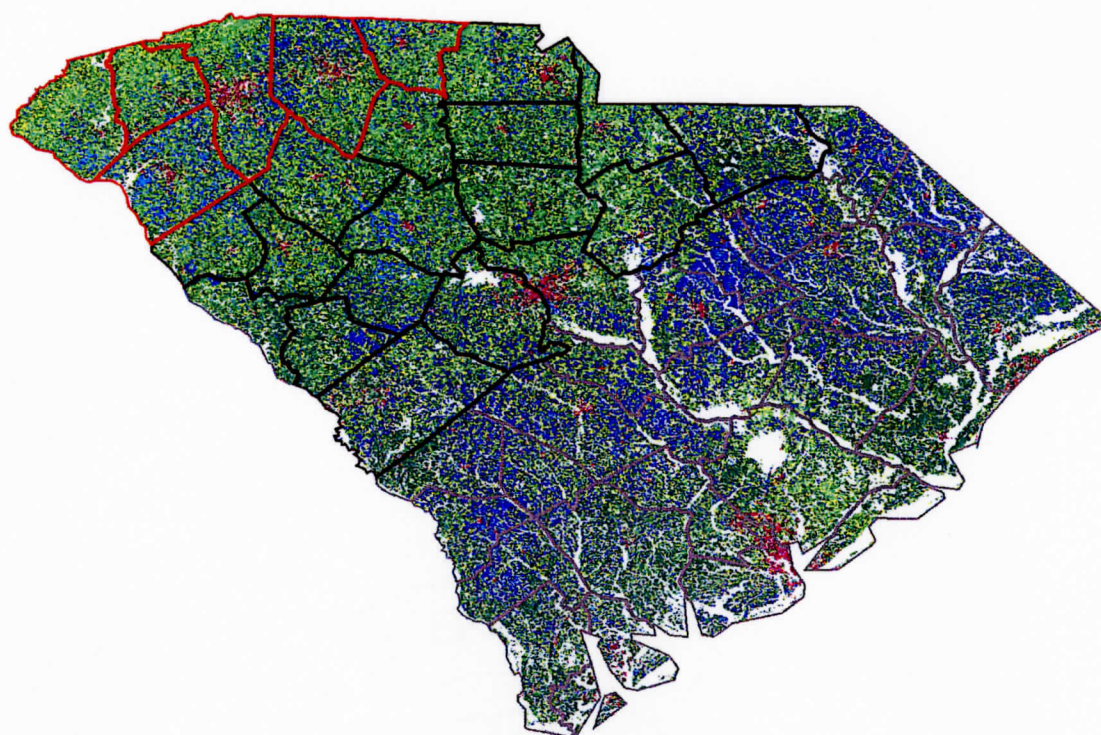


Figure 4. United State Geological Survey (USGS) 200m land cover (solid colors) and rufous screech owl density (outlined in color by county) for counties in South Carolina.

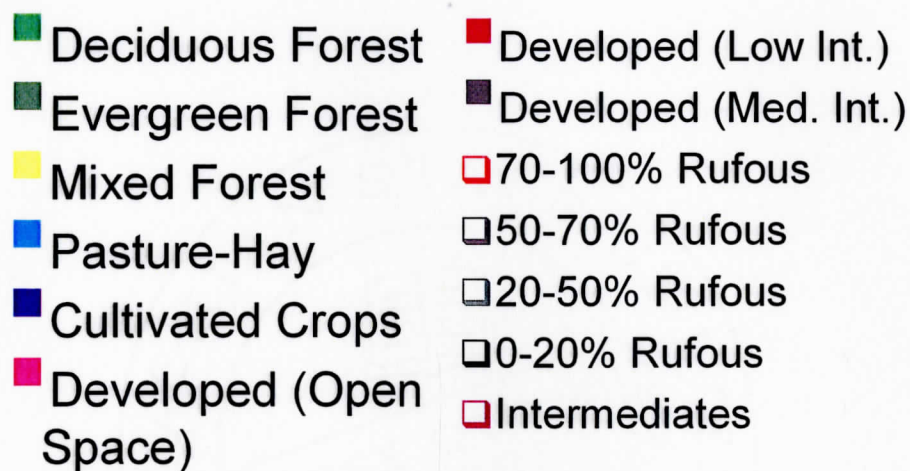
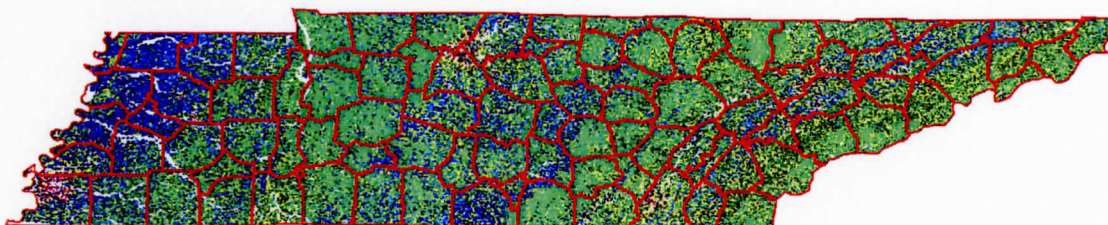


Figure 5. United State Geological Survey (USGS) 200m land cover (solid colors) and rufous screech owl density (outlined in color by county) for counties in Tennessee.

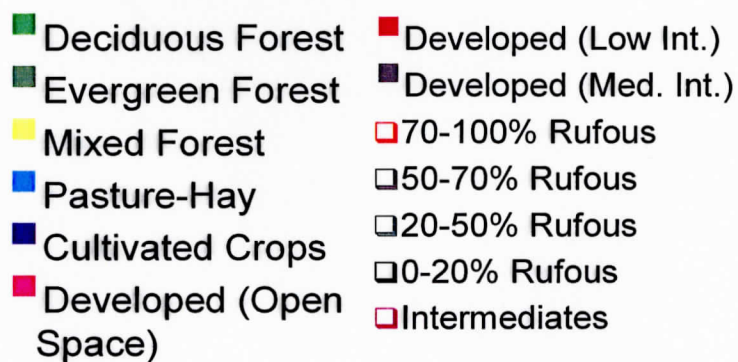
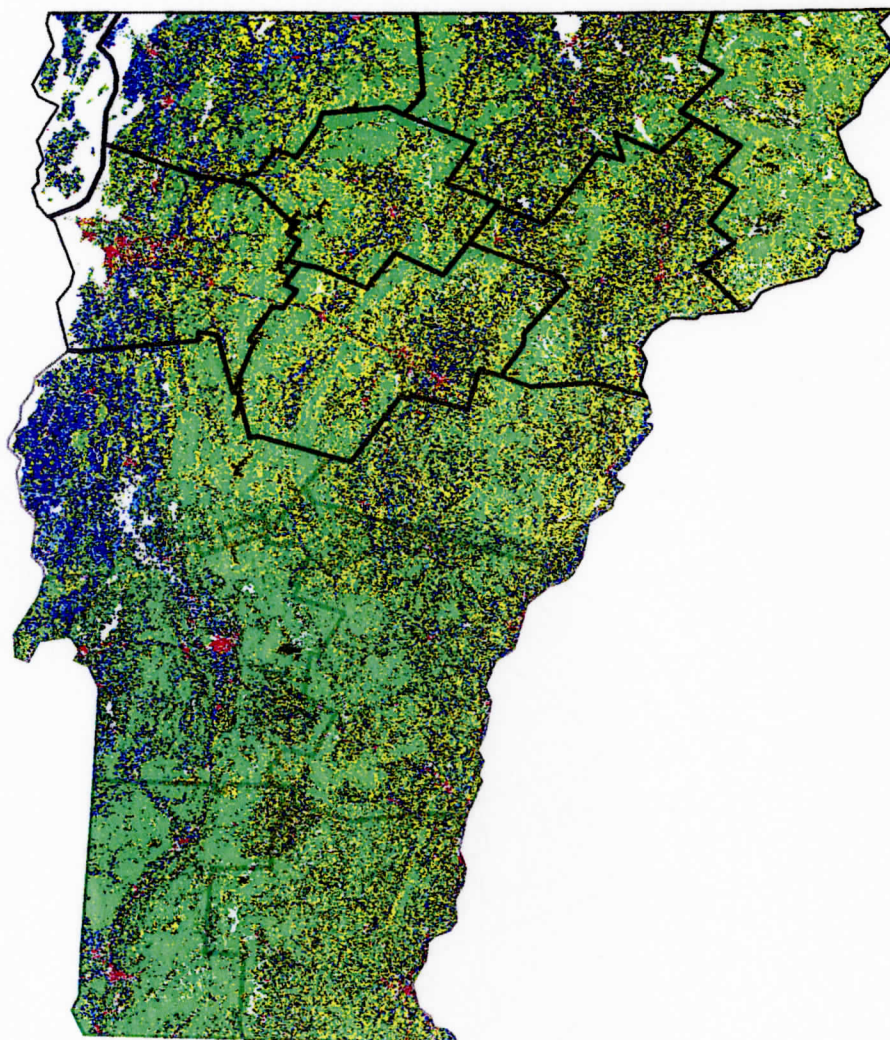


Figure 6. United State Geological Survey (USGS) 200m land cover (solid colors) and rufous screech owl density (outlined in color by county) for counties in Vermont.

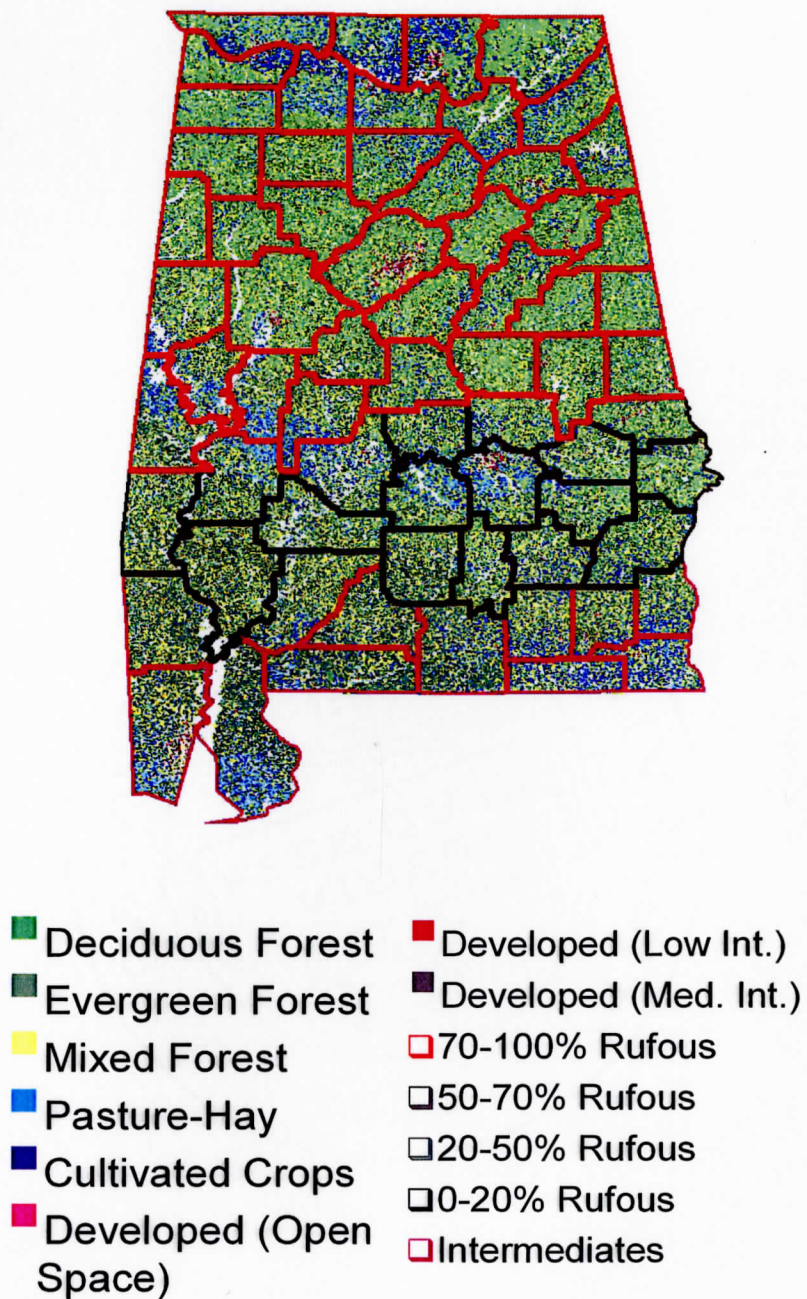


Figure 7. United State Geological Survey (USGS) 200m land cover (solid colors) and rufous screech owl density (outlined in color by county) for counties in Alabama.

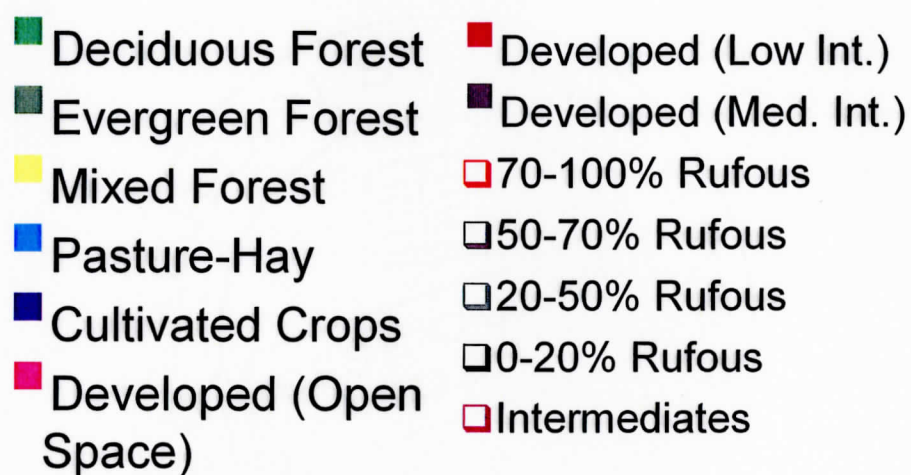
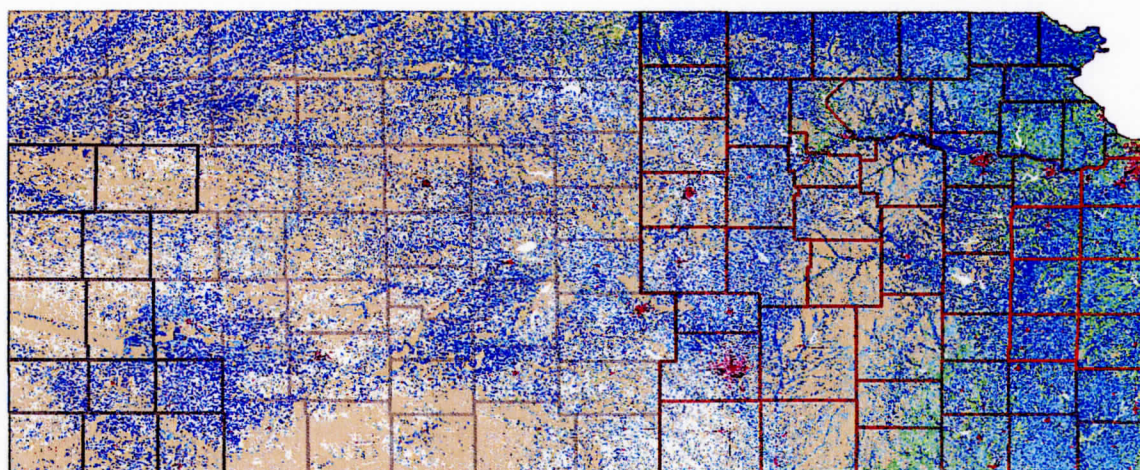


Figure 8. United State Geological Survey (USGS) 200m land cover (solid colors) and rufous screech owl density (outlined in color by county) for counties in Kansas.

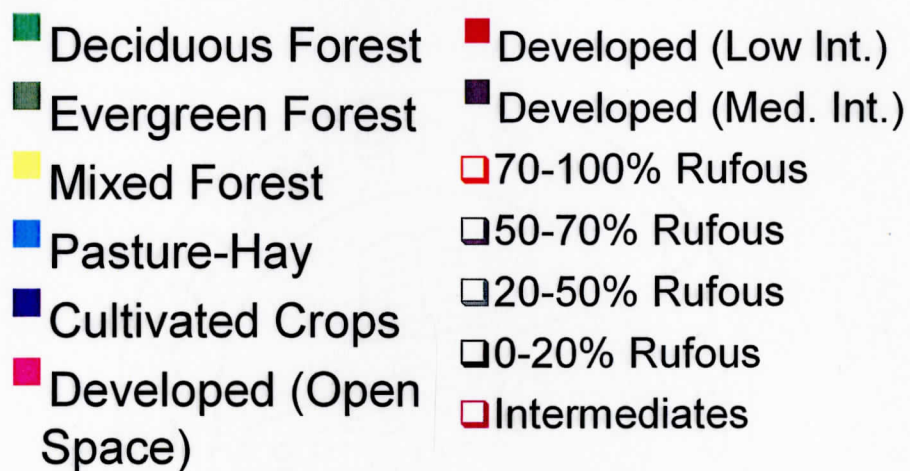
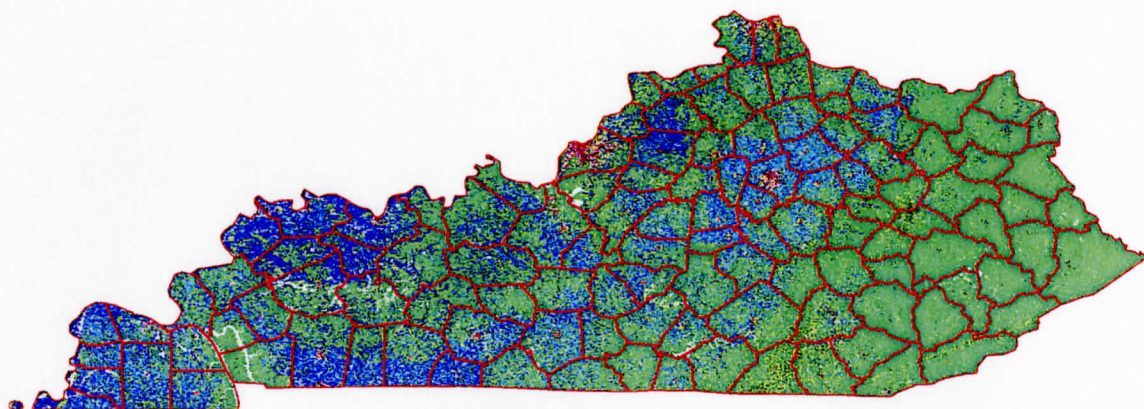


Figure 9. United State Geological Survey (USGS) 200m land cover (solid colors) and rufous screech owl density (outlined in color by county) for counties in Kentucky.

DISCUSSION

The GIS land cover majority zonal statistics exhibited patterns that have been previously reported by other researchers (Hasbrouck 1893a, 1893b; Owen 1963a, 1963b; VanCamp and Henny 1975; Gehlbach 1995; Dexter 1996). The eastern screech owl inhabits many types of land cover from suburban to rural habitats (Smith and Gilbert 1984; Sparks et al. 1994; DeCandido 2005; Richards et al. 2006; Proudfoot et al. 2007). Lower rufous frequencies linked with the presence of evergreen and mixed forest while higher rufous frequencies associated with forests dominated by deciduous trees except in northern habitats. Rufous morphs mortality is higher in cold temperature than gray morphs, hence the gray morphs dominate in northern climates (VanCamp and Henny 1975; Mosher and Henny 1976; Dexter 1996), which may influence results in Vermont where there was a majority of deciduous forest in the counties with the lowest rufous frequency (0-20%). In Kansas, grasslands, pastures, and cultivated crops dominated the landscape. However, total screech owl density is lower in the Midwest because eastern screech owl prefers forest edges and limbs approximately twelve feet high for hunting purposes and have home ranges of ~50 ha (Smith and Gilbert 1984; North 1985; Belthoff and Ritchison 1989, 1990; Belthoff et al. 1993; Dorn and Dorn 1994; Klatt and Ritchison 1994; Sparks et al. 1994; Belthoff and Dufty 1998; Buhay and Ritchison 2002). Rufous morphs seem to dominate in 'prime' screech owl habitats while gray morphs dominate in apparently suboptimal habitats (Dexter, personal communication), but the reason for this pattern is unclear.

The above GIS analysis data should be interpreted with caution because the screech owl data were gathered from over a century of published papers. Human activity has drastically changed the nature of the American landscape since the earliest papers on color polymorphism in screech owls (Hasbrouck 1893a, 1893b) and color morph frequencies may have changed. Unfortunately, many publications on the eastern screech owl ignore color morphs (Sparks et al. 1994) or owl density (Fitton 1993). A current study on eastern screech owl color morph frequency coupled with owl density and possible correlations with landscape composition and environmental factors would be of great interest to any researcher interested in color polymorphism.

CHAPTER 3

MACRO- AND MICROSTRUCTURAL ANATOMY OF EASTERN SCREECH OWL FEATHERS

INTRODUCTION

The microstructural anatomy of feathers has been extensively studied (Mascha 1905; Chandler 1916; Sick 1937; Lucas and Stettenheim 1972). Mascha (1905) wrote one of the first detailed papers on feather anatomy and included hand drawn illustrations of feathers. More recently, Chandler (1916) and Brom (1986) used descriptive feather anatomy to study taxonomic relationships. Sick (1937) extended anatomical descriptions in his doctoral thesis, but a consistent terminology for avian integumentary anatomy was not established until Lucas and Stettenheim (1972). Researchers still use microscopic analysis of feather anatomy to elucidate avian evolutionary relationships (Prum and Brush 2002).

Research also focuses on how feather microstructure relates to the function of feathers (Shawkey et al. 2003, 2006a, 2006b). One use of feathers is thermoregulation. Downy feathers and the plumulaceous region of contour feathers lack hooklets and phalanges, and reinforce insulation by creating pockets of dead air near the skin (Stettenheim 2000). Birds can control thermoregulation by allowing heat to escape through piloerection of contour feathers (Stettenheim 2000). Contour feathers vary greatly in morphology (Lucas and Stettenheim 1972). If these feathers vary at the macro- and microstructural level in the eastern screech owl morphs the effectiveness in insulation could also vary. Differences in the anatomy of eastern screech owl color variant feathers have not been studied.

The purpose of the present chapter is to describe the anatomy of eastern screech owl contour and downy feathers and compare the morphology according to color. Light microscopy will be utilized to compare lengths of the rachis, barb, and barbules morphological dimensions, SEM will be utilized to describe the nodal features of the eastern screech owl barbules, and TEM will be used to describe the cross section of feather barbs. By describing the anatomy of the eastern screech owl plumage, differences between color variants that may impact the owls' clinal variation can be elucidated and also differences between the eastern screech owl and other species in the order Strigiformes can be used for future taxonomic study.

MATERIALS AND METHODS

Owl Collection:

Frozen eastern screech owls were obtained from the Blue Ridge Raptor Rehabilitation Clinic, the American Museum of Natural History, Audubon Society of Florida, North Carolina Museum of Natural History, and the Avian and Exotic Animal Clinic of Indianapolis. Taxidermy specimens were obtained from the North Carolina Museum of Natural History and the Appalachian State University collections. Feathers removed from frozen specimens were used for all experiments. Taxidermy specimens were only used for light microscopy due to the confounding results that could result from using aging study skins for tensile strength tests or TEM. Only owls from NC were used for light microscopy measurements.

Color Score:

Owls used for transmission electron microscopy and tensile strength were laid out on a dissecting tray according to color. Owl color was scored by eye. A digital camera image from a controlled setting was used to check for human error in the visual index (Dale 2000; Montgomerie 2006; Rudh et al. 2007). The picture was opened in Adobe Photoshop 7.0.1, an area of the dorsum was chosen, and the histogram function was used to obtain luminosity and red, green, and blue (RGB) color tristimulus values. One owl was excluded from analysis due to damage to the plumage.

Light Microscopy and Macroscopic Measurements:

Measurements of down and contour feathers were made using a Leica ATC 2000 compound light microscope, an Olympus SZX12 dissecting scope equipped with an Olympus DP10 digital camera, and a WILD Heerbrugg Switzerland dissecting microscope. Four owls from three color categories (gray, brown, rufous) were used for light microscopy. Two feathers were removed from three areas (anterior, posterior, and intermediate) of four pterylae tracts. The down feathers of the femoral tract and contour feathers from the medial pectoral, femoral, humeral, and dorsal tracts were quantified (Figure 10-11). If two contour feathers could not be obtained from a specified area of a pterylae, a down feather was substituted. Feathers were cleaned by vigorously shaking them in a borax solution (~1/3 gram in ~50 ml) followed by shaking in 75% and 95% ethanol respectively according to standard methods (Lucas and Stettenheim 1972). Two barbs were removed from the intermediate plumulaceous region of each feather, fixed to glass slides with double sided tape, and measurements recorded (Figure 12-13, Table 2). Barbs were taken from the left side of the rachis on one feather and the right side of the rachis on the second feather so the data would not be a biased representation of one side of the feather.

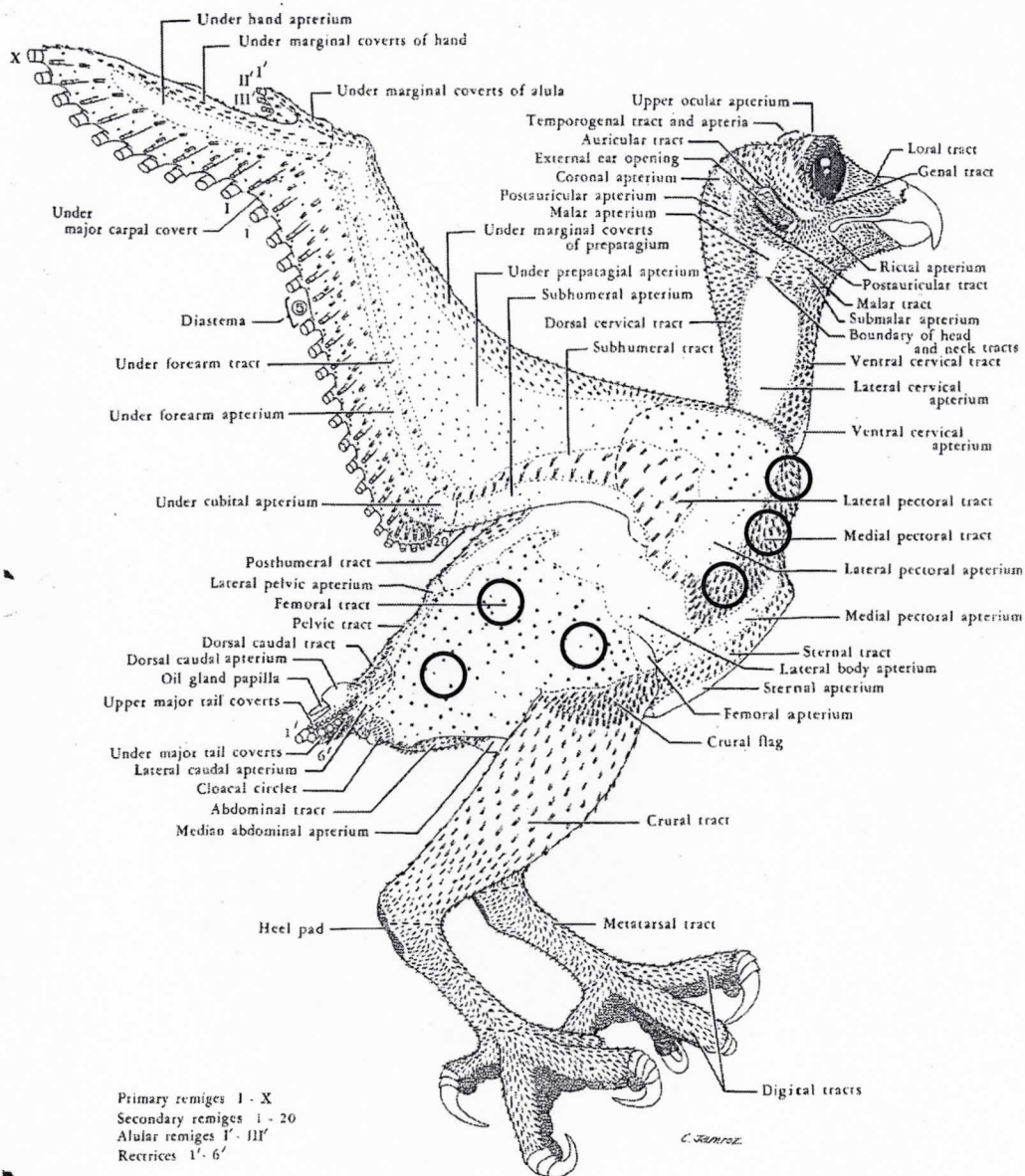


Figure 10. Lateral pterylae of the great-horned owl (*Bubo virginianus*). Feathers were removed from areas with bolded circles (modified from Lucas and Stettenheim 1972).

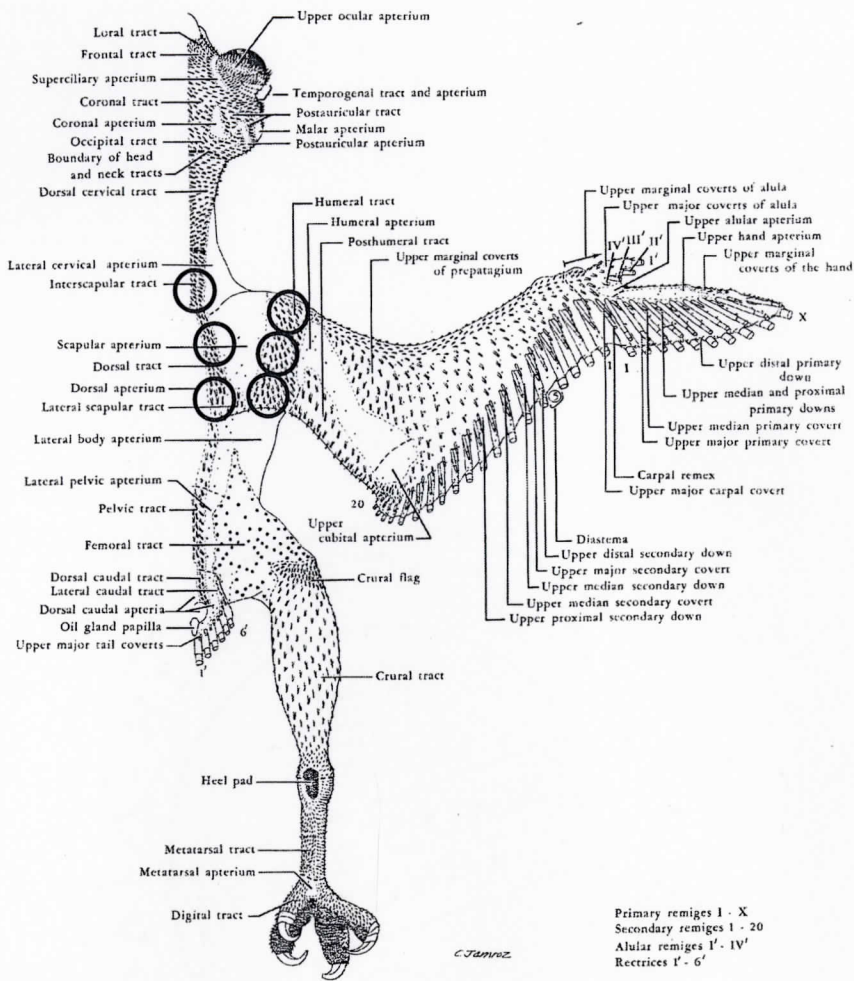


Figure 11. Dorsal pterylae of the great-horned owl (*Bubo virginianus*). Feathers were removed from areas with bolded circles (modified from Lucas and Stettenheim 1972).

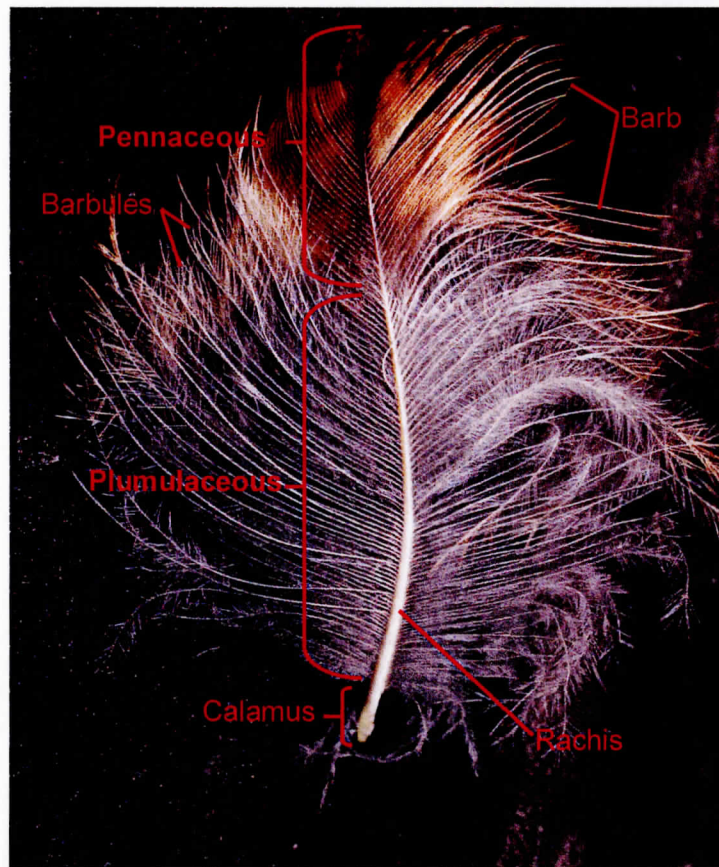


Figure 12. Topographic anatomy of an eastern screech owl dorsal contour feather.

Feather Morphology

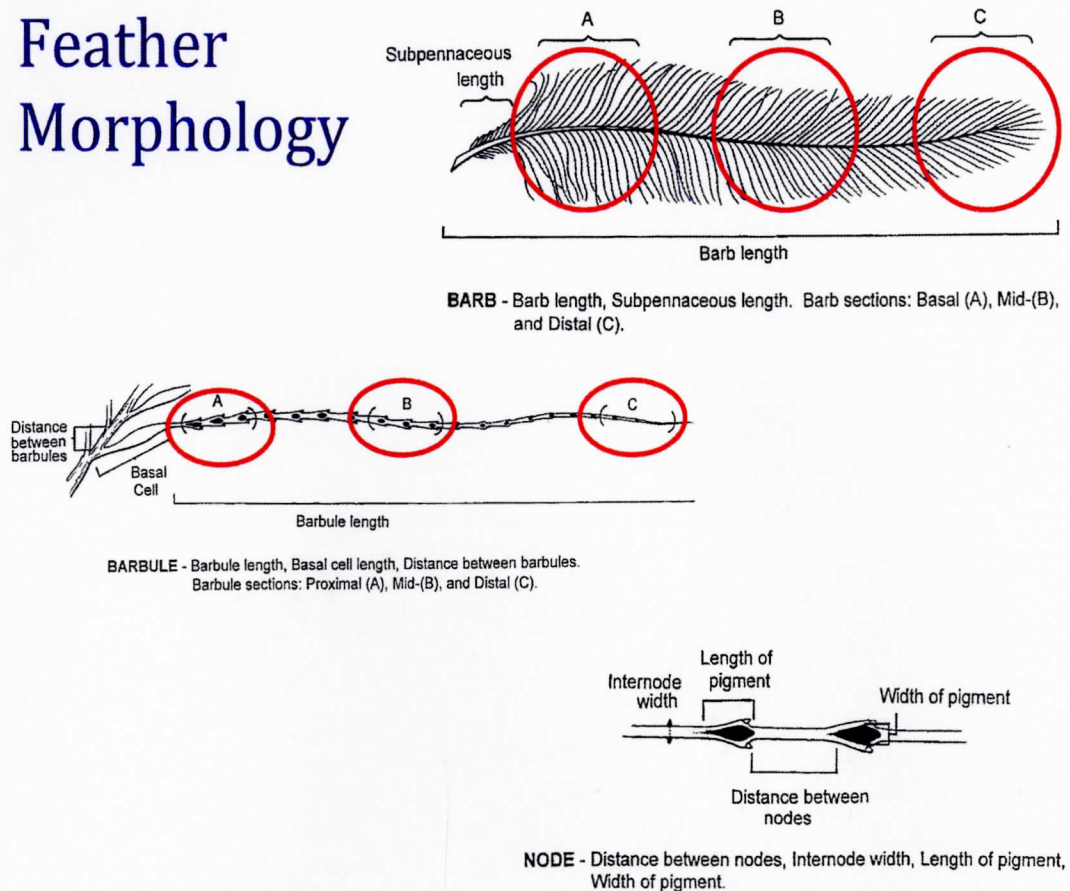


Figure 13. Feather morphology at the barb, barbule, and barbule segment levels (modified from Dove 1997).

Measurements were taken of the bill length (culmen to cere), wing length, tail length, and mass (Table 2). All measurements were compiled in Excel. One way analysis of variance (ANOVA) was used to determine whether birds of different color morphs varied on body, feather, barb and barbule levels and was performed in SAS 9.1 for Windows 2002-2003 (Zar 2005; Cody and Smith 2006). A principle components analysis (PCA) was used to create composite variables and an ANOVA was performed on the principle components (PC) scores for the body and barbule segment (Figure 13) levels (Olvera et al. 2006; Hayashida et al. 2007; Hund et al. 2007; Teodori et al. 2007). The PCA analysis and subsequent ANOVAs

was performed in SAS 9.1 for Windows 2002-2003 (Zar 2005; Cody and Smith 2006). At the barbule segment level, the basal cell of distal barbules could not be measured because, in many cases, cell differentiation could not be observed. Color was the treatment for each level of analyses and the morphological measurements were the independent variables.

Due to the variability and intricacy of feathers, the analyses had to be conducted on multiple levels. The owls chosen for analysis were all from NC and were of similar size. However, need for a precise color gradation limited the overall homogenization of body level measurements. At the feather and barb level, feathers were randomly chosen and were susceptible to great size variability. PCA analysis was performed at both the body and barbule segment levels because multiple variables were highly intercorrelated with each other. Composite scores from the factor analyses on the body and barbule segment levels reduced the chances of a type I statistical error.

Table 2. Levels of analysis of eastern screech owl feather morphological measurements. (p-d=proximal to distal)

Body	Feather and Barb	Barbule	Barbule Segments
Bill Length (mm)	Pennaceous Rachis Length (mm)	Barbule Length (mm)	p-d Nodal Length (μm)
Wing Length (mm)	Pennaceous Barb Number	Basal Cell Length (μm)	p-d Pigment Length (μm)
Tail Length (mm)	Plumulaceous Rachis Length (mm)	Length Between Barbules (μm)	Internode Width (μm)
Mass (g)	Plumulaceous Barb Number	Number of Nodes per Barbule	Spine Length (μm)
	Barb Length (mm)	Number of Pigmented Nodes per Barbule	

Scanning Electron Microscopy:

One feather from the four tracts of a brown intermediate eastern screech owl was prepared for scanning electron microscopy following standard methodology (Bozzola and Russell 1999; Shawkey et al. 2005). The rachis of the intermediate plumulaceous region was removed, attached to a stub with a double sided carbon disc, and sputter-coated with gold. Micrographs were obtained with a FEI Quanta 200 environmental scanning electron microscope (ESEM) of the barb base, barbule base, proximal, intermediate, and distal regions of the barbule. The nodal characteristics of the barbules were described.

Transmission Electron Microscopy:

Samples from the distal one cm of the rachis from two feathers from the dorsal tract of one owl in each of eight color categories were prepared for scanning transmission electron microscopy (STEM) following standard methods (Andersson 1999; Bozzola and Russell 1999; Shawkey et al. 2003). Transmission electron microscopy produces a cross-sectional view of feather barbs so the arrangement of the feather constituents (melanin, keratin layers, etc...) can be determined. Barbs were removed and incubated in 0.25 M NaOH and 0.2% Tween-20 for 30 minutes on an orbital shaker. Barbs were transferred to 2.5% glutaraldehyde in a Na phosphate buffer (pH = 7) and incubated for three days at 4°C. Barbs were washed in Na phosphate buffer (pH = 7) for five minute durations three times and incubated in 2% osmium tetroxide (OsO₄) and Na phosphate buffer (pH = 7) for 16 hours at 4°C. Two Na phosphate buffer (pH = 7) washes were performed for five minutes followed with successive two hour incubations in 50%, 70%, 85%, 95%, and 100% ethanol (EtOH). The barbs were washed twice with propylene oxide for five minutes each and twice with a mix of half propylene oxide and half Spurr's resin for one hour and 12 hours respectively.

The samples were then placed in molds with Spurr's resin and incubated at 65°C for 14 hrs. The molds were sectioned using a Reichert-Jung ultra-cut E ultramicrotome and sections were placed on 50 mesh copper grids.

The distal most portions of the barbs were visualized with a Phillips CM-12 STEM electron microscope ($n = 3-4$ for each sample) at 3,000x and 17,000x. Micrographs of a parallel line diffraction grating replica (Electron Microscopy Sciences) were used for calibration. TEM micrograph negatives were scanned at 600 d.p.i. with a Microtek ScanMaker 8700 scanner and analyzed using AxioVision AC Release 4.3 software. Surface areas of the anterior portion of the barb, cortex, spongy layer, and melanin granules were calculated following Shawkey et al. (2003, 2006a, 2006b). Surface areas of the cortex, spongy layer, and melanin granules were divided by total barb surface area to find proportional representations. All measurements were compiled in Excel. A student's *t*-test was performed in SAS 9.1 for Windows 2002-2003 comparing the percentage of melanin and cortex that occupied the feather cross-sections from TEM micrographs of gray and rufous color morphs (Zar 2005; Cody and Smith 2006).

RESULTS

Color Score:

The amount of redness from the color tristimulus matched the initial color rank order (Table 3).

Table 3. Average color tristimulus scores on a number of pixels from the eastern screech owl dorsum. Each column represents one individual owl (mean \pm standard deviation).

Pixels	Gray						Rufous
	17760	18060	19008	24800	20128	21216	21120
Luminosity	104.61 \pm 24.76	108.05 \pm 31.71	109.60 \pm 27.54	127.28 \pm 22.83	126.29 \pm 30.19	130.34 \pm 25.85	136.64 \pm 21.98
Red	122.24 \pm 25.25	124.45 \pm 34.09	135.32 \pm 31.05	152.20 \pm 25.33	166.92 \pm 31.98	176.59 \pm 25.61	185.04 \pm 20.45
Blue	102.11 \pm 25.52	106.10 \pm 32.13	105.34 \pm 27.79	123.68 \pm 23.03	118.01 \pm 31.21	120.39 \pm 27.62	126.83 \pm 24.19
Green	70.92 \pm 21.78	74.75 \pm 24.48	63.46 \pm 19.49	79.69 \pm 17.16	60.96 \pm 23.98	58.69 \pm 22.03	58.23 \pm 18.59

Light Microscopy and Macroscopic Measurements:*Differences Between Colors:**Body Level:*

The first three PC's accounted for 97.4% (PC1 = 60.4%, PC2 = 25.9%, PC3 = 11.1%) of the variation at the body level (Table 4). There were no significant effects from subsequent ANOVAs on the first three PC's. Color morphs did not differ significantly in any morphological body measurements.

Table 4. Eigenvectors and percentage of variation for the first 3 principle components (PC) of morphological body measurements of eastern screech owl color variants. The *P*-values and *F*-values from subsequent univariate one-way analysis of variance (ANOVA) on the first 3 PC's are also listed.

Measurement	Loading Factors		
	Prin1	Prin2	Prin3
Bill Length (mm)	0.53	-0.04	0.85
Wing Length (mm)	0.60	-0.08	-0.08
Tail Length (mm)	-0.05	0.98	0.98
Mass (g)	0.60	0.19	0.19
% of Variation Explained	60.4	25.9	11.1
F-Value	3.38	1.50	0.70
P-Value	0.09	0.28	0.53

Feather and Barb Level:

Only one significant difference between owls of different color morphs at the feather and barb level was found. The brown owl feather sample had a significantly shorter pennaceous rachis length ($F = 12.95$, $df = 2$, $P = 0.03$) in the medial pectoral tract than red or gray morphs (Table 5).

Table 5. *P*-values and *F*-values for a univariate one-way analysis of variance (ANOVA) and summary statistics for morphological measurements at the feather and barb level of eastern screech owl color variants. Means \pm Standard error, $n=2$, significant models are in bold print.

Measurement	Color			P-value	F-value
	Gray	Brown	Rufous		
Dorsal Tract (Contour)					
Pennaceous Rachis Length (mm)	21.26 \pm 1.73	22.27 \pm 1.74	22.15 \pm 2.10	P = 0.83	F = 0.21
Pennaceous Barb Number	34.56 \pm 1.19	40.94 \pm 3.80	27.91 \pm 4.65	P = 0.08	F = 6.74
Plumulaceous Rachis Length (mm)	22.14 \pm 1.06	21.73 \pm 0.96	22.71 \pm 1.04	P = 0.79	F = 0.25
Plumulaceous Barb Number	55.65 \pm 4.07	58.44 \pm 4.23	61.17 \pm 5.96	P = 0.80	F = 0.24
Barb Length (mm)	19.65 \pm 0.82	18.35 \pm 0.69	19.74 \pm 0.71	P = 0.31	F = 1.77
Femoral Tract (Down)					
Plumulaceous Rachis Length (mm)	32.48 \pm 1.84	29.30 \pm 1.50	27.49 \pm 1.03	P = 0.14	F = 4.13
Plumulaceous Barb Number	101.83 \pm 8.91	95.67 \pm 5.48	106.67 \pm 7.30	P = 0.67	F = 0.46
Barb Length (mm)	17.82 \pm 1.01	19.10 \pm 0.97	19.75 \pm 0.81	P = 0.20	F = 2.88
Humeral Tract (Contour)					
Pennaceous Rachis Length (mm)	20.18 \pm 1.09	22.67 \pm 1.23	20.98 \pm 1.35	P = 0.37	F = 1.42
Pennaceous Barb Number	41.64 \pm 3.08	42.61 \pm 1.99	36.25 \pm 3.07	P = 0.32	F = 1.71
Plumulaceous Rachis Length (mm)	26.07 \pm 1.75	25.12 \pm 1.18	24.69 \pm 1.76	P = 0.60	F = 0.62
Plumulaceous Barb Number	77.17 \pm 7.38	67.6 \pm 4.82	75.92 \pm 9.04	P = 0.25	F = 2.32
Barb Length (mm)	19.26 \pm 0.83	19.10 \pm 0.55	19.54 \pm 0.72	P = 0.40	F = 1.28
Medial Pectoral Tract (Contour)					
Pennaceous Rachis Length (mm)	17.43 \pm 1.15	13.80 \pm 0.71^A	16.70 \pm 1.31	P = 0.03	F = 12.95
Pennaceous Barb Number	31.06 \pm 2.91	27.44 \pm 1.41	26.83 \pm 2.52	P = 0.31	F = 1.80
Plumulaceous Rachis Length (mm)	25.76 \pm 1.37	24.50 \pm 1.09	28.78 \pm 1.68	P = 0.06	F = 8.75
Plumulaceous Barb Number	79.78 \pm 5.39	74.94 \pm 3.75	83.92 \pm 8.69	P = 0.47	F = 0.97
Barb Length (mm)	19.89 \pm 0.83	18.09 \pm 0.51	19.04 \pm 0.98	P = 0.30	F = 1.86

Barbule Level:

At the barbule level in the dorsal tract the length between barbules (proximal $F = 15.21$, $df = 2$, $P = 0.03$, intermediate $F = 24.79$, $df = 2$, $P = 0.03$) was significantly longer in rufous feathers at the proximal and intermediate barbules. However, at the distal barbules, the length between barbules ($F = 9.64$, $df = 2$, $P = 0.05$) was significantly greater in rufous feathers than gray but not brown feathers (Table 6). Rufous barbules

(intermediate $F = 32.03$, $df = 2$, $P = 0.01$, distal $F = 52.14$, $df = 2$, $P = <0.01$) were significantly longer at the intermediate and distal barbules in the dorsal tract.

In the femoral tract, rufous feathers had a significantly greater length between barbules (proximal $F = 17.57$, $df = 2$, $P = 0.02$, intermediate $F = 73.58$, $df = 2$, $P = <0.01$) at the proximal and intermediate barbs and fewer pigmented nodes ($F = 50.60$, $df = 2$, $P = <0.01$) per barbule at the intermediate barb (Table 6). Rufous feathers also had a longer basal cell ($F = 9.13$, $df = 2$, $P = 0.05$) at the proximal barb. For intermediate barbs, brown feathers had significantly longer barbules ($F = 16.26$, $df = 2$, $P = 0.02$), which may have been responsible for more nodes per barb ($F = 31.56$, $df = 2$, $P = 0.01$). Rufous feathers had fewer nodes per barbules ($F = 20.70$, $df = 2$, $P = 0.02$) at the distal barb but also had longer nodes in all three barbule segments (Appendix A).

Rufous feathers had fewer pigmented nodes per barbules ($F = 39.28$, $df = 2$, $P = 0.01$) at the distal barbule of the humeral tract, but there were no other significant differences between eastern screech owl color variants at the humeral intermediate and distal barbs (Table 6). Proximal barbs of brown feathers had a shorter barbule length ($F = 17.16$, $df = 2$, $P = 0.02$) while rufous feathers had a greater length between barbules ($F = 30.82$, $df = 2$, $P = 0.01$). Gray feathers had a shorter basal cell length ($F = 24.27$, $df = 2$, $P = 0.01$) and more nodes per barbules ($F = 12.20$, $df = 2$, $P = 0.04$) at the proximal barb of the humeral tract.

In the medial pectoral tract rufous feathers had longer barbules ($F = 43.94$, $df = 2$, $P = 0.01$) and basal cells ($F = 23.24$, $df = 2$, $P = 0.01$) at the proximal barb, a greater length between barbules ($F = 16.72$, $df = 2$, $P = 0.02$) at the intermediate barb, and fewer pigmented nodes ($F = 18.74$, $df = 2$, $P = 0.02$) at the distal barb (Table 6). Brown feathers had shorter barbules ($F = 15.12$, $df = 2$, $P = 0.03$) at the distal barb.

Table 6. *P*-values and *F*-values for a univariate one-way analysis of variance (ANOVA) and summary statistics for morphological measurements at the barbule level of eastern screech owl color variants. Means \pm Standard error, $n=2$, significant models are in bold print.

Measurement	Color			P-value	F-value
	Gray	Brown	Rufous		
Dorsal Tract (Contour): Proximal Barb					
Barbule Length (mm)	1.71 \pm 0.04	1.69 \pm 0.04	1.87 \pm 0.05	P = 0.18	F = 3.23
Basal Cell Length (μ m)	115.21 \pm 3.75	127.42 \pm 6.50	143.91 \pm 7.91	P = 0.08	F = 6.39
Length Between Barbules (μ m)	23.70 \pm 3.75	26.51 \pm 1.79	35.47 \pm 1.74^A	P = 0.03	F = 15.21
Number of Nodes per Barbule	31.00 \pm 0.60	30.77 \pm 0.72	30.21 \pm 0.81	P = 0.86	F = 0.16
# of Pigmented Nodes per Barbule	31.00 \pm 0.60	30.77 \pm 0.72	30.21 \pm 0.81	P = 0.86	F = 0.16
Femoral Tract (Down): Proximal Barb					
Barbule Length (mm)	1.96 \pm 0.05	2.03 \pm 0.06	2.05 \pm 0.90	P = 0.70	F = 0.41
Basal Cell Length (μ m)	103.13 \pm 4.48	101.25 \pm 3.39	123.58 \pm 5.60^A	P = 0.05	F = 9.13
Length Between Barbules (μ m)	25.26 \pm 1.28	24.69 \pm 1.36	32.78 \pm 1.58^A	P = 0.02	F = 17.57
Number of Nodes per Barbule	34.10 \pm 0.90	34.85 \pm 0.82	33.55 \pm 0.83	P = 0.58	F = 0.65
# of Pigmented Nodes per Barbule	34.13 \pm 0.90	34.85 \pm 0.82	33.55 \pm 0.83	P = 0.58	F = 0.65
Humeral Tract (Contour): Proximal Barb					
Barbule Length (mm)	1.90 \pm 0.05	1.68 \pm 0.05^A	1.92 \pm 0.06	P = 0.02	F = 17.16
Basal Cell Length (μ m)	104.83 \pm 5.31^A	132.24 \pm 6.04	124.90 \pm 6.83	P = 0.01	F = 24.27
Length Between Barbules (μ m)	22.05 \pm 1.09	25.47 \pm 1.49	31.82 \pm 1.52^A	P = 0.01	F = 30.82
Number of Nodes per Barbule	34.52 \pm 0.96^A	30.77 \pm 0.80	31.48 \pm 0.85	P = 0.04	F = 12.20
# of Pigmented Nodes per Barbule	34.52 \pm 0.96^A	30.77 \pm 0.80	31.48 \pm 0.85	P = 0.04	F = 12.20
Medial Pectoral Tract (Contour): Proximal Barb					
Barbule Length (mm)	1.84 \pm 0.05	1.81 \pm 0.06	2.12 \pm 0.06^A	P = 0.01	F = 43.94
Basal Cell Length (μ m)	122.30 \pm 5.59	124.53 \pm 5.17	153.69 \pm 8.76^A	P = 0.01	F = 23.24
Length Between Barbules (μ m)	25.09 \pm 1.63	25.05 \pm 1.37	31.48 \pm 1.56	P = 0.08	F = 6.43
Number of Nodes per Barbule	33.79 \pm 0.78	33.90 \pm 0.97	35.75 \pm 1.05	P = 0.32	F = 1.68
# of Pigmented Nodes per Barbule	33.79 \pm 0.78	33.90 \pm 0.97	35.55 \pm 1.08	P = 0.35	F = 1.51

Measurement	Color			P-value	F-value
	Gray	Brown	Red		
Dorsal Tract (Contour): Intermediate Barb					
Barbule Length (mm)	1.85 ± 0.04	1.89 ± 0.04	2.09 ± 0.05^A	P = 0.01	F = 32.03
Basal Cell Length (µm)	99.79 ± 3.60	108.23 ± 4.04	121.30 ± 4.41	P = 0.08	F = 6.49
Length Between Barbules (µm)	36.46 ± 1.75	38.39 ± 1.59	47.42 ± 1.94^A	P = 0.01	F = 24.79
Number of Nodes per Barbule	35.38 ± 0.70	34.60 ± 0.51	33.48 ± 0.81	P = 0.13	F = 4.47
# of Pigmented Nodes per Barbule	35.38 ± 0.70	34.60 ± 0.51	33.48 ± 0.81	P = 0.13	F = 4.47
Femoral Tract (Down): Intermediate Barb					
Barbule Length (mm)	1.88 ± 0.06	2.13 ± 0.06^A	1.97 ± 0.07	P = 0.02	F = 16.26
Basal Cell Length (µm)	89.23 ± 3.11	91.67 ± 2.20	103.64 ± 4.60	P = 0.14	F = 4.06
Length Between Barbules (µm)	29.48 ± 1.16^A	33.07 ± 1.41^B	38.98 ± 1.61^C	P = <0.01	F = 73.58
Number of Nodes per Barbule	35.17 ± 0.87	37.42 ± 0.81^A	34.05 ± 0.73	P = 0.01	F = 31.56
# of Pigmented Nodes per Barbule	35.17 ± 0.87	37.42 ± 0.81^A	33.91 ± 0.76	P = <0.01	F = 50.60
Humeral Tract (Contour): Intermediate Barb					
Barbule Length (mm)	1.81 ± 0.04	1.82 ± 0.04	1.91 ± 0.06	P = 0.51	F = 0.84
Basal Cell Length (µm)	93.98 ± 2.84	105.89 ± 5.63	105.89 ± 3.13	P = 0.06	F = 8.84
Length Between Barbules (µm)	33.18 ± 1.60	36.35 ± 1.73	38.65 ± 1.31	P = 0.24	F = 2.35
Number of Nodes per Barbule	34.61 ± 0.80	33.92 ± 0.68	33.40 ± 0.87	P = 0.45	F = 1.07
# of Pigmented Nodes per Barbule	34.61 ± 0.80	33.92 ± 0.68	33.40 ± 0.87	P = 0.45	F = 1.07
Medial Pectoral Tract (Contour): Intermediate Barb					
Barbule Length (mm)	1.88 ± 0.04	1.87 ± 0.03	1.93 ± 0.04	P = 0.41	F = 1.23
Basal Cell Length (µm)	111.72 ± 2.89	101.04 ± 2.73	117.85 ± 4.32	P = 0.17	F = 3.42
Length Between Barbules (µm)	37.19 ± 1.39	35.27 ± 1.76	42.28 ± 1.63^A	P = 0.02	F = 16.72
Number of Nodes per Barbule	37.04 ± 0.82	36.75 ± 0.59	36.02 ± 0.64	P = 0.72	F = 0.36
# of Pigmented Nodes per Barbule	35.67 ± 1.35	36.75 ± 0.59	36.02 ± 0.64	P = 0.77	F = 0.29

Measurement	Color			P-value	F-value
	Gray	Brown	Red		
Dorsal Tract (Contour): Distal Barb					
Barbule Length (mm)	1.79 ± 0.05	1.70 ± 0.04	2.04 ± 0.05 ^A	P = <0.01	F = 52.14
Length Between Barbules (µm)	71.51 ± 2.96 ^B	79.22 ± 4.01 ^{A,B}	86.93 ± 3.89 ^A	P = 0.05	F = 9.64
Number of Nodes per Barbule	29.27 ± 0.71	27.94 ± 0.63	27.98 ± 0.74	P = 0.12	F = 4.76
# of Pigmented Nodes per Barbule	29.13 ± 0.73	27.94 ± 0.63	27.54 ± 0.78	P = 0.07	F = 7.10
Femoral Tract (Down): Distal Barb					
Barbule Length (mm)	1.62 ± 0.05	1.66 ± 0.04	1.65 ± 0.04	P = 0.35	F = 1.52
Length Between Barbules (µm)	61.56 ± 4.24	76.25 ± 4.44	82.05 ± 4.40	P = 0.07	F = 7.31
Number of Nodes per Barbule	29.38 ± 0.87	27.73 ± 0.65	25.95 ± 0.49 ^A	P = 0.02	F = 20.70
# of Pigmented Nodes per Barbule	25.27 ± 1.64	25.52 ± 1.15	17.61 ± 1.89 ^A	P = 0.03	F = 15.47
Humeral Tract (Contour): Distal Barb					
Barbule Length (mm)	1.67 ± 0.04	1.76 ± 0.05	1.85 ± 0.04	P = 0.24	F = 2.36
Length Between Barbules (µm)	69.60 ± 3.41	75.00 ± 3.78	81.04 ± 4.59	P = 0.39	F = 1.29
Number of Nodes per Barbule	29.32 ± 0.58	28.15 ± 0.65	26.90 ± 0.71	P = 0.32	F = 1.69
# of Pigmented Nodes per Barbule	26.68 ± 1.40	26.68 ± 1.04	20.88 ± 1.65 ^A	P = 0.01	F = 39.28
Medial Pectoral Tract (Contour): Distal Barb					
Barbule Length (mm)	1.80 ± 0.03	1.63 ± 0.02 ^A	1.88 ± 0.04	P = 0.03	F = 15.12
Length Between Barbules (µm)	86.61 ± 4.54	78.96 ± 3.57	95.23 ± 4.23	P = 0.09	F = 5.99
Number of Nodes per Barbule	30.40 ± 0.63	27.44 ± 0.52	28.55 ± 0.69	P = 0.10	F = 5.36
# of Pigmented Nodes per Barbule	10.29 ± 1.96	12.73 ± 1.86	0.70 ± 0.70 ^A	P = 0.02	F = 18.74

Barbule Segment Level:

P-values for subsequent ANOVAs performed on the first three principle components (PC1, PC2, PC3) are listed (Table 7) and also inserted in text below only for significant *P*-values. Due to the high amount of analyses conducted, loading factors for the first three PC's, percentage of variation explained by the first three PC's, *P*-values and *F*-values from subsequent ANOVAs performed on the first three PC's are listed (Table 8) and inserted in text below by tract for significant *P*-values only (Table 7). Loading factors ($\sim > 0.50$) for morphological characteristics with the highest impact on significant effects are listed below in parentheses for each pterylae.

Dorsal Tract:

At the proximal barb of the dorsal tract, the first three PC's explained 95.0% (PC1 = 60.3%, PC2 = 29.7%, PC3 = 5.0%) of the variation at the proximal barbule segment and 97.2% (PC1 = 46.9%, PC2 = 31.4%, PC3 = 18.9%) of the variation at the intermediate barbule segment in the dorsal tract (Table 8). The proximal-distal pigment length (0.60 proximal, 0.59 intermediate) at the proximal and intermediate barbule segments, spine length (0.59) at the proximal barbule segment, and internode width (-0.51) at the intermediate barbule segment all contributed to an overall color effect. There were significant differences detected by subsequent ANOVAs on PC1 ($F = 14.20$, $P = 0.03$) at the proximal portion of the proximal barb and PC3 ($F = 12.51$, $P = 0.04$) at the intermediate portion of the proximal barb (Table 7-8).

The first three PC's explained 98.8% (PC1 = 52.9%, PC2 = 24.5%, PC3 = 21.4%) of the variation at the intermediate barbule portion of the intermediate barb in the dorsal tract (Table 8). At the intermediate barbule segment of the intermediate barb the proximal-distal pigment length (0.67) and internode width (-0.63) contributed to a significant color effect. The subsequent ANOVA detected a significant difference at PC1 ($F = 108.02$, $P = <0.01$) at the intermediate portion of the intermediate barb (Table 7-8).

At the distal barb of the dorsal tract, the first three PC's explained 97.8% (PC1 = 63.7%, PC2 = 20.4%, PC3 = 13.7%) of the variation at the proximal barbule segment and 93.0% (PC1 = 49.4%, PC2 = 36.1%, PC3 = 8.0%) of the variation at the intermediate barbules segment (Table 8). At the distal barb, the internode width (-0.59) at the proximal barbule and the proximal-distal nodal length (-0.64) and spine length (0.65) at the intermediate barbule segment contributed the most to a color effect. The subsequent

ANOVA detected a significant difference at PC2 (proximal $F = 11.99$, $P = 0.04$, and intermediate $F = 27.35$, $P = 0.01$) at the proximal and intermediate portions of the barbule of the distal barb (Table 7-8).

Femoral Tract:

The first three PC's explained 99.6% (PC1 = 68.2%, PC2 = 19.9%, PC3 = 11.5%) of the variation at the proximal portion of the proximal barb in the femoral tract (Table 8). Proximal-distal pigment length (-0.49), internode width (0.47), and spine length (0.58) contributed to a significant color effect at the proximal barbule segment of the proximal barb in the femoral tract. The subsequent ANOVA detected a significant difference at PC1 ($F = 49.00$, $P = 0.01$) at the proximal portion of the proximal barb (Table 7-8).

At the intermediate barb in the femoral tract, the first three PC's explained 96.8% (PC1 = 55.1%, PC2 = 25.9%, PC3 = 15.8%) of the variation at the proximal barbule segment, 99.6% (PC1 = 47.7%, PC2 = 35.5%, PC3 = 16.4%) of the variation at the intermediate barbule segment, and 92.4% (PC1 = 49.8%, PC2 = 30.2%, PC3 = 12.4%) of the variation at the distal barbule segment (Table 8). Proximal-distal nodal length (0.62) and spine length (-0.63) contributed the most to a color effect at the proximal barbule segment. Proximal-distal pigment length (0.68) and spine length (-0.70) contributed the most to a color effect at the intermediate segment. Proximal-distal nodal length (0.60), proximal-distal pigment length (0.52), and internode width (-0.54) contributed the most to a color effect at the distal segment. The ANOVA detected a significant difference at PC1 (proximal $F = 18.54$, $P = 0.02$, intermediate $F = 11.48$, $P = 0.04$ and distal $F = 16.55$, $P = 0.02$) at all three portions of the intermediate barb (Table 7-8).

The first three PC's explained 100.0% (PC1 = 50.3%, PC2 = 36.6%, PC3 = 9.8%) of the variation at the intermediate barbule segment at the distal barb of the femoral tract (Table 8). Internode width (0.66) and spine length (0.68) at the intermediate barbule segment at the distal barb contributed to a color effect. The ANOVA detected a significant difference at PC2 ($F = 9.31$, $P = 0.05$) at the intermediate portion of the distal barb (Table 7-8).

Humeral Tract:

The first three PC's explained 99.3% (PC1 = 90.0%, PC2 = 7.6%, PC3 = 1.7%) of the variation at the distal barbule segment of the proximal barb in the humeral tract (Table 8). At the proximal barb in the humeral tract the proximal-distal nodal length (-0.51), internode width (0.50), and spine length (0.52) contributed to a color effect at the distal barbule segment. The subsequent ANOVA detected a significant difference at PC3 ($F = 15.35$, $P = 0.03$) at the distal barbule portion of the proximal barb (Table 7-8).

The first three PC's explained 98.2% (PC1 = 54.1%, PC2 = 32.3%, PC3 = 11.8%) of the variation at the proximal barbule segment of the intermediate barb in the humeral tract (Table 8). The proximal-distal nodal length (-0.56), internode width (0.54), and spine length (0.61) contributed to a color effect at the proximal barbule segment of the intermediate barb. The subsequent ANOVA detected a significant difference at PC3 ($F = 12.76$, $P = 0.03$) at the proximal barbule portion of the intermediate barb (Table 7-8).

At the distal barb of the humeral tract, the first three PC's explained 95.1% (PC1 = 58.4%, PC2 = 20.9%, PC3 = 15.8%) of the variation at the proximal barbule segment, 96.4% (PC1 = 60.2%, PC2 = 28.2%, PC3 = 8.0%) of the variation at the intermediate barbule segment, and 94.1% (PC1 = 52.8%, PC2 = 30.2%, PC3 = 11.1%) of the variation at the distal barbule segment (Table 8). The proximal-distal nodal length (proximal 0.53, intermediate

0.56, and distal 0.56) and internode width (proximal -0.61, intermediate -0.60, and distal -0.53) contributed to a color effect at all three barbule segments of the distal barb and the proximal-distal pigment length (0.62) contributed to a color effect at the distal barbule segment of the distal barb. The ANOVA detected a significant difference at PC1 (proximal $F = 22.49$, $P = 0.02$, intermediate $F = 20.53$, $P = 0.02$ and distal $F = 24.74$, $P = 0.01$) at all three portions of the distal barb (Table 7-8).

Medial Pectoral Tract:

The first three PC's explained 98.3% (PC1 = 68.4%, PC2 = 20.4%, PC3 = 9.5%) of the variation at the distal barbule segment of the proximal barb in the medial pectoral tract (Table 8). Proximal-distal nodal length (-0.59), internode width (0.50), and spine length (0.53) contributed to a color effect at the distal barbule segment of the proximal barb in the medial pectoral tract. The subsequent ANOVA detected a significant difference at PC1 ($F = 56.99$, $P < 0.01$) and PC2 ($F = 28.25$, $P = 0.01$) at the distal barbule portion of the proximal barb (Table 7-8).

The first three PC's explained 97.6% (PC1 = 68.6%, PC2 = 18.3%, PC3 = 10.7%) of the variation at the proximal barbule segment of the intermediate barb in the medial pectoral tract (Table 8). At the intermediate barb the proximal-distal pigment length (0.52), internode width (0.58) and spine length (-0.51) contributed to a color effect at the proximal barbule segment. The subsequent ANOVA detected a significant difference at PC1 ($F = 9.38$, $P = 0.05$) and PC3 ($F = 9.88$, $P = 0.05$) at the proximal barbule portion of the intermediate barb (Table 7-8).

At the distal barb of the medial pectoral tract, the first three PC's explained 99.5% (PC1 = 79.8%, PC2 = 16.2%, PC3 = 3.5%) of the variation at the proximal barbule segment,

100.0% (PC1 = 84.4%, PC2 = 12.9%, PC3 = 2.7%) of the variation at the intermediate barbule segment, and 95.8% (PC1 = 67.8%, PC2 = 28.0%, PC3 = 0.04%) of the variation at the distal barbule segment (Table 8). Proximal-distal nodal length (0.55), internode width (0.51), and spine length (0.48) contributed to a significant color effect at the proximal barbule portion of the distal barb. Proximal-distal nodal length (0.50), proximal-distal pigment length (0.53), and internode width (0.52) contributed to a significant color effect at the intermediate barbule portion of the distal barb. Proximal-distal pigment length (0.57), internode width (-0.59), and spine length (0.56) contributed to a significant color effect at the distal barbule portion of the distal barb. The ANOVA detected a significant difference at PC1 (proximal $F = 28.66$, $P = 0.03$, intermediate $F = 402.67$, $P = <0.01$ and distal $F = 576.07$, $P = <0.01$) at all three barbule portions of the distal barb. The ANOVA detected a significant difference at PC2 ($F = 17.83$, $P = 0.05$) at the proximal barbule portion of the distal barb (Table 7-8).

Table 7. *P*-values from subsequent univariate one-way analysis of variance (ANOVA) on the first 3 principle components (PC) for morphological measurements at the barbule segment level of eastern screech owl color variants. Significant models are in bold print.

Measurement	Barbule Segment		
	Proximal	Intermediate	Distal
Dorsal Tract (Contour): Proximal Barb			
Prin 1	P = 0.03	P = 0.34	P = 0.10
Prin 2	P = 0.73	P = 0.60	P = 0.46
Prin 3	P = 0.15	P = 0.04	P = 0.82
Femoral Tract (Down): Proximal Barb			
Prin 1	P = 0.01	P = 0.08	P = 0.21
Prin 2	P = 0.98	P = 0.43	P = 0.46
Prin 3	P = 0.47	P = 0.85	P = 0.20
Humeral Tract (Contour): Proximal Barb			
Prin 1	P = 0.19	P = 0.09	P = 0.16
Prin 2	P = 0.47	P = 0.82	P = 0.83
Prin 3	P = 0.43	P = 0.36	P = 0.03
Medial Pectoral Tract (Contour): Proximal Barb			
Prin 1	P = 0.11	P = 0.11	P = <0.01
Prin 2	P = 0.92	P = 0.48	P = 0.01
Prin 3	P = 0.26	P = 0.70	P = 0.96

Measurement	Barbule Segment		
	Proximal	Intermediate	Distal
Dorsal Tract (Contour): Intermediate Barb			
Prin 1	P = 0.27	P = <0.01	P = 0.53
Prin 2	P = 0.34	P = 0.72	P = 0.21
Prin 3	P = 0.45	P = 0.29	P = 0.30
Femoral Tract (Down): Intermediate Barb			
Prin 1	P = 0.02	P = 0.04	P = 0.02
Prin 2	P = 0.62	P = 0.15	P = 0.44
Prin 3	P = 0.89	P = 0.77	P = 0.80
Humeral Tract (Contour): Intermediate Barb			
Prin 1	P = 0.12	P = 0.92	P = 0.22
Prin 2	P = 0.72	P = 0.26	P = 0.51
Prin 3	P = 0.03	P = 0.60	P = 0.47
Medial Pectoral Tract (Contour): Intermediate Barb			
Prin 1	P = 0.05	P = 0.09	P = 0.12
Prin 2	P = 0.94	P = 0.65	P = 0.37
Prin 3	P = 0.05	P = 0.53	P = 0.41

Measurement	Barbule Segment		
	Proximal	Intermediate	Distal
Dorsal Tract (Contour): Distal Barb			
Prin 1	P = 0.34	P = 0.81	P = 0.14
Prin 2	P = 0.04	P = 0.01	P = 0.98
Prin 3	P = 0.43	P = 0.12	P = 0.44
Femoral Tract (Down): Distal Barb			
Prin 1	P = 0.11	P = 0.17	P = 0.20
Prin 2	P = 0.28	P = 0.05	P = 0.08
Prin 3	P = 0.87	P = 0.80	P = 0.72
Humeral Tract (Contour): Distal Barb			
Prin 1	P = 0.02	P = 0.02	P = 0.01
Prin 2	P = 0.98	P = 0.11	P = 0.57
Prin 3	P = 0.38	P = 0.78	P = 0.71
Medial Pectoral Tract (Contour): Distal Barb			
Prin 1	P = 0.03	P = <0.01	P = <0.01
Prin 2	P = 0.05	P = 0.65	P = 0.98
Prin 3	P = 0.92	P = 0.84	P = 0.94

Table 8. Principle component loading factors for the first three principle components (PC) and P-values, percentage of variation, and *F*-values from subsequent analysis of variance (ANOVA) with significant *P*-values for morphological measurements at the barbule segment level of eastern screech owl color variants ($n=2$). Significant models are in bold print.

Measurement	Loading Factors		
	Prin1	Prin2	Prin3
Dorsal Tract (Contour): Proximal Barb, Proximal Barbule			
Proximal-Distal Nodal Length (μm)	-0.24	0.84	0.30
Proximal-Distal Pigment Length (μm)	0.60	-0.17	-0.08
Internode Width (μm)	0.49	0.52	-0.62
Spine Length (μm)	0.59	0.08	0.72
Percentage of Variation	60.3	29.7	5.0
F-value	14.20	0.36	3.90
P-Value	0.03	0.73	0.15
Femoral Tract (Down): Proximal Barb, Proximal Barbule			
Proximal-Distal Nodal Length (μm)	-0.44	0.56	0.71
Proximal-Distal Pigment Length (μm)	-0.49	0.43	-0.64
Internode Width (μm)	0.47	0.67	-0.24
Spine Length (μm)	0.58	0.24	0.18
Percentage of Variation	68.2	19.9	11.5
F-value	49.00	0.02	0.97
P-Value	0.01	0.98	0.47

Measurement	Loading Factors		
	Prin1	Prin2	Prin3
Dorsal Tract (Contour): Proximal Barb, Intermediate Barbule			
Proximal-Distal Nodal Length (μm)	0.57	0.51	-0.17
Proximal-Distal Pigment Length (μm)	0.59	0.15	0.63
Internode Width (μm)	-0.51	0.33	0.70
Spine Length (μm)	0.27	-0.78	0.30
Percentage of Variation	46.9	31.4	18.9
F-value	1.60	0.61	12.51
P-Value	0.34	0.60	0.04

Measurement	Loading Factors		
	Prin1	Prin2	Prin3
Humeral Tract (Contour): Proximal Barb, Distal Barbule			
Proximal-Distal Nodal Length (μm)	-0.51	-0.10	0.85
Proximal-Distal Pigment Length (μm)	-0.46	0.85	-0.17
Internode Width (μm)	0.50	0.46	0.33
Spine Length (μm)	0.52	0.21	0.37
Percentage of Variation	90.0	7.6	1.7
F-value	3.67	0.20	15.35
P-Value	0.16	0.83	0.03
Medial Pectoral Tract (Contour): Proximal Barb, Distal Barbule			
Proximal-Distal Nodal Length (μm)	-0.59	0.09	0.07
Proximal-Distal Pigment Length (μm)	0.35	0.88	-0.27
Internode Width (μm)	0.50	-0.47	-0.55
Spine Length (μm)	0.53	-0.04	0.78
Percentage of Variation	68.4	20.4	9.5
F-value	56.99	28.25	0.05
P-Value	<0.01	0.01	0.96

Measurement	Loading Factors		
	Prin1	Prin2	Prin3
Femoral Tract (Down): Intermediate Barb, Proximal Barbule			
Proximal-Distal Nodal Length (μm)	0.62	0.11	-0.36
Proximal-Distal Pigment Length (μm)	0.38	-0.60	0.69
Internode Width (μm)	0.28	0.78	0.55
Spine Length (μm)	-0.63	0.10	0.30
Percentage of Variation	55.1	25.9	15.8
F-value	18.54	0.56	0.12
P-Value	0.02	0.62	0.89
Humeral Tract (Contour): Intermediate Barb, Proximal Barbule			
Proximal-Distal Nodal Length (μm)	-0.56	0.38	0.50
Proximal-Distal Pigment Length (μm)	0.17	-0.82	0.38
Internode Width (μm)	0.54	0.29	0.72
Spine Length (μm)	0.61	0.61	-0.29
Percentage of Variation	54.1	32.3	11.8
F-value	4.52	0.37	12.76
P-Value	0.12	0.72	0.03
Medial Pectoral Tract (Contour): Intermediate Barb, Proximal Barbule			
Proximal-Distal Nodal Length (μm)	0.37	0.92	-0.10
Proximal-Distal Pigment Length (μm)	0.52	-0.17	0.73
Internode Width (μm)	0.58	-0.15	0.01
Spine Length (μm)	-0.51	0.32	0.68
Percentage of Variation	68.6	18.3	10.7
F-value	9.38	0.06	9.88
P-Value	0.05	0.94	0.05

Measurement	Loading Factors		
	Prin1	Prin2	Prin3
Dorsal Tract (Contour): Intermediate Barb, Intermediate Barbule			
Proximal-Distal Nodal Length (μm)	0.35	-0.34	0.85
Proximal-Distal Pigment Length (μm)	0.67	0.19	-0.05
Internode Width (μm)	-0.63	-0.27	0.30
Spine Length (μm)	-0.19	-0.88	0.43
Percentage of Variation	52.9	24.5	21.4
F-value	108.02	0.36	1.93
P-Value	<0.01	0.72	0.29
Femoral Tract (Down): Intermediate Barb, Intermediate Barbule			
Proximal-Distal Nodal Length (μm)	0.20	0.67	0.67
Proximal-Distal Pigment Length (μm)	0.68	-0.07	-0.37
Internode Width (μm)	-0.02	-0.73	0.61
Spine Length (μm)	-0.70	0.14	-0.20
Percentage of Variation	47.7	35.5	16.4
F-value	11.48	3.73	0.28
P-Value	0.04	0.15	0.77
Measurement	Loading Factors		
	Prin1	Prin2	Prin3
Femoral Tract (Down): Intermediate Barb, Distal Barbule			
Proximal-Distal Nodal Length (μm)	0.60	0.30	0.12
Proximal-Distal Pigment Length (μm)	0.52	-0.41	0.65
Internode Width (μm)	-0.54	0.34	0.75
Spine Length (μm)	0.27	0.79	-0.03
Percentage of Variation	49.8	30.2	12.4
F-value	16.55	1.10	0.24
P-Value	0.02	0.44	0.80

Measurement	Loading Factor		
	Prin1	Prin2	Prin3
Dorsal Tract (Contour): Distal Barb, Proximal Barbule			
Proximal-Distal Nodal Length (μm)	0.43	-0.58	0.68
Proximal-Distal Pigment Length (μm)	-0.59	0.10	0.35
Internode Width (μm)	0.37	0.81	0.46
Spine Length (μm)	0.58	0.01	-0.45
Percentage of Variation	63.7	20.4	13.7
F-value	1.60	11.99	1.12
P-Value	0.34	0.04	0.43
Humeral Tract (Contour): Distal Barb, Proximal Barbule			
Proximal-Distal Nodal Length (μm)	0.53	-0.17	-0.66
Proximal-Distal Pigment Length (μm)	0.38	0.84	0.28
Internode Width (μm)	-0.61	0.01	0.11
Spine Length (μm)	0.45	-0.51	0.69
Percentage of Variation	58.4	20.9	15.8
F-value	22.49	0.02	1.36
P-Value	0.02	0.98	0.38
Medial Pectoral Tract (Contour): Distal Barb, Proximal Barbule			
Proximal-Distal Nodal Length (μm)	0.55	0.23	0.15
Proximal-Distal Pigment Length (μm)	0.46	0.71	0.03
Internode Width (μm)	0.51	-0.36	-0.77
Spine Length (μm)	0.48	-0.55	0.62
Percentage of Variation	79.8	16.2	3.5
F-value	28.66	17.83	0.08
P-Value	0.03	0.05	0.92

Measurement	Loading Factor		
	Prin1	Prin2	Prin3
Dorsal Tract (Contour): Distal Barb, Intermediate Barbule			
Proximal-Distal Nodal Length (μm)	0.08	0.77	0.63
Proximal-Distal Pigment Length (μm)	-0.64	-0.18	0.21
Internode Width (μm)	0.65	0.10	-0.30
Spine Length (μm)	0.40	-0.60	0.69
Percentage of Variation	49.4	36.1	8.0
F-value	0.22	27.35	4.59
P-Value	0.81	0.01	0.12
Femoral Tract (Down): Distal Barb, Intermediate Barbule			
Proximal-Distal Nodal Length (μm)	0.10	0.74	-0.66
Proximal-Distal Pigment Length (μm)	-0.32	0.65	0.68
Internode Width (μm)	0.66	0.15	0.30
Spine Length (μm)	0.68	0.05	0.12
Percentage of Variation	50.3	36.6	9.8
F-value	3.45	9.31	0.24
P-Value	0.17	0.05	0.80
Humeral Tract (Contour): Distal Barb, Intermediate Barbule			
Proximal-Distal Nodal Length (μm)	0.56	0.20	0.79
Proximal-Distal Pigment Length (μm)	0.46	0.57	-0.56
Internode Width (μm)	-0.60	0.19	0.22
Spine Length (μm)	0.34	-0.77	-0.15
Percentage of Variation	60.2	28.2	8.0
F-value	20.53	5.20	0.27
P-Value	0.02	0.11	0.78
Medial Pectoral Tract (Contour): Distal Barb, Intermediate Barbule			
Proximal-Distal Nodal Length (μm)	0.50	-0.44	0.63
Proximal-Distal Pigment Length (μm)	0.53	0.09	-0.68
Internode Width (μm)	0.52	-0.35	-0.19
Spine Length (μm)	0.44	0.82	0.33
Percentage of Variation	84.4	12.9	2.7
F-value	402.67	0.53	0.20
P-Value	<0.01	0.05	0.80

Measurement	Loading Factor		
	Prin1	Prin2	Prin3
Humeral Tract (Contour): Distal Barb, Distal Barbule			
Proximal-Distal Nodal Length (μm)	0.56	0.43	0.20
Proximal-Distal Pigment Length (μm)	0.62	0.15	0.34
Internode Width (μm)	-0.53	0.35	0.77
Spine Length (μm)	-0.18	0.82	-0.50
Percentage of Variation	52.8	30.2	11.1
F-value	24.74	0.68	0.38
P-Value	0.01	0.57	0.71
Medial Pectoral Tract (Contour): Distal Barb, Distal Barbule			
Proximal-Distal Nodal Length (μm)	-0.06	0.94	0.10
Proximal-Distal Pigment Length (μm)	0.57	<0.01	0.80
Internode Width (μm)	-0.59	0.19	0.26
Spine Length (μm)	0.56	0.28	-0.53
Percentage of Variation	67.8	28.0	0.04
F-value	576.07	0.00	0.01
P-Value	<0.01	0.98	0.94

Scanning Electron Microscopy:

Due to the low resolution of light microscopy, SEM was used to image the nodal structures of the intermediate plumulaceous region of eastern screech owl contour feathers. Only one owl was used for SEM micrographs due to the high amount of computer memory that micrographs consume. The proximal nodes described are the third node from the proximal end, distal nodes are the third node from the distal end, and intermediate nodes are from approximately the middle of the barbule. Definitions and descriptions of nodal structures are presented in Lucas and Stettenheim (1972) and Gilroy (1980). One modification on nodal terminology from Gilroy (1980) is a distinction between rough transitional nodes and smooth rounded transitional nodes.

Dorsal Tract:

The nodal structures of the proximal barbules at the proximal portion had elongated nodal prongs and reduced swelling, which is typical of a crocus node (Figure 14). The proximal nodes from barbules on other tracts did not have elongated nodal prongs. The amount of nodal prongs was variable. The intermediate nodes were crocus or spined but rarely transitional. The distal nodes were spined with a variable number of nodal prongs.

The nodal structures of the intermediate barbules at the proximal portion were typical or crocus. The intermediate nodes were usually smooth transitional and sometimes coronal or rough transitional. The distal nodes were usually spined but sometimes were reduced to a coronal node.

The proximal and intermediate nodes of the distal barbule were usually spined or crocus. Some of the intermediate nodes were rough transitional. The distal nodes were spined and sometimes coronal.

Femoral Tract:

The proximal nodes of the proximal barbule were perfect or typical. Rarely were bent and asymmetrical nodes present (Figure 15). The intermediate nodes were always transitional, usually of the smooth variety. The distal nodes usually lacked long distinctive spines and were considered rough transitional or coronal.

The intermediate barbule nodal structures on the proximal portion were typical or coronal. The intermediate nodes were usually smooth or rough transitional or coronal. The distal nodes were usually spined; however, the nodal prongs could be reduced thereby classifying the node as rough transitional.

The proximal nodes on the proximal barbule were typical or crocus. The intermediate nodes were spined or coronal, rarely rough transitional. The distal nodes were spined.

Humeral Tract:

The proximal nodes of the proximal barbule were typical or perfect (Figure 16). The intermediate nodes were smooth and rough transitional, crocus, or coronal. The distal nodes were spined or coronal.

The proximal nodes of the intermediate barbule were typical or perfect. The proximal portion of the intermediate barbule resembled the proximal portion of the proximal barbule. The intermediate nodes were smooth or rough transitional or coronal. The distal nodes were spined, rough transitional, or coronal.

The distal barbule nodes were reduced in swelling and had elongated nodal prongs. The proximal nodes were coronal with a variable number of nodal prongs. The intermediate nodes were variable and can range from spined, rough transitional, coronal, or crocus. None of the intermediate transitional nodes were smooth or rounded. The distal nodes were spined.

Medial Pectoral Tract:

The nodes across the barbules in the medial pectoral tract were not as variable between each other as the nodes in the femoral, humeral, or dorsal tracts (Figure 17). The nodes on the proximal portion of the proximal barbule were typical, perfect, and some nodes were crocus. The intermediate nodes were smooth transitional. The distal nodes were rough transitional and in some cases the nodal prongs were long enough to be considered spined.

The proximal nodes of the intermediate barbule were perfect or typical. The intermediate nodes were smooth transitional and rarely rough transitional. The distal nodes were coronal, rough transitional, or spined.

The proximal nodes of the distal barbule were mostly crocus. The nodes were rarely swollen enough to be considered typical. The intermediate nodes were rough transitional, spined, or crocus. The distal nodes were spined.

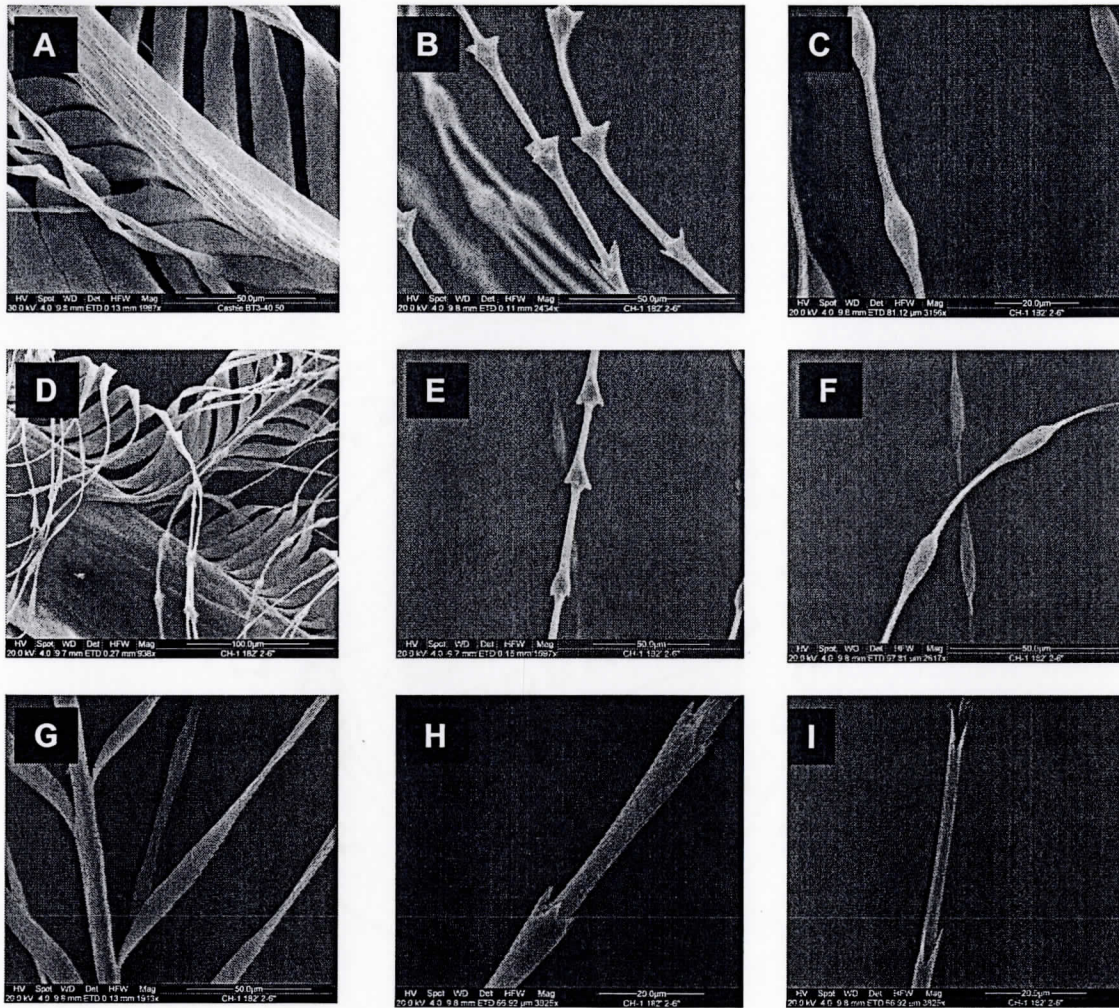


Figure 14. Scanning electron microscopy (SEM) micrographs of contour feathers from dorsal tract of the eastern screech owl. (A) proximal barbule base (B) proximal barbule, proximal nodes (C) proximal barbule, intermediate nodes (D) barb base (E) intermediate barbule, proximal nodes (F) intermediate barbule, intermediate nodes (G) distal barbule base (H) distal barbule, proximal nodes (I) distal barbule, distal nodes

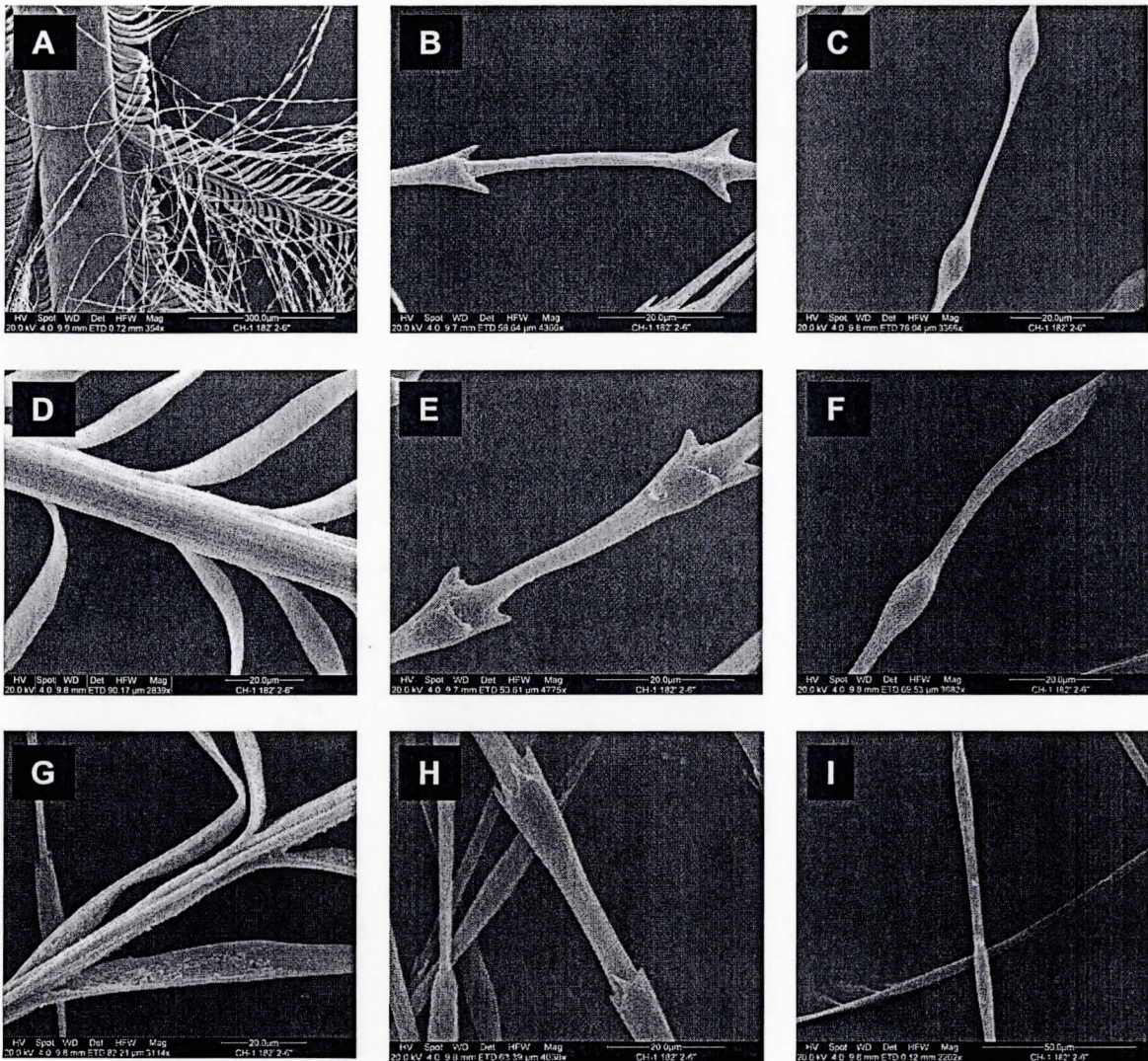


Figure 15. Scanning electron microscopy (SEM) micrographs of contour feathers from femoral tract of the eastern screech owl. (A) barb base (B) proximal barbule, proximal nodes (C) proximal barbule, intermediate nodes (D) intermediate barbule base (E) intermediate barbule, proximal nodes (F) intermediate barbule, intermediate nodes (G) distal barbule base (H) distal barbule, proximal nodes (I) distal barbule, intermediate nodes

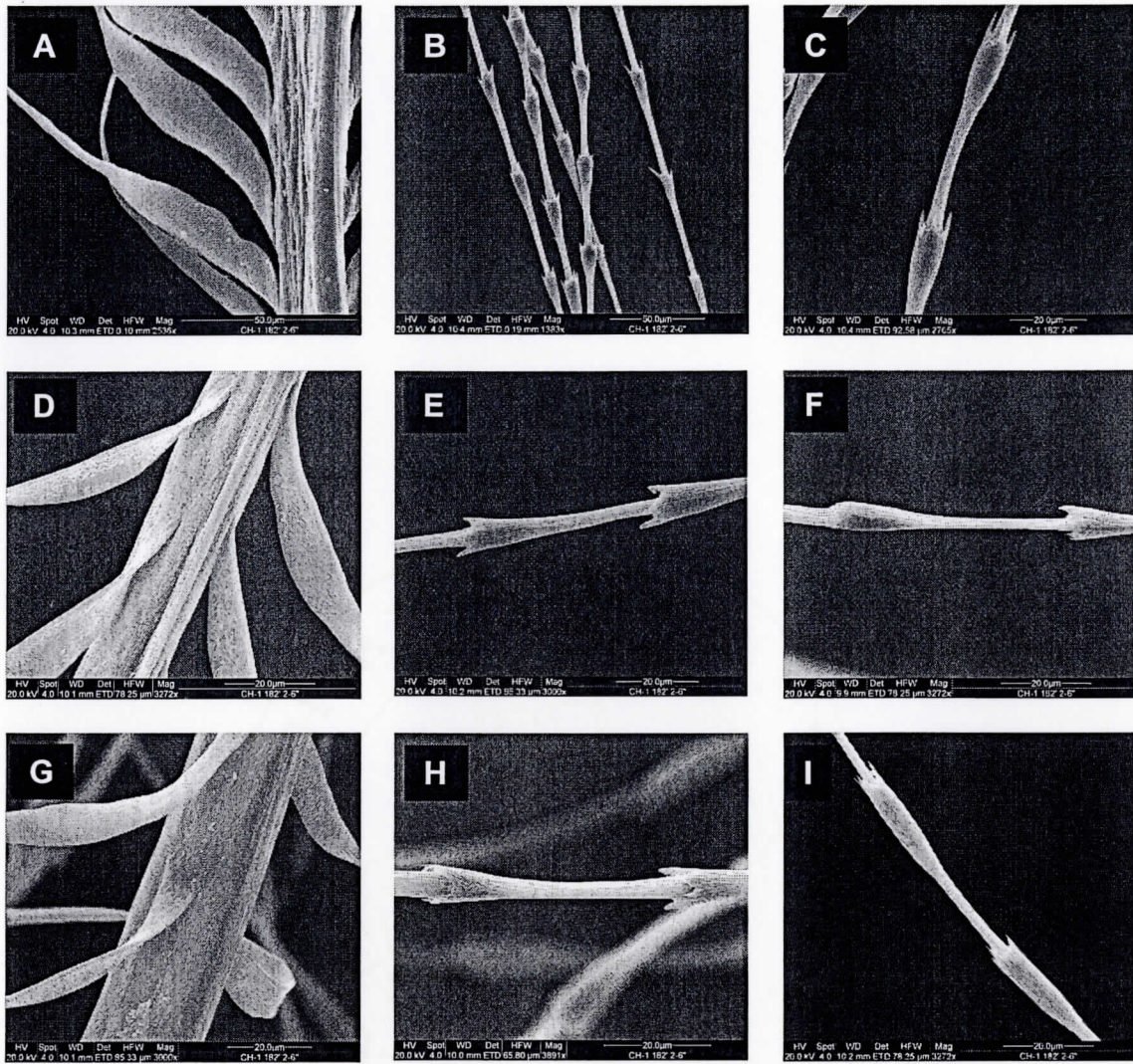


Figure 16. Scanning electron microscopy (SEM) micrographs of contour feathers from humeral tract of the eastern screech owl. (A) proximal barbule base (B) proximal barbule, proximal nodes (C) proximal barbule, intermediate nodes (D) intermediate barbule base (E) intermediate barbule, proximal nodes (F) intermediate barbule, intermediate nodes (G) distal barbule base (H) distal barbule, proximal nodes (I) distal barbule, intermediate nodes

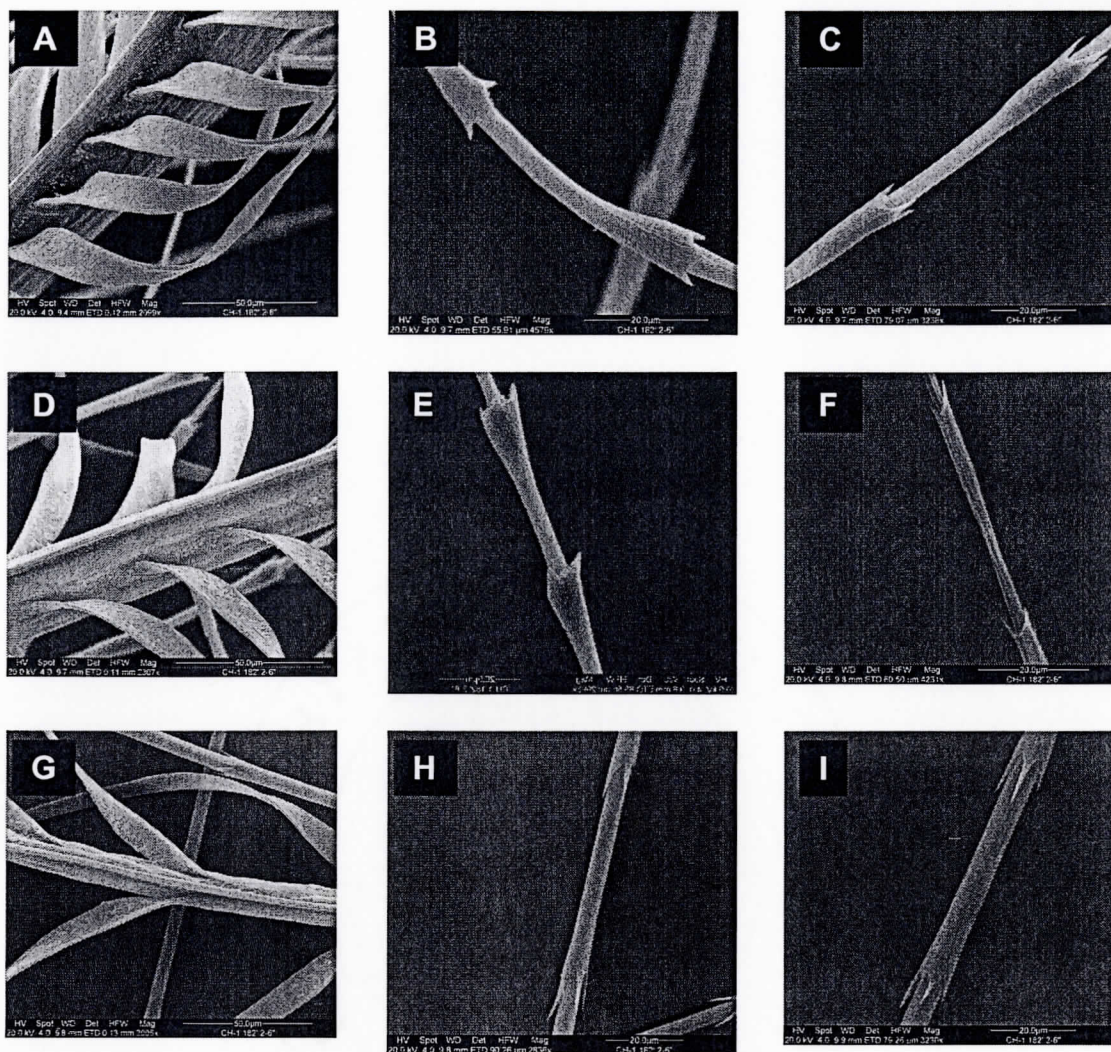


Figure 17. Scanning electron microscopy (SEM) micrographs of contour feathers from medial pectoral tract of the eastern screech owl. (A) proximal barbule base (B) proximal barbule, proximal nodes (C) proximal barbule, intermediate nodes (D) intermediate barbule base (E) intermediate barbule, proximal nodes (F) intermediate barbule, distal nodes (G) distal barbule base (H) distal barbule, proximal nodes (I) distal barbule, intermediate nodes

Transmission Electron Microscopy:

TEM visualizations of feather cross-sections revealed a central vacuole that was surrounded by a spongy layer which was surrounded by a keratin cortex with melanin globules present (Figure 18) and were similar to previous descriptions (Dyck 1971; Shawkey et al. 2006a, 2006b). Intraspecific melanin percentage of the cortex or cortex percentage of

the entire feather did not vary significantly between gray and rufous feathers (Table 9). Interindividual differences of feather physical constituents from the proximal to the distal barb described by Dyck (1971) and Shawkey et al. (2005) were not investigated in the present study and remain open for further research.

Dorsal eastern screech owl feathers have a distinct dorsal and ventral ridge which probably serves as support for the feather (Mascha 1909; Chandler 1916; Lucas and Stettenheim 1972; Shawkey personal communication), however, the dorsal ridge varied considerably between micrographs and was thus discarded from quantitative analysis.

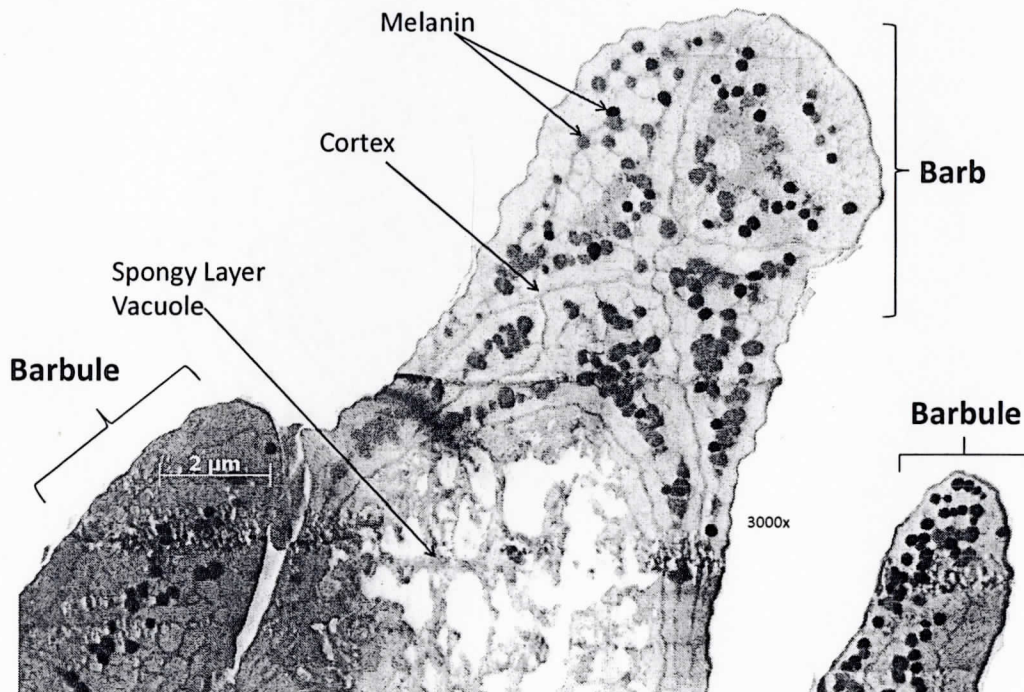


Figure 18. Transmission electron microscopy (TEM) micrograph (3000x) of the distal region of a rufous eastern screech owl dorsal feather barb and barbule.

Table 9. Summary statistics, *P*-value, and *T*-value from student's *t*-test of physical and chemical constituent percentages in eastern screech owl color variant feathers. Means \pm Standard error, $n=3$.

Measurement	Color		P-value	T-value
	Gray	Rufous		
Cortex % of the Feather	51.07 \pm 5.39	58.57 \pm 8.38	0.49	-0.75
Melanin % of the Cortex	9.11 \pm 2.42	9.17 \pm 2.60	0.98	-0.02

DISCUSSION

Light Microscopy and Macroscopic Measurements:

Body Level and Feather and Barb Level:

The main focus of this study was to assess microstructural differences between eastern screech owl color morphs, thus obtaining a homogenous body and feather size while maintaining a heterogenous color sample was of paramount importance. None of the comparisons of owls of different colors yielded significant results at the body level (see Gehlbach 2003 for a more thorough compilation of eastern screech owl body measurements). The only significant difference between owl color morphs at the feather and barb level was a shorter pennaceous rachis length in the medial pectoral tract of brown owls. Thus, the macroscopic size of the owls and feathers used in this study should not have affected the microscopic results obtained.

Barbule Level:

My results indicate that the length between barbules was significantly different at three tracts of each of the proximal and intermediate barbules and one tract of the distal barbules. In all seven of the above cases, the rufous morph length between barbules was greater than gray morphs and in six cases greater than brown morphs. If the contour feathers of the rufous morph have a greater length between barbules then the thermal efficiency of the feathers would not be as great. The above result is interesting because Pittaway (1995) noted that the density of feathers on the legs of rufous morphs was not as great as gray morphs.

The rufous morphs also exhibited significantly lower numbers of pigmented nodes than gray or brown morphs, primarily in the distal barb. The possibility exists that rufous pigments are harder to detect with light microscopy than gray or brown pigmentation. However, if the rufous morphs had lower nodal pigmentation then higher amounts of light would be refracted from the plumage (Cena and Monteith 1975a) and may account for the decreased radiative transfer observed in rufous morphs (Dexter 1996). Although a larger sample size is desirable, the hypothesis that there may be microstructural differences in feather morphology that may influence morph clinal variation has been supported at the barbule level.

Barbule Segment Level:

Significant differences of owls of different color morphs at the barbule segment level at the proximal and intermediate barbs do not seem to correlate with any one specific tract or barbule portion. Most significant differences between colors are between the distal barbules. The distal portions of feather barbs are morphologically less defined than the proximal portions and therefore more “unique” morphological structures occur, especially spine and pigment lengths. A majority of the significant differences were due to rufous owls. When proximal-distal pigment length had high loading factors the significant differences may be due to the resolution of the different melanin subtype colors in the microscope. Overall analyses did not exhibit a consistent pattern according to color or feather tract and the assumption cannot be made that there are morphological differences between eastern screech owl color variant feathers at the barbule segment level that would contribute to the observed clinal variation.

Scanning Electron Microscopy:

Scanning electron microscopy allows for high quality and high resolution views of feather nodal structures. Nodal structures remain similar within a species (Mascha 1905; Chandler 1916; Sick 1937; Dyck 1966; Brom 1986; Brom and Prins 1989; Brom and Frank 1992; Dove 1997; Dyck 1999; Stettenheim 2000) but can vary between pterylae from individuals and between families (Gilroy 1980; Perremans et al. 1992; Koch and Wagner 2002). Due to the variation observed in nodal structures between taxonomic groups, they have been used for taxonomic differentiation (Chandler 1916; Reaney et al. 1978; Dove 1997; Lei et al. 2002). Within the Strigiformes, there is little variation in the feather anatomy between any of the species (Mascha 1905; Chandler 1916; Sick 1937; Robertson et al. 1984; personal observation). Owls have highly specialized feathers for dampened sound production (Lucas and Stettenheim 1972; Gill 1995). Fishing owls (genus *Scotopelia*) tend to have shortened pennulums for a possible increase in water repellency (Sick 1937) and barn owls tend to have longer spines (personal observation); however, the eastern screech owl had 'typical strigiform' nodes.

Transmission Electron Microscopy:

There have been many published transmission electron micrographs of feather cross-sections (Andersson 1999; Shawkey et al. 2003, 2005, 2006a, 2006b; Doucet et al. 2004; Shawkey and Hill 2006); however, to date, there have been no TEM visualizations of an owl feather. TEM micrographs of bird feathers reveal that in bird feathers, melanin deposition can occur in the spongy layer and vacuole (Steller's jay and eastern bluebird) in the barbule (red-winged blackbird, screaming cowbird, giant cowbird, bronzed cowbird, shiny cowbird, brown-headed cowbird, western meadowlark, bobolink, scrub blackbird, great-tailed grackle,

and boat-tailed grackle) and in the cortex (eastern and western bluebird) (Shawkey et al. 2005, 2006a, 2006b; Shawkey and Hill 2006). Melanin is present in the cortex of the eastern screech owl, and the subtype of melanin reflects light of different wavelengths which we then perceive as rufous (phaeomelanin) or gray (eumelanin) (McGraw et al. 2005; Cuthill 2006; McGraw 2006; They 2006; Shawkey et al. 2006b). To determine if differential pigmentation can lead to differential strength, we must understand how the feather constituents are arranged. The results of the TEM micrographs reveal that the microstructural constituents of the gray and rufous morphs are arranged in the same way. Further, the lack of significant difference between the percentage area that the constituents occupy in the feather cross-sections suggests that melanin subtype does not cause differential strength through a difference in cortex thickening as has been previously implicated in melanic vs. non-melanic feathers (Butler and Johnson 2004). However, tensile strength tests (Chapter 4) have not previously been employed along with TEM to understand if the melanin subtypes could be responsible for differential strength (such as through amino acid side chain interactions).

CHAPTER 4

MELANIN ENDOCRINOLOGY, BIOCHEMISTRY, AND BIOMECHANICS

INTRODUCTION

Melanin is the most ubiquitous light absorbing pigment found in the animal kingdom (McGraw 2006). The production of melanin involves interplay between the endocrine and integumentary system. Melanin coloration is responsible for much black, gray, brown, and rufous coloration observed in animals and is strongly heritable (McGraw 2006). While quantitative analysis of melanin coloration has been difficult (Ito and Fujita 1985), the function of melanin deposition in biological tissue has been implicated in disease (Hadley 1999), protection and strength (reviewed in Bortolotti 2006), crypsis (reviewed in Bortolotti 2006), and sexual signaling (reviewed in Jawor and Breitwisch 2003).

Melanin production is a product of chemical reactions of the endocrine system and the formation and appearance of melanin has been described in detail (Brumbaugh 1968; Kobayashi et al. 1995; Hadley 1999; Roulin and Dijkstra 2003; Boswell and Takeuchi 2005). In birds, melanin production occurs as a cutaneous melanocortin system or the pars distalis synthesizes melanocyte stimulating hormone (MSH) (Brandstatter and Abraham 2003; Boswell and Takeuchi 2005). MSH can be antagonized by the hypothalamus releasing a catecholamine, most likely dopamine, or chlorpromazine (Hadley 1999). Pigmentation will take place if MSH initiates a specific cascade of events.

Melanin is produced by melanocytes or melanophores in the feather follicle (Stevens 1996; Hadley 1999; Boswell and Takeuchi 2005). Melanocytes are differentiated neural crest

cells which are then distributed throughout the skin and produce plumage patterns in avian species (Stevens 1996). Melanocytes are nested within melanosomes or melanin granules (Boswell and Takeuchi 2005). The melanocytes grow dendritic processes and the melanosomes travel to surrounding cells through cytotrine mechanisms and secrete melanin into other cells (Hadley 1999). The type of melanin produced is dependent on many factors.

There are two different types of melanin, pheomelanin (red) and eumelanin (gray) (Figure 19), that can produce different colors depending on the concentrations (Hadley 1995; Stevens 1996; Roulin and Dijkstra 2003; Boswell and Takeuchi 2005). Agouti stimulating protein (ASP) is a melanocortin-1-receptor (MC1R) antagonist and inhibits eumelanin synthesis (Boswell and Takeuchi 2005). If eumelanin synthesis is inhibited then pheomelanin will be produced, which Boswell and Takeuchi (2005) refer to as the “default product of the melanin biosynthetic pathway”. Pheomelanin (N=8-11%, S=9-12%) can also be produced if sufficient sulfhydryls are available (Figure 20). The rate reaction for the first pheomelanin intermediary, cysteinyl-dopa, is 8.8×10^5 M/s (Figure 21) and cysteinyl-dopa is preferred if the cysteine concentration is greater than $1 \mu\text{M}$ (Wakamatsu and Ito 2002). Pheomelanogenesis is preferred if the cysteinyl-dopa concentration is above $10 \mu\text{M}$. If tyrosinase oxidizes dopaquinone to leucodopachrome, black melanin or eumelanin (N=6-9%, S=0-1%) is produced (Kobayashi et al. 1995). The rate reaction for dopachrome is 7×10^5 M/s (Wakamatsu and Ito 2002). If tyrosinase does not oxidize dopaquinone then pheomelanin will be produced, due to the incorporation of glutathione or cysteine (Ito 2003). Eumelanin is a rod shaped molecule (Brumbaugh 1968), while pheomelanin is more rounded than eumelanin. Pheomelanin contains more sulfhydryls than eumelanin, which could lead to a decreased uptake of tyrosine. The form of melanin deposited into tissues from these initial biochemical

steps could have important implications on tissue biomechanics. Differential pigmentation influencing tissue biomechanics could affect the ecological distribution of color polymorphic birds.

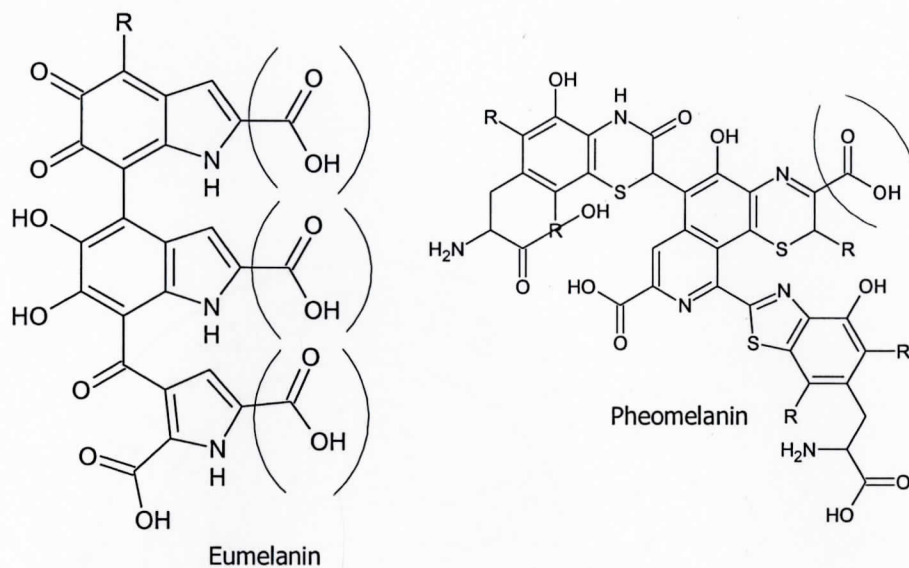


Figure 19. Structure of eumelanin and pheomelanin (redrawn from Wakamatsu and Ito 2002).

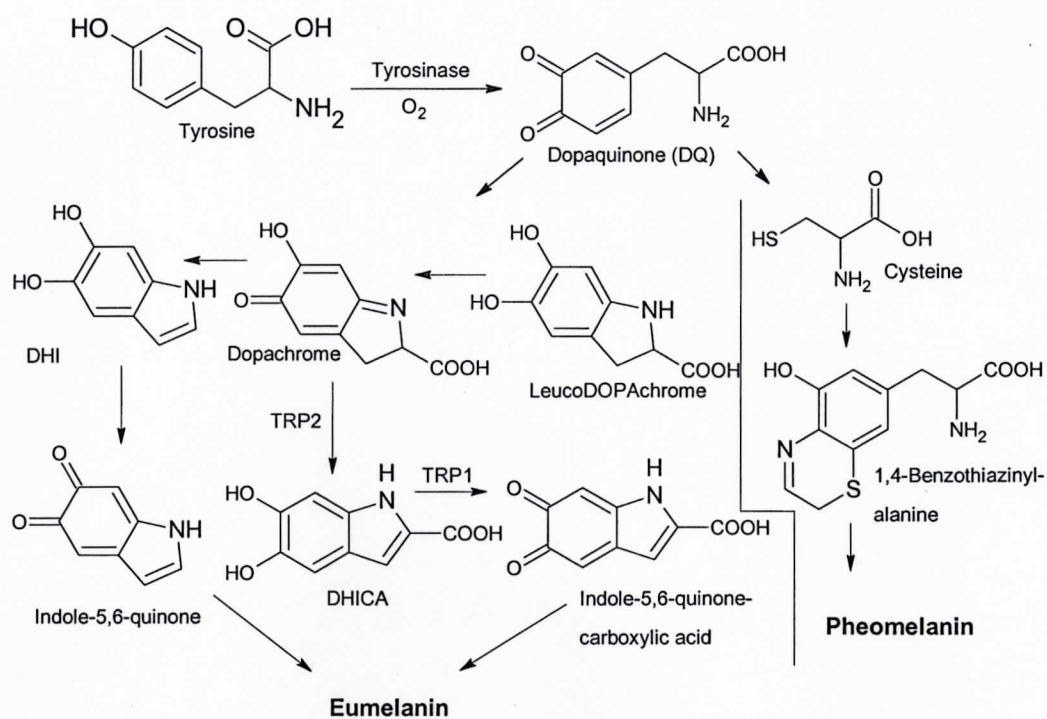


Figure 20. The biochemical pathway for eumelanin and pheomelanin (DHICA-5,6-dihydroxyindole-2-carboxylic acid, DHI-dihydroxyindole, TRP-tyrosinase related enzyme) (redrawn from Kobayashi et al. 1995).

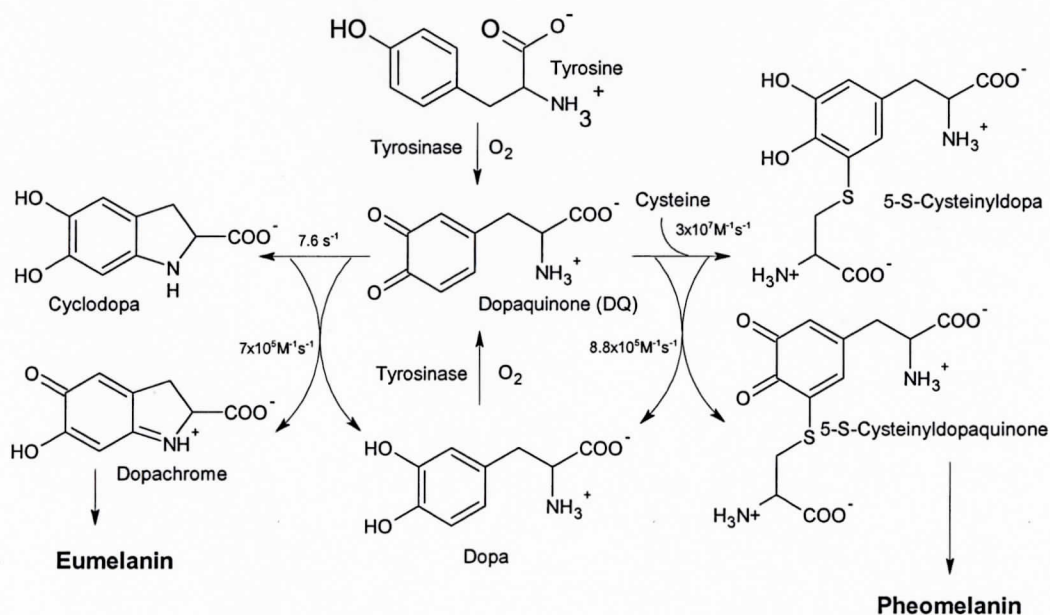


Figure 21. Rate reactions for beginning intermediates in pheomelanin and eumelanin production (redrawn from Ito 2003).

The effect of melanin deposition on abrasion resistance of feathers has been debated for years. Some scientists have speculated that increased melanin concentration or the presence of melanin serves to harden feathers (reviewed in Bortolotti 2006). An increase in strength of melanized keratin has been alluded to by Bonser (1995, 1996a, 1996b) who studied Vicker's hardness, or the materials' ability to resist mechanical deformation, of the European starling's bill, feathers, and claws. Burt (1986) blew glass beads on feathers and determined that melanized barbs fractured less than unmelanized barbs. Goldstein et al. (2004) found that melanized feathers responded more slowly to bacterial degradation than unmelanized feathers, and hypothesized that melanin may somehow bond and make a stronger feather. Conversely, a lack of melanin may result in weaker feathers. For example, an albino great frigatebird was found with a higher degree of feather wear than its pigmented counterparts (Schreiber et al. 2006). However, Butler and Johnson (2004) measured tensile strength from the flight feather of an osprey and showed that if the morphological placement, cross-sectional area, breaking force, breaking stress, breaking strain, and toughness of the feather are taken into consideration then the melanin does not strengthen the feather material but thickens it and possibly leads to higher resistance to mechanical deformation by secreting melanoproteins into the cortex. Butler and Johnson (2004) used flight feathers, which would theoretically be strengthened for flight. Perhaps the gray morph of the eastern screech owl is more abundant in dry dusty environments because of their thicker or stronger feathers. However, rufous melanin has a higher sulfur content which may increase di-sulfide bonding and increase feather toughness (Figure 19) (Brumbaugh 1968; Jawor and Breitwisch 2003).

The purpose of the present chapter is to determine the tensile strength of eastern screech owl feathers of different colors and use SEM analysis to determine the cross-sectional area of

the breakage point. The force required to break the feathers will be normalized with the cross-sectional area to investigate if different melanin subtype leads to differential strength through dissimilar molecular interactions.

MATERIALS AND METHODS

Tensile strength tests of barbs from dorsal feathers of eastern screech owl color variants were performed under the supervision of Dr. Louis T. Germinario of the Physical Chemistry Research Laboratory of the Eastman Chemical Company; Kingsport, TN. Barbs were removed from the proximal pennaceous portion of the rachis of dorsal feathers. Barbs were chosen from the opposite side of barbs used in TEM (chapter 3) so cross-sections of barbs could be compared to tensile strength results. Breaking strength was collected from at least three barbs from a dorsal feather from eight individuals, but five data points from each individual were desired. Dorsal feathers were chosen because the only other study to consider morphological and mechanical variables together (Butler and Johnson 2004) used a primary flight feather, which should naturally be strengthened for flight requirements. Since dorsal feathers are not required to sustain airflow for flight like flight feathers, then a more realistic representation of a possible link between pigment deposition and tissue strength should theoretically be obtained.

Barbs were superglued between two pieces of polyethylene and inserted into brass tension grips. The barbs were extended at a controlled strain (preload force of 0.0010 Newtons (N), an initial displacement of 10.0 μm , and a ramp displacement of 100.0 $\mu\text{m}/\text{min}$) until breakage in a Q800 dynamic mechanical analyzer (DMA). The tensile strength was measured using Thermal Analysis Q series and Universal Analysis 2000 data analysis software. Breakage points were examined using SEM using the procedures of Butler and Johnson (2004). Height, width, and cross-sectional area of breakage points were measured

using AxioVision AC Release 4.3 software. Data points for mechanical and morphological variables were averaged together for each of the eight individual owls to avoid pseudoreplication. Breakage force and breakage stress of rufous and gray barbs were compared using a student's *t*-test in SAS 9.1 for Windows 2002-2003 (Zar 2005; Cody and Smith 2006).

RESULTS

The average height at the breakage point of eastern screech owl dorsal feather barbs was $107.91 \mu\text{m} \pm 0.03$ and mean width was $53.48 \mu\text{m} \pm 0.01$ (Table 10-11). There was no significant difference between the breaking force (F_{brk}) (Figure 22, Table 12), the N required to break the barb, or breaking stress (σ_{brk}) (Figure 23, Table 12), the F_{brk} divided by the cross-sectional area of the cortex (s_c), of the differently pigmented feather barbs (Table 12). Rufous barbs had a significantly higher s_c (Figure 24, Table 12), but when F_{brk} was normalized with s_c there was no significant difference between the two colors (Table 12).

The results of the present study indicate that there are no significant differences between the feather tensile strength of the color morphs and differential tensile strength does not covary with the eastern screech owls clinal variation.

Table 10. Terms and abbreviations for tensile strength tests of eastern screech owl dorsal feather barbs.

Tensile Strength Terms and Variables	
Breaking Force= F_{brk}	Mean Radius= r
Cross-sectional area of Barb= s_o	Breaking extension= l_{brk}
Cross-sectional area of Cortex= s_c	Original Length= l_o
Cross-sectional area of Vacuole= s_m	Breaking Stress (σ_{brk})= F_{brk}/s_c
Outer Radius= r_o	Breaking Strain (ϵ_{brk})= l_{brk}/l_o
Inner Radius= r_i	Wall Thickness= t

Table 11. Pooled summary statistics of morphological measurements of the breakage point of eastern screech owl dorsal contour feathers ($n = 33$).

Variable	Mean	Std Dev
Cross-sectional area of Cortex (s_c) (mm^2)	0.00033	<0.01
Cross-sectional area of Vacuole (s_m) (mm^2)	0.00052	<0.01
Height (μm)	107.91	0.03
Width (μm)	53.48	0.01

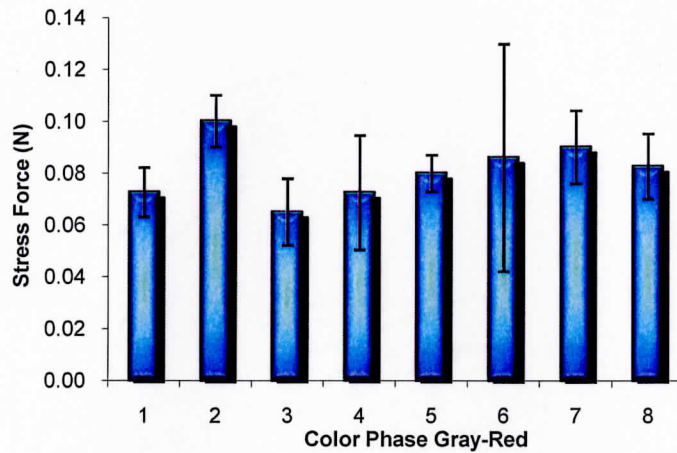


Figure 22. Average mean breaking force (N) and standard deviation for eastern screech owl dorsal barbs (1=grayest, 8=reddest; $n=3$ for 1 and 2; $n=4$ for 3, 4, and 8; $n=5$ for 5, 6, and 7).

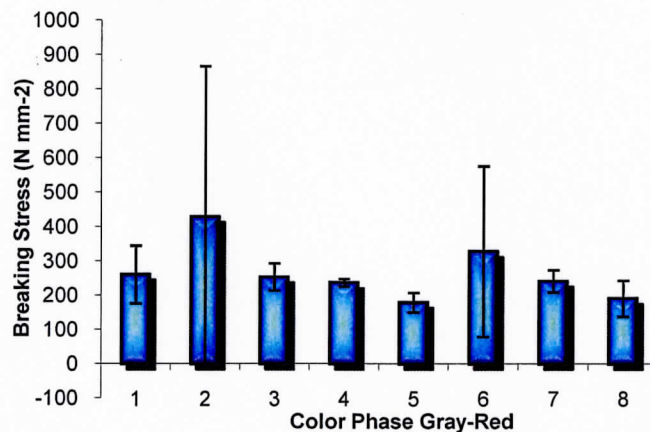


Figure 23. Average breaking stress (N mm^{-2}) and standard deviation for eastern screech owl dorsal barbs (1=grayest, 8=reddest; $n=3$ for 1 and 2; $n=4$ for 3, 4, and 8; $n=5$ for 5, 6, and 7).

Table 12. Summary statistics of morphological measurements and mechanical variables of the breakage point of eastern screech owl color variant dorsal feather barbs. Means \pm Standard Error, $n = 4$, significant models are in bold.

Variable	Color		P-Value	T-Value
	Gray	Red		
Breaking Force (F_{brk}) (N)	0.08 \pm 0.01	0.08 \pm 0.01	0.54	-0.65
Breaking Stress (σ_{brk}) (N mm ⁻²)	293.7 \pm 44.80	213.7 \pm 17.08	0.14	-1.67
Displacement (mm)	0.32 \pm 0.02	0.43 \pm 0.05	0.09	-2.01
Cross-sectional area of Barb (s_o) (mm ²)	0.00083 \pm <0.01	0.0010 \pm <0.01	0.12	-1.81
Cross-sectional area of Cortex (s_c) (mm ²)	0.00027 \pm <0.01	0.00039 \pm <0.01	0.05	-2.53
Cross-sectional area of Vacuole (s_m) (mm ²)	0.00047 \pm <0.01	0.00057 \pm <0.01	0.32	-1.08
Dorsal Ridge Length (μ m)	44.25 \pm 0.03	21.80 \pm 0.01	0.52	0.69
Height (μ m)	153.68 \pm 0.11	83.83 \pm 0.03	0.55	0.63
Width (μ m)	66.13 \pm 0.04	47.90 \pm 0.02	0.71	0.40

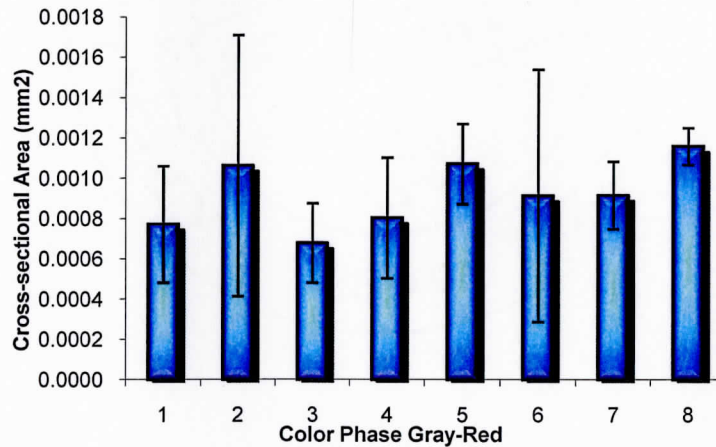


Figure 24. Average cross-sectional area (mm²) and standard deviation for eastern screech owl dorsal barbs (1=grayest, 8=reddest; $n=3$ for 1 and 2; $n=4$ for 3, 4, and 8; $n=5$ for 5, 6, and 7).

DISCUSSION

The present study failed to find any significant differences in the tensile strength of eastern screech owl color variants. Differential strength conferred by type of melanin deposition should not influence low rufous frequency in dry dusty parts of the eastern screech owls range. Because the microstructural anatomy of the feather was considered, the evidence suggests that melanin subtype does not influence pigment amount and pheomelanin does not provide greater strength through molecular interactions. Gehlbach (1994) attributed high rufous frequencies in humid environments to the scattering of red wavelengths of light by water (Cena and Monteith 1975a); however, dust has the same effect on red light and would theoretically benefit rufous morphs in crypsis (Cena and Monteith 1975a, 1975c). Factors for the gray morphs dominance in dry dusty environments remain to be elucidated if low rufous frequency cannot be explained by crypsis or abrasion resistance.

The hypothesis that differential pigmentation may lead to differential strength has been rejected but the importance of quantifying morphological parameters of feathers in conjunction with biomechanical testing has been supported. The physical properties and dynamics of feathers have been studied extensively yet the potential relationship between pigmentation and feather strength has been controversial (Burt 1986; Bonser 1996a, 1996b; Corning and Biewener 1998; Fitzpatrick 1998; Niecke et al. 1999; Burt and Ichida 2004; Butler and Johnson 2004; Goldstein et al. 2004; Schreiber et al. 2006; Saranathan and Burt 2007). Many researchers have found that different pigments, such as melanin, tended to lower the amount of feather breakage or inhibit bacterial degradation (Burt 1986; Burt and

Ichida 2004; Schreiber et al. 2006). However, until Butler and Johnson (2004) no study investigated the microstructural size of the feathers. Because the microstructural size of feathers vary considerably within a single bird and even within a single feather, feather size must be considered a confounding factor in all studies that do not incorporate cross-sectional area of breakage points (Lucas and Stettenheim 1972). Although tensile strength tests may not mimic natural conditions as well as the abrasion experiments done by Burt (1986), the logistics of obtaining cross-sectional areas after an abrasion experiment are daunting.

CHAPTER 5

GENERAL CONCLUSIONS

Researchers in the past have produced hand drawn maps to find land composition or environmental variables that may be associated with eastern screech owl color morph frequency; however no previous attempts have utilized GIS capabilities (Hasbrouck 1893a, 1893b; Owen 1963a, 1963b; Dexter 1996). My research on the current GIS land cover analysis did not result in any new correlations between color morph frequency and land composition from previously published work. However, by using GIS future studies should have higher accuracy and reproducibility. Rufous morphs tend to be located in counties with high levels of deciduous forests while gray morphs dominate in areas of mixed and evergreen forests and cultivated land (Figures 2-9, Table 1). In general, rufous morphs dominate in 'prime' eastern screech owl habitats while gray morphs dominate at the peripheries of the range.

The light microscope is a tool that has been used to describe and quantify the morphological parameters of feathers for over a century (Mascha 1905; Chandler 1916; Sick 1937; Lucas and Stettenheim 1972). Morphological quantification of feathers with light microscopy has mainly been used for taxonomic differentiation at the family level (Brom 1986; Dove 1997) and has never been utilized to investigate a single color polymorphic species. The present study used a sample size that consisted of owls and feathers of similar size (Tables 4-5). Light microscopy revealed that the rufous morphs of the eastern screech owl may have morphological differences from gray morphs in the plumage anatomy that may

affect the clinal variation observed. Rufous morphs tend to have a greater length between barbules (Table 6) and less nodal pigmentation (Table 6) that may decrease thermal efficiency and increase radiative transfer, but more analysis with higher sample sizes is required at the barbule level. No consistent patterns emerged from the PCA at the barbule segment level that would indicate morphological differences between colors that would influence the clinal variation.

SEM analysis is useful in the qualitative analysis of feathers because higher resolution micrographs of feather nodes can be produced than could be achieved with light microscopy. Nodal structures of barbules are used extensively for taxonomic differentiation in birds; however, SEM analysis did not demonstrate any defining differences in nodal structures in the eastern screech owl from the rest of the Strigiformes (Figures 14-18). TEM analysis is useful for determining cross-sections of biological tissue at very small scales. TEM visualization demonstrated a coordination of feather constituents similar to previously published micrographs (Figure 18), but there was no significant difference between color morphs for placement or amount of any feather constituent (Table 9). Melanin amount or placement was not affected by melanin subtype.

There have been conflicting results in the literature concerning differential pigmentation affecting strength in biological tissue (reviewed in Bortolotti 2006). Studies that concluded melanin deposition or subtype could strengthen feathers did not consider morphological parameters (Burt 1986). If feather morphology is considered along with the force applied to break the feather then differential pigmentation does not result in differential strength (Butler and Johnson 2004). In the eastern screech owl, feather tensile strength was not significantly different between color morphs due to differential pigmentation (Figure 23,

Table 12). The hypothesis that melanin subtype could affect feather strength and possibly clinal variation in eastern screech owls was rejected.

I conclude that the microstructural anatomy in the eastern screech owl color variant plumage may be significantly different in rufous morphs at the barbule level, specifically greater length between barbules and decreased nodal pigmentation, and may lead to a decrease in thermal efficiency. A decrease in the thermal efficiency of the plumage of rufous morphs may inhibit occupation of colder habitats. The tensile strength of eastern screech owl feathers is not different due to differential melanin subtype deposition and does not contribute to the observed clinal variation in the eastern screech owl color morphs.

REFERENCES

- American Museum of Natural History (AMNH). 2006. Personal communication.
- Andersson, S. 1999. Morphology of UV reflectance in a whistling-thrush: implications for the study of structural colour signaling in birds. *Journal of Avian Biology* 30:193-204.
- Audubon Society of FL and NC (Audubon). 2006. Personal communication.
- Avise, J. C., and D. Walker. 1998. Pleistocene phylogeographic effects on avian populations and the speciation process. *Royal Society of Biology* 265:457-463.
- Baker, A. J. 1974. Melanin pigmentation in the dorsal plumage of New Zealand oystercatcher. *New Zealand Journal of Zoology* 1:159-164.
- Banks, R. C., C. Cicero, J. L. Dunn, A. W. Kratter, P. C. Rasmussen, J. V. Remsen, Jr., J. D. Rising, and D. F. Stotz. 2003. Forty-fourth supplement to the American Ornithologists' Union Checklist of North American Birds. *The Auk* 120:923-931.
- Belthoff, J. R., and A. M. Dufty Jr. 1998. Corticosterone, body condition and locomotor activity: A model for dispersal in screech owls. *Animal Behavior* 55:405-415.
- Belthoff, J. R., and G. Ritchison. 1990. Nest-site selection by eastern screech-owls in central Kentucky. *The Condor* 92:982-990.
- . 1989. Natal dispersal of eastern screech-owls. *The Condor* 91:254-265.
- Belthoff, J. R., E. J. Sparks, and G. Ritchison. 1993. Home ranges of adult and juvenile eastern screech owls: Size, seasonal variation and extent of overlap. *Journal of Raptor Research* 27:8-15.
- Bond, A. B., and A. C. Kamil. 2006. Spatial heterogeneity, predator cognition, and the evolution of color polymorphism in virtual prey. *Proceedings of the National Academy of Sciences* 103:3214-3219.
- Bonser, R. H. C. 1995. Melanin and the abrasion resistance of feathers. *Condor* 97:590-591.
- . 1996a. The mechanical properties of feather keratin. *Journal of Zoology (London)* 239:477-484.

- . 1996b. Comparative mechanics of bill, claw and feather keratin in the common starling *Sturnus vulgaris*. *Journal of Avian Biology* 27:175-176.
- Bortolotti, G. R. 2006. Natural selection and coloration: Protection, concealment, advertisement, or deception? Chap. 3 in G. E. Hill and K. J. McGraw, eds. *Bird coloration: Function and evolution*. Harvard University Press, Cambridge, MA.
- Boswell, T., and S. Takeuchi. 2005. Recent developments in our understanding of the avian melanocortin system: Its involvement in the regulation of pigmentation and energy homeostasis. *Peptides* 26:1733-1743.
- Bozzola, J. J., and L. D. Russell. 1999. *Electron microscopy: Principles and techniques for biologists*. 2nd Ed. Jones and Bartlett Publishers. Sudbury, MA.
- Brandstaetter, R., and U. Abraham. 2003. Hypothalamic circadian organization in birds. I. Anatomy, functional morphology, and terminology of the suprachiasmatic region. *Chronobiology International* 20:637-655.
- Bretagnolle, V. 1993. Adaptive significance of seabird coloration: The case of Procellariiforms. *The American Naturalist* 142:141-173.
- Brito, P. H. 2005. The influence of Pleistocene glacial refugia on tawny owl genetic diversity and phylogeography in western Europe. *Molecular Ecology* 14:3077-3094.
- Brittan-Powell, E. F., B. Lohr, D. C. Hahn, and R. J. Dooling. 2005. Auditory brainstem responses in the Eastern Screech Owl: An estimate of auditory thresholds. *Journal of the Acoustical Society of America* 118:314-321.
- Brom, T. G. 1986. Microscopic identification of feathers and feather fragments of Palearctic birds. *Bigdragen Tot de Dierkunde* 56:181-204.
- Brom, T. G., and T. G. Prins. 1989. Microscopic investigation of feather remains from the head of the Oxford dodo, *Raphus cucullatus*. *The Zoological Society of London* 218:233-246.
- Brom, T. G., and U. Frank. 1992. The diagnostic and phylogenetic significance of widened and pronged hamuli in feathers. *Scanning Microscopy* 6:597-602.
- Brommer, J. E., K. Ahola, and T. Karstinen. 2005. The colour of fitness: Plumage coloration and lifetime reproductive success in the tawny owl. *Proceedings of the Royal Society of London: Series B* 272:935-940.
- Brumbaugh, J. A. 1968. Ultrastructural differences between forming eumelanin and pheomelanin as revealed by the pink-eye mutation in the fowl. *Developmental Biology* 18:375-390.

- Buhay, J. E., and G. Ritchison. 2002. Hunting behavior of and space use by eastern screech owls during the breeding season. *Journal of Raptor Research* 36:194-199.
- Bull, J. L. 1964. *Birds of the New York area*. Harper and Row, NY.
- Burleigh, T. D. 1958. *Georgia birds*. University of Oklahoma Press. Norman, OK.
- Burt, E. H. Jr. 1986. An analysis of physical, physiological, and optical aspects of avian coloration with emphasis on wood-warblers. *Ornithological Monographs No.* 38:1-128.
- Burt, E. H. Jr., and J. M. Ichida. 2004. Gloger's rule, feather-degrading bacteria, and color variation among song sparrows. *The Condor* 106:681-686.
- Butler, M., and A. S. Johnson. 2004. Are melanized feather barbs stronger? *Journal of Experimental Biology* 207:285-293.
- Cena, K., and J. L. Monteith. 1975a. Transferprocesses in animal coats I. Radiative transfer. *Proceedings of the Royal Society of London: Series B* 188:377-393.
- . 1975b. Transferprocesses in animal coats II. Conduction and convection. *Proceedings of the Royal Society of London: Series B* 188:395-411.
- . 1975c. Transferprocesses in animal coats III. Water vapour diffusion. *Proceedings of the Royal Society of London: Series B* 188:413-423.
- Cody, R. P., and J. K. Smith. 2006. *Applied statistics and the SAS programming language*. 5th Ed. Pearson Prentice Hall, NJ.
- Chandler, A. C. 1916. A study of the structure of feathers, with reference to their taxonomic significance. *University of California Publications Zoology* 13:243-446.
- Cooke, F., D. T. Parkin, and R. F. Rockwell. 1988. Evidence of former allopatry of the two color phases of lesser snow geese *Chen caerulescens caerulescens*. *Auk* 105:467-479.
- Corning, W. R., and A. A. Biewener. 1998. *In vivo* strains in pigeon flight feather shafts: Implications for structural design. *The Journal of Experimental Biology* 201:3057-3065.
- Cuthill, I. C. 2006. Color perception. Chap. 1 in G. E. Hill and K. J. McGraw, eds. *Bird coloration: Mechanisms and mechanics*. Harvard University Press, Cambridge, MA.
- Dale, J. 2000. Ornamental plumage does not signal male quality in red-billed queleas. *The Royal Society of London: Series B* 267:2143-2149.

- Daniels, K., and G. E. Duke. 1980. Factors influencing respiratory rates in four species of raptors. *Comparative Biochemistry and Physiology* 664:703-706.
- DeCandido, R. 2005. History of the eastern screech-owl (*Megascops asio*) in New York City, 1867-2005. *Urban Habitats* 3:117-133.
- Dexter, M. A. 2006. Personal communication.
- . 1996. Plumage dichromatism and thermal ecology of the eastern screech owl (*Otus asio*). M.S. thesis, Wake Forest University, Winston-Salem, NC.
- Dorn, R. D., and J. L. Dorn. 1994. Further data on screech owl distribution and habitat use in Wyoming. *Western Birds* 25:35-42.
- Doucet, S. M., M. D. Shawkey, M. K. Rathburn, H. L. Mays Jr., and R. Montgomerie. 2004. Concordant evolution of plumage colour, feather microstructure and a melanocortin receptor gene between mainland and island populations of a fairy-wren. *Proceedings of the Royal Society of London: Series B* 271:1663-1670.
- Dove, C. J. 1997. Quantification of microscopic feather characters used in the identification of North American Plovers. *The Condor* 99:47-57.
- Duley, L. J. 1979. Life history aspects of the screech owl (*Otus asio*) in Tennessee. M.S. thesis, University of Tennessee, Knoxville, TN.
- Dyck, J. 1966. Determination of plumage colours, feather pigments and structures by means of reflection spectrophotometry. *Dansk Ornithologiske Forenings Tidsskrift* 60:50-76.
- . 1971. Structure and colour-production of the blue barbs of *Agapornis roseicollis* and *Cotinga maynana*. *Z. Zellforsch* 115:17-29.
- . 1999. Feather morphology at the ultrastructural level. *Acta Ornithologica* 34:131-134.
- Endler, J. A. 1978. A predator's view of animal color patterns. *Evolutionary Biology* 11:319-364.
- Environmental Systems Research Institutes. 2005. ArcGIS desktop. <http://www.esri.com/>. Access date, December 1, 2006.
- Fitton, S. 1993. Screech-owl distribution in Wyoming. *Western Birds* 24:182-188.
- Fitzpatrick, S. 1998. Birds' tails as signaling devices: Markings, shape, length, and feather quality. *The American Naturalist* 151:157-173.

- Fowler, L. J. 1985. Breeding birds and vegetation along the Duck River in Middle Tennessee. *Tennessee Academy of Science Journal* 60:40-43.
- Fowlie, M. K., and O. Kruger. 2003. The evolution of plumage polymorphism in birds of prey and owls: The apostatic selection hypothesis revisited. *Journal of Evolutionary Biology* 16:577-583.
- Galeotti, P., and C. Cesaris. 1996. Rufous and grey colour morphs in the Italian tawny owl: Geographical and environmental influences. *Journal of Avian Biology* 27:15-20.
- Galeotti, P., and R. Sacchi. 2003. Differential parasitaemia in the tawny owl (*Strix aluco*): effects of colour morph and habitat. *Journal of Zoology* 261:91-99.
- Galeotti, P., D. Rubolini, P. O. Dunn, and M. Fasola. 2003. Colour polymorphism in birds: Causes and functions. *Journal of Evolutionary Biology* 16:635-646.
- Galeotti, P., and D. Rubolini. 2004. The niche variation hypothesis and the evolution of colour polymorphism in birds: A comparative study of owls, nightjars and raptors. *Biological Journal of the Linnean Society* 82:237-248.
- Gehlbach, F. R. 1994. *The eastern screech-owl: Life history, ecology, and behavior in the suburbs and countryside*. Texas A&M University Press, College Station, TX.
- . 1995. Eastern screech-owl. *Birds of North America* 165:1-24.
- . 2003. Body size variation and evolutionary ecology of eastern and western screech-owls. *Southwestern Naturalist* 48:70-80.
- Gill, F. B. 1995. *Ornithology*. 2nd Ed. W.H. Freeman and Company, NY.
- Gilroy, B. A. 1980. Microscopic variation in plumulaceous barbules of the rock dove, *Columba livia* (Aves: Columbidae). M.S. thesis, George Mason University, Fairfax, VA.
- GIS data depot. 2007. <http://data.geocomm.com/>. Access date, April 24, 2006.
- Goldstein, G., K. R. Flory, B. A. Browne, S. Majid, J. M. Ichida, and E. H. Burt Jr. 2004. Bacterial degradation of black and white feathers. *The Auk* 121:656-659.
- Grant, B. R., and P. R. Grant. 2003. What Darwin's finches can teach us about the evolutionary origin and regulation of biodiversity. *Bioscience* 53:965-975.
- Gullion, G. W., and W. H. Marshall. 1968. Survival of Ruffed Grouse in a Boreal Forest *Bonasa umbellus*. *Living Bird* 7:117-167.
- Hadley, M. E. 1999. *Endocrinology*. 5th Ed. Prentice Hall, Upper Saddle River.

- Hasbrouck, E. M. 1893a. Evolution and dichromatism in the genus *Megascops*. American Naturalist 27:521-533.
- . 1893b. Evolution and dichromatism in the genus *Megascops*. American Naturalist 27:638-649.
- Hayashida, A., H. Endo, M. Sasaki, T. Oshida, J. Kimura, S. Waengothorn, N. Kitamura, and J. Yamada. 2007. Geographical variation in skull morphology of gray-bellied squirrel *Callosciurus caniceps*. Journal of Veterinary and Medical Science 69:149-157.
- Hoffman, E. C. 1931. Plumage pattern of the screech owl. Journal of Field Ornithology 2:38.
- Hrubant, H. E. 1955. An analysis of the color phases of the eastern screech owl, *Otus asio*, by the gene frequency method. American Naturalist 89:223-230.
- Hughes, J. M., A. M. Baker, G. De Zylva, and P. B. Mather. 2001. A phylogeographic analysis of southern and eastern populations of the Australian magpie: Evidence for selection in maintenance of the distribution of two plumage morphs. Biological Journal of the Linnean Society 74:25-34.
- Hund, A., W. Richner, A. Soldati, Y. Fracheboud, and P. Stamp. 2007. Root morphology and photosynthetic performance of maize inbred lines at low temperature. European Journal of Agronomy 27:52-61.
- Huxley, J. S. 1955. Morphism in birds. Acta 6th International Ornithological Congress Basel 1954:309-328.
- Ito, S, and K. Fujita. 1985. Microanalysis of eumelanin and pheomelanin in hair and malanomas by chemical degradation and liquid chromatography. Analytical Biochemistry 144:527-536.
- Ito, S. 2003. A chemist's view of melanogenesis. Pigment Cell Research 16:230-236.
- Jawor, J. M., and R. Breitwisch. 2003. Melanin ornaments, honesty, and sexual selection. The Auk 120:249-265.
- Johnsgard, P. A., 1988. North American owls: biology and natural history. Smithsonian Institution Press, Washington, D.C.
- Johnson, N. K., and A. H. Brush. 1972. Analysis of polymorphism in the sooty-capped bush tanager. Systematic Zoology 21:245-262.
- Kelso, L. H. 1938. A study of the screech owl (*Otus asio*). M.S. thesis, Cornell University, Ithaca, NY.

- Klatt, P. H., and G. Rithcison. 1994. The effect of mate removal on the vocal behavior and movement patterns of male and female eastern screech owls. *The Condor* 96:485-493.
- Kobayashi, T., W. D. Vieira, B. Potterf, C. Sakai, G. Imokawa, and V. J. Hearing. 1995. Modulation of melanogenic protein expression during the switch from eu- to pheomelanogenesis. *Journal of Cell Science* 108:2301-2309.
- Koch, U. R., and H. Wagner. 2002. Morphometry of auricular feathers of barn owls (*Tyto alba*). *European Journal of Morphology* 40:15-21.
- Lank, D. B. 2002. Diverse processes maintain plumage polymorphisms in birds. *Journal of Avian Biology* 33:327-330.
- Lei, F., Y. Qu, Y. Gan, A. Gebauer, and M. Kaiser. 2002. The feather microstructure of passerine sparrows in China. *Journal of Ornithology* 143:205-213.
- Lohrer, F. E. 1985. Ontogeny of thermoregulation in the eastern screech owl. *Journal of Field Ornithology* 56:65-66.
- Lucas, A. M., and P. Stettenheim. 1972. Avian anatomy: Integument Vol. 1 and 2. U.S. Department of Agriculture, Washington D.C.
- Matics, R., G. Hoffmann, T. Nagy, and A. Roulin. 2002. Random pairing with respect to plumage coloration in Hungarian barn owls (*Tyto alba*). *Journal of Ornithology* 143:493-495.
- Mascha, E. 1905. The structure of wing-feathers. *Smithsonian Miscellaneous Collection* 48:1-30.
- Mayr, E. 1963. Animal species and evolution. The Belknap Press of Harvard University, Cambridge, MA.
- McGraw, K., R. J. Safran, and K. Wakamatsu. 2005. How feather colour reflects its melanin content. *Functional Ecology* 19:816-821.
- McGraw, K. 2006. Mechanics of melanin-based coloration. Chap. 6 in G. E. Hill and K. J. McGraw, eds. *Bird coloration: Mechanisms and mechanics*. Harvard University Press, Cambridge, MA.
- Montgomerie, R. 2006. Analyzing colors. Chap. 3 in G. E. Hill and K. J. McGraw, eds. *Bird coloration: Mechanisms and mechanics*. Harvard University Press, Cambridge, MA.
- Mosher, J. A., and C. J. Henny. 1976. Thermal adaptiveness of plumage color in screech owls. *The Auk* 93:614-619.

- Mundy, N. I., and J. Kelly. 2003. Evolution of a pigmentation gene, the melanocortin-1 receptor, in primates. *American Journal of Physical Anthropology* 121:67-80.
- Mundy, N. I., J. Kelly, E. Theron, and K. Hawkins. 2003. Evolutionary genetics of the melanocortin-1 receptor in vertebrates. *Annals of the New York Academy of Science* 994:307-312.
- Needham, A. E. 1974. *The significance of zoochromes*. Springer-Verlag, NY.
- Niecke, M., M. Heid, and A. Kruger. 1999. Correlations between melanin pigmentation and element concentration in feathers of white-tailed eagles (*Haliaeetus albicilla*). *Journal of Ornithology* 140:355-362.
- Niecke, M., S. Rothlaender, and A. Roulin. 2003. Why do melanin ornaments signal individual quality? Insights from metal element analysis of barn owl feathers. *Oecologia* 137:153-158.
- North, P. M. 1985. A computer modeling study of the population dynamics of the screech owl (*Otus asio*). *Ecological Modelling* 30:105-143.
- North Carolina State Museum of Natural History (NCSM). 2006. Personal communication.
- Olsen, B., and P. Mooney. 2001. Effect of colour phase on winter habitat characteristics of the eastern screech owl, *Otus asio*, in central Pennsylvania. *Journal of Ecological Research* 3:53-61.
- Olvera, H. F., S. Fuentes-Soriano, and E. M. Hernandez. 2006. Pollen morphology and systematics of Atripliceae (Chenopodiaceae). *Grana* 45:175-194.
- Owen, D. F. 1963a. Screech owl polymorphism. *The Wilson Bulletin* 75:183-189.
- . 1963b. Variation in North American screech owls and the subspecies concept. *Systematic Zoology* 12:8-14.
- Paulson, D. R. 1973. Predator polymorphism and apostatic selection. *Evolution* 27:269-277.
- Perremans, K., A. DeBont, and F. Ollevier. 1992. A study of featherprints by scanning electron microscopy. *Belgium Journal of Zoology* 122:113-121.
- Pittaway, R. 1995. Recognizable forms: Morphs of the eastern screech owl. *Ontario Birds* 13:66-71.
- Preston, C. R. 1980. Differential perch site selection by color morphs of the red-tailed hawk (*Buteo jamaicensis*). *The Auk* 97:782-789.

- Price, T., and A. Bontrager. 2001. Evolutionary genetics: The evolution of plumage patterns. *Current Biology* 11:R405-R408.
- Proudfoot, G. A., F. R. Gehlbach, and R. L. Honeycutt. 2007. Mitochondrial DNA variation and phylogeography of the eastern and western screech-owls. *The Condor* 109:617-627.
- Prum, R. O. and A. H. Brush. 2002. The evolutionary origin and diversification of feathers. *Quarterly Review of Biology*. 77: 261-295
- Py, I., A. Ducrest, N. Duvoisin, L. Fumagalli, and A. Roulin. 2006. Ultraviolet reflectance in a melanin-based plumage trait is heritable. *Evolutionary Ecology Research* 8:483-491.
- Reaney, B. A., S. M. Richner, and W. P. Cunningham. 1978. A preliminary scanning electron microscope study of the minute morphological features of feathers and their taxonomic significance. *Scanning Electron Microscopy* 1:471-478.
- Richards, N. L., P. Mineau, and D. M. Bird. 2006. The case for sampling eastern screech owls (*Megascops asio*) admitted to rehabilitation facilities for evidence of exposure to pesticides and persistent contaminants. *Journal of Wildlife Rehabilitation* 28:4-9.
- Robertson, J., C. Harkin, and J. Govan. 1984. The identification of bird feathers. Scheme for feather examination. *Forensic Science Society Journal* 24:85-98.
- Roulin, A. 1999. Nonrandom pairing by male barn owls (*Tyto alba*) with respect to a female plumage trait. *Behavioral Ecology* 10:688-695.
- . 2004a. The evolution, maintenance and adaptive function of genetic colour polymorphism in birds. *Biological Reviews* 79:815-848.
- . 2004b. Covariation between plumage colour polymorphism and diet in the barn owl *Tyto alba*. *Ibis* 146:509-517.
- . 2004c. Proximate basis of the covariation between a melanin-based female ornament and offspring quality. *Oecologia* 140:668-675.
- . 2006. Linkage disequilibrium between a melanin-based colour polymorphism and tail length in the barn owl. *Biological Journal of the Linnean Society* 88:475-488.
- . 2007. Melanin pigmentation negatively correlates with plumage preening effort in barn owls. *Functional Ecology* 21:264-271.
- Roulin, A., and C. Dijkstra. 2003. Genetic and environmental components of variation in eumelanin and pheomelanin sex-traits in the barn owl. *Heredity* 90:359-364.

- Roulin, A., B. Ducret, P. Ravussin, and R. Altwegg. 2003. Female colour polymorphism covaries with reproductive strategies in the tawny owl *Strix aluco*. *Journal of Avian Biology* 34:393-401.
- Roulin, A., and M. Wink. 2004. Predator-prey relationships and the evolution of colour polymorphism: a comparative analysis in diurnal raptors. *Biological Journal of the Linnean Society* 81:565-578.
- Roulin, A., T. Dauwe, R. Blust, M. Eens, and M. Beaud. 2006. A link between eumelanism and calcium physiology in the barn owl. *Naturwissenschaften* 93:426-430.
- Roulin, A., and R. Altwegg. 2007. Breeding rate is associated with pheomelanism in male and with eumelanism in female barn owls. *Behavioral Ecology* 18:563-570.
- Roulin, A., J. Gasparini, P. Bize, M. Ritschard, and H. Richner. 2008. Melanin-based colorations signal strategies to cope with poor and rich environments. *Behavioral and Ecological Sociobiology* 62:507-519.
- Rudh, A., B. Rogell, and J. Hoglund. 2007. Non-gradual variation in colour morphs of the strawberry poison frog *Dendrobates pumilio*: genetic and geographical isolation suggest a role for selection in maintaining polymorphism. *Molecular Ecology* 16:4284-4294.
- Saranathan, V., and E. H. Burt Jr. 2007. Sunlight on feathers inhibits feather-degrading bacteria. *The Wilson Journal of Ornithology* 119:239-245.
- Schluter, D. 2001. Ecology and the origin of species. *Trends in Ecology & Evolution* 16:372-380.
- Schorger, A. W. 1954. Color phases of the screech owl between Madison, Wisconsin, and Freeport, Illinois. *The Auk* 71:205.
- Schreiber, R. W., E. A. Schreiber, A. M. Peele, and E. H. Burt Jr. 2006. Pattern of damage to albino great frigatebird flight feathers supports hypothesis of abrasion by airborne particles. *The Condor* 108:736-741.
- Shawkey, M. D., A. M. Estes, L. M. Siefferman, and G. E. Hill. 2003. Nanostructure predicts intraspecific variation in ultraviolet-blue plumage colour. *Proceedings of the Royal Society Biological Sciences Series B* 270:1455-1460.
- . 2005. The anatomical basis of sexual dichromatism in non-iridescent ultraviolet-blue structural coloration of feathers. *Biological Journal of the Linnean Society* 84:259-271.

- Shawkey, M. D., and G. E. Hill. 2006. Significance of a basal melanin layer to production of non-iridescent structural plumage color: evidence from an amelanotic Steller's jay (*Cyanocitta stelleri*). *The Journal of Experimental Biology* 209:1245-1250.
- Shawkey, M. D., S. L. Balenger, G. E. Hill, L. S. Johnson, A. J. Keyser, and L. Siefferman. 2006a. Mechanisms of evolutionary change in structural plumage coloration among bluebirds (*Sialia* spp.). *Journal of the Royal Society Interface* 3:527-532.
- Shawkey, M. D., M. E. Hauber, L. K. Estep, and G. E. Hill. 2006b. Evolutionary transitions and mechanisms of matte and iridescent plumage coloration in grackles and allies (Icteridae). *Journal of the Royal Society Interface* 3:777-786.
- Shawkey, M. D. 2007. Personal communication.
- Sick, H. 1937. Morphologisch-funktionelle untersuchungen uber die feinstruktur der vogelfeder. *Journal fur Ornithologie* 85:206-372.
- Smith, D. G., and R. Gilbert. 1984. Eastern screech owl home range and use of suburban habitats in southern Connecticut. *Journal of Field Ornithology* 55:322-329.
- Soule, M., and B. R. Stewart. 1970. The "niche-variation" hypothesis: A test and alternatives. *The American Naturalist* 104:85-97.
- Sparks, E. J., J. R. Belthoff, and G. R. Ritchison. 1993. Habitat use by eastern screech-owls in central Kentucky. *Journal of Field Ornithology* 65:83-95.
- Stettenheim, P. R. 2000. The integumentary morphology of modern birds- An overview. *American Zoology* 40:461-477.
- Stevens, L. 1996. *Avian biochemistry and molecular biology*. Cambridge University Press, Cambridge.
- Stupka, A. 1963. *Notes on the birds of Great Smoky National Park*. University of Tennessee Press, Knoxville, TN.
- Sutton, G. M. 1986. Dichromatism of the screech owl in central Oklahoma. *Oklahoma Ornithological Society* 19:17-20.
- Teodori, L., A. Accorsi, F. Ugucioni, M. Rocchi, R. Baldoni, E. Piatti, and M. C. Albertini. 2007. Erythrocyte morphology automated analysis: Proposal for a new prediction tool of essential hypertension diagnosis. *Cytometry Part B (Clinical Cytometry)* 72B:211-214.
- Theron, E., K. Hawkins, E. Bermingham, R. E. Ricklefs, and N. I. Mundy. 2001. The molecular basis of an avian plumage polymorphism in the wild: A melanocortin-1-

- receptor point mutation is perfectly associated with the melanic plumage morph of the bananaquit, *Coereba flaveola*. *Current Biology* 11:550-557.
- Thery, M. 2006. Effects of light environment on color communication. Chap. 4 in G. E. Hill and K. J. McGraw, eds. *Bird coloration: Mechanisms and mechanics*. Harvard University Press, Cambridge, MA.
- United States Geological Survey (USGS). 2007. USGS seamless data distribution. <http://seamless.usgs.gov/>. Access date, June 28, 2006.
- VanCamp, L. F., and C. J. Henny. 1975. The screech owl its life history and population ecology in Northern Ohio. *North America Fauna* 1-65.
- Van Valen, L. V. 1965. Morphological variation and the width of ecological niche. *American Naturalists* 99:377-390.
- Wakamatsu, K., and S. Ito. 2002. Advanced chemical methods in melanin determination. *Pigment Cell Research* 15:174-183.
- Willson, M. F. 1969. Avian niche size and morphological variation. *American Naturalist* 103:531-542.
- Wunderle, J. M. Jr. 1981. An analysis of a morph Ratio cline in the bananaquit (*Coereba flaveola*) on Grenada, West Indies. *Evolution* 35:333-344.
- Zar, J. H. 2005. *Biostatistical analysis*. 4th Ed. Pearson Education, Singapore.

APPENDIX A

Pooled Morphological Measurements at the Barbule Segment Level

APPENDIX A

Appendix A. Pooled summary statistics for morphological measurements at the barbule segment level of eastern screech owl color variants. Coefficient of variation in parenthesis, Means \pm Standard Error. ($n=2$).

Measurement	Barbule Segment			P-value	F-value
	Proximal	Intermediate	Distal		
Dorsal Tract (Contour): Proximal Barb					
Proximal-Distal Nodal Length (μm)	31.74 \pm 0.75 (28.40)	30.74 \pm 0.57 (22.21)	25.90 \pm 0.77 ^A (35.31)	P = 0.01	F = 25.86
Proximal-Distal Pigment Length (μm)	19.43 \pm 0.52 (31.91)	22.53 \pm 0.58 (30.91)	22.19 \pm 0.55 (29.61)	P = 0.07	F = 7.41
Internode Width (μm)	4.11 \pm 0.09 ^A (26.14)	3.36 \pm 0.09 ^B (32.02)	2.70 \pm 0.09 ^C (39.75)	P = <0.01	F = 130.93
Spine Length (μm)	4.00 \pm 0.11 ^A (33.31)	3.07 \pm 0.17 ^B (50.26)	4.95 \pm 0.30 ^C (70.22)	P = <0.01	F = 571.33
Femoral Tract (Down): Proximal Barb					
Proximal-Distal Nodal Length (μm)	30.16 \pm 0.54 ^A (21.00)	37.32 \pm 0.75 (23.91)	37.24 \pm 1.04 (33.14)	P = 0.01	F = 47.99
Proximal-Distal Pigment Length (μm)	14.57 \pm 0.32 ^A (26.21)	17.54 \pm 0.24 ^B (15.95)	21.96 \pm 0.40 ^C (21.32)	P = <0.01	F = 106.14
Internode Width (μm)	3.99 \pm 0.08 ^A (25.05)	2.73 \pm 0.08 ^B (36.19)	2.07 \pm 0.04 ^C (24.33)	P = <0.01	F = 338.63
Spine Length (μm)	4.50 \pm 0.10 ^A (26.07)	2.33 \pm 0.19 (40.35)	2.73 \pm 0.21 (79.60)	P = 0.02	F = 17.96
Humeral Tract (Contour): Proximal Barb					
Proximal-Distal Nodal Length (μm)	29.96 \pm 0.60 (23.77)	30.73 \pm 0.48 (18.53)	26.75 \pm 0.68 ^A (29.91)	P = 0.04	F = 11.60
Proximal-Distal Pigment Length (μm)	18.88 \pm 0.46 ^A (27.94)	20.62 \pm 0.40 ^B (22.95)	21.84 \pm 0.40 ^C (21.69)	P = <0.01	F = 78.41
Internode Width (μm)	4.21 \pm 0.09 ^A (24.27)	3.32 \pm 0.09 ^B (31.57)	2.50 \pm 0.07 ^C (34.05)	P = <0.01	F = 538.21
Spine Length (μm)	4.08 \pm 0.11 (30.75)	2.83 \pm 0.17 ^A (51.61)	4.17 \pm 0.27 (71.54)	P = 0.01	F = 26.49
Medial Pectoral Tract (Contour): Proximal Barb					
Proximal-Distal Nodal Length (μm)	33.13 \pm 0.63 (22.21) ^A	30.59 \pm 0.46 ^B (17.38)	25.74 \pm 0.62 ^C (29.26)	P = <0.01	F = 2879.00
Proximal-Distal Pigment Length (μm)	18.35 \pm 0.37 ^A (23.53)	20.17 \pm 0.38 (21.88)	20.57 \pm 0.28 (16.41)	P = 0.05	F = 9.92
Internode Width (μm)	4.09 \pm 0.09 ^A (24.67)	3.38 \pm 0.09 ^B (30.45)	2.79 \pm 0.08 ^C (33.70)	P = <0.01	F = 277.69
Spine Length (μm)	4.19 \pm 0.12 (32.96)	2.93 \pm 0.14 ^A (45.42)	4.86 \pm 0.28 (66.40)	P = 0.01	F = 25.49

Measurement	Barbule Segment			P-value	F-value
	Proximal	Intermediate	Distal		
Dorsal Tract (Contour): Intermediate Barb					
Proximal-Distal Nodal Length (μm)	25.73 \pm 0.46 (21.25)	30.78 \pm 0.51 ^A (19.75)	26.60 \pm 0.58 (25.97)	P = 0.01	F = 25.23
Proximal-Distal Pigment Length (μm)	19.62 \pm 0.48 ^A (29.24)	22.74 \pm 0.36 ^B (19.12)	25.05 \pm 0.64 ^C (30.88)	P = 0.05	F = 9.76
Internode Width (μm)	4.88 \pm 0.06 ^A (15.59)	3.44 \pm 0.10 ^B (24.48)	2.49 \pm 0.05 ^C (26.32)	P = <0.01	F = 241.03
Spine Length (μm)	4.22 \pm 0.11 ^A (30.50)	2.02 \pm 0.07 ^B (24.48)	2.73 \pm 0.12 ^C (51.33)	P = <0.01	F = 89.40
Femoral Tract (Down): Intermediate Barb					
Proximal-Distal Nodal Length (μm)	26.07 \pm 0.52 ^A (23.66)	32.85 \pm 0.82 ^B (29.46)	30.75 \pm 0.82 ^C (31.52)	P = <0.01	F = 68.62
Proximal-Distal Pigment Length (μm)	16.46 \pm 0.44 ^A (31.49)	19.48 \pm 0.27 ^B (16.68)	23.08 \pm 0.04 ^C (23.81)	P = <0.01	F = 118.44
Internode Width (μm)	4.37 \pm 0.07 ^A (19.25)	3.30 \pm 0.10 ^B (36.44)	2.25 \pm 0.04 ^C (23.01)	P = <0.01	F = 253.24
Spine Length (μm)	4.39 \pm 0.10 ^A (27.40)	1.95 \pm 0.05 ^B (16.73)	2.41 \pm 0.08 ^C (37.16)	P = <0.01	F = 791.48
Humeral Tract (Contour): Intermediate Barb					
Proximal-Distal Nodal Length (μm)	24.89 \pm 0.48 (22.60)	28.71 \pm 0.49 ^A (20.26)	25.11 \pm 0.53 (25.11)	P = <0.01	F = 77.45
Proximal-Distal Pigment Length (μm)	19.47 \pm 0.39 ^A (23.78)	22.63 \pm 0.43 (22.35)	23.50 \pm 0.45 (22.86)	P = 0.02	F = 22.97
Internode Width (μm)	4.84 \pm 0.08 ^A (18.81)	3.69 \pm 0.10 ^B (31.15)	2.46 \pm 0.05 ^C (24.83)	P = <0.01	F = 649.63
Spine Length (μm)	3.81 \pm 0.11 ^A (33.64)	2.38 \pm 0.23 ^B (74.50)	3.00 \pm 0.18 ^{A,B} (66.72)	P = 0.03	F = 12.80
Medial Pectoral Tract (Contour): Intermediate Barb					
Proximal-Distal Nodal Length (μm)	26.82 \pm 0.47 (20.31)	26.74 \pm 0.49 (21.24)	22.87 \pm 0.44 ^A (23.18)	P = <0.01	F = 69.07
Proximal-Distal Pigment Length (μm)	18.84 \pm 0.32 ^A (19.16)	21.74 \pm 0.35 (18.62)	21.71 \pm 0.35 (19.49)	P = <0.01	F = 94.24
Internode Width (μm)	4.78 \pm 0.07 ^A (17.26)	3.80 \pm 0.10 ^B (30.83)	2.70 \pm 0.08 ^C (34.18)	P = <0.01	F = 88.28
Spine Length (μm)	3.94 \pm 0.11 (32.11)	2.53 \pm 0.16 ^A (49.32)	3.42 \pm 0.18 (62.55)	P = 0.03	F = 14.28

Measurement	Barbule Segment			P-value	F-value
	Proximal	Intermediate	Distal		
Dorsal Tract (Contour): Distal Barb					
Proximal-Distal Nodal Length (μm)	26.96 \pm 0.63 ^A (27.61)	32.90 \pm 0.76 (27.59)	30.39 \pm 0.87 (33.11)	P = 0.03	F = 15.89
Proximal-Distal Pigment Length (μm)	24.50 \pm 0.70 ^A (34.40)	30.63 \pm 0.69 (27.19)	33.96 \pm 1.16 (40.57)	P = 0.03	F = 13.87
Internode Width (μm)	5.78 \pm 0.08 ^A (17.25)	4.44 \pm 0.12 ^B (61.43)	2.86 \pm 0.07 ^C (29.65)	P = <0.01	F = 66.99
Spine Length (μm)	3.65 \pm 0.11 (36.61)	3.02 \pm 0.18 (61.43)	4.82 \pm 0.23 ^A (55.41)	P = 0.03	F = 13.17
Femoral Tract (Down): Distal Barb					
Proximal-Distal Nodal Length (μm)	32.45 \pm 1.06 (38.48)	37.16 \pm 1.37 (43.62)	32.97 \pm 1.24 (43.94)	P = 0.07	F = 7.36
Proximal-Distal Pigment Length (μm)	20.47 \pm 0.46 ^A (24.16)	26.35 \pm 0.63 ^B (25.79)	29.50 \pm 0.93 ^C (32.95)	P = <0.01	F = 1113.32
Internode Width (μm)	4.98 \pm 0.08 ^A (18.05)	3.91 \pm 0.11 ^B (32.25)	2.26 \pm 0.06 ^C (32.95)	P = <0.01	F = 121.17
Spine Length (μm)	3.96 \pm 0.14 (41.59)	3.04 \pm 0.14 ^A (47.57)	4.46 \pm 0.21 (54.00)	P = 0.03	F = 13.62
Humeral Tract (Contour): Distal Barb					
Proximal-Distal Nodal Length (μm)	32.14 \pm 0.99 (36.29)	36.02 \pm 1.22 (39.49)	32.11 \pm 1.22 (42.84)	P = 0.09	F = 6.07
Proximal-Distal Pigment Length (μm)	24.64 \pm 0.65 ^A (29.43)	30.00 \pm 0.92 ^B (34.15)	32.06 \pm 1.51 ^C (42.84)	P = <0.01	F = 556.95
Internode Width (μm)	5.49 \pm 0.08 ^A (16.32)	4.69 \pm 0.10 ^B (26.25)	2.97 \pm 0.08 ^C (51.42)	P = <0.01	F = 514.38
Spine Length (μm)	3.87 \pm 0.13 (40.49)	4.32 \pm 0.19 (49.39)	6.44 \pm 0.24 ^A (42.40)	P = 0.03	F = 16.06
Medial Pectoral Tract (Contour): Distal Barb					
Proximal-Distal Nodal Length (μm)	51.91 \pm 1.24 (28.20)	53.08 \pm 1.45 (31.91)	45.07 \pm 1.09 ^A (29.12)	P = 0.02	F = 19.15
Proximal-Distal Pigment Length (μm)	19.29 \pm 0.90 (30.34)	24.25 \pm 1.12 (29.08)	N/A	P = N/A	F = N/A
Internode Width (μm)	6.02 \pm 0.07 ^A (13.73)	5.72 \pm 0.09 ^B (17.72)	3.57 \pm 0.10 ^C (34.59)	P = <0.01	F = 2615.01
Spine Length (μm)	4.80 \pm 0.16 (38.77)	5.23 \pm 0.20 (43.60)	7.82 \pm 0.25 ^A (38.37)	P = <0.01	F = 192.61

VITA

Evan Lacy Pannkuk was born in Raleigh, North Carolina, on May 18, 1982. He attended Raleigh Christian Academy and Wake Christian Academy in Raleigh, North Carolina. He then attended West Lake Middle School for 8th grade and then four years at Cary High School where he graduated in 2000. He entered the college transfer program at Wake Technical Community College where he planned on being a Psychology major. Evan decided to depart from Psychology to enter the pre-professional Biology program at Appalachian State University in 2002. He graduated with a B.S. in Biology in 2005 and entered the graduate program in Biology at Appalachian State University the same year. He graduated with a M.S. in Biology in August 2008 and continued his research on avian pigmentation for a PhD.